Doctoral theses at NTNU, 2021:348

Magnus Nystad

Real-Time Data-Driven Drilling Optimization

an Extremum Seeking Approach

Doctoral thesis

NTNU
Norwegian University of Science and Technology
Thesis for the Degree of
Philosophiae Doctor
Faculty of Engineering
Department of Geoscience and Petroleum

NTNU
Norwegian University of
Science and Technology

Magnus Nystad

Real-Time Data-Driven Drilling Optimization

an Extremum Seeking Approach

Thesis for the Degree of Philosophiae Doctor

Trondheim, November 2021

Norwegian University of Science and Technology
Faculty of Engineering
Department of Geoscience and Petroleum

NTNU
Norwegian University of
Science and Technology

NTNU
Norwegian University of Science and Technology

Thesis for the Degree of Philosophiae Doctor

Faculty of Engineering
Department of Geoscience and Petroleum

ISBN 978-82-326-5854-1 (printed ver.)
ISBN 978-82-326-6290-6 (electronic ver.)
ISSN 1503-8181 (printed ver.)
ISSN 2703-8084 (online ver.)

Doctoral theses at NTNU, 2021:348

Printed by NTNU Grafisk senter

Abstract

Drilling a well for exploration or production of petroleum resources is a costly and complicated procedure. On the Norwegian Continental Shelf (NCS), it is estimated that approximately 50 percent of field development costs are related to drilling and well activities, with 80 percent of these costs being related to time [1]. There is in other words a great potential for cost reduction by drilling safer, faster and with less Non-Productive Time (NPT). Reducing the time spent on drilling will not only save costs, it also provides the benefit of lowering the environmental impact of drilling operations.

From a mechanical standpoint, achieving high efficiency drilling can be realized by optimizing the applied Weight on Bit (WOB) and drillstring rotational speed (Revolutions per Minute - RPM). However, selection of optimal values for WOB and RPM is a complex task. The drilling action at the bit happens at distances often several kilometers away from the rig, and only indirect measurements performed at the surface are routinely available to gauge what is happening down the hole. The task is further complicated by uncontrollable changes in downhole conditions such as variations in rock properties and wear and tear on the bit, which can alter the bit/rock interaction so that the WOB and RPM that was optimal a few minutes ago might no longer be the most efficient solution. Furthermore, the information required to accurately model the downhole conditions might not be directly measurable or available in real-time, which could preclude available models from predicting the optimal WOB and RPM.

In this work, an adaptive model-free algorithm called Extremum Seeking (ES) is investigated for the purpose of optimizing the WOB and RPM in real-time. The method is data-driven and relies on continuously performing small tests with the applied WOB and RPM while drilling ahead, to gather information about the current downhole conditions. The test results are used to generate a local linear model, based on which the ES algorithm continuously performs automatic adjustments in WOB and RPM in the direction that increases Rate of Penetration (ROP) or reduces Mechanical Specific Energy (MSE). This process is designed to iteratively drive the WOB and RPM to their optimal values and maintain optimal drilling by adapting to changes in downhole conditions. The ES method does not require an a priori model of the drilling process and can thus be applied even in instances when sufficiently accurate drilling models are not available.

To ensure that the ES algorithm does not steer the WOB or RPM to values which might be detrimental to drilling equipment or personnel, several constraint handling techniques are included in the proposed methodology. The ES algorithm employed in this thesis is a product of modifications proposed by the authors, as well as different algorithms and tools found in the literature, which are assembled to make the routine better suited for drilling applications. The outlined optimization strategy is tested in a variety of scenarios with simulations and experiments on a small-scale drilling rig. The experiments and simulations demonstrate the ES algorithm's ability to seek out optimal values for WOB and RPM, adapt to changes in downhole conditions, and avoid violation of process constraints. Therefore, this study indicates a potential for significant improvement in drilling efficiency from applying the ES method for real-time drilling optimization.

Preface

This dissertation is submitted to the Norwegian University of Science and Technology (NTNU) for partial fulfilment of the requirements for the degree of Philosophiae Doctor. The work was conducted at the Department of Geoscience and Petroleum (IGP), NTNU. The project was supervised by Professor Alexey Pavlov and co-supervised by Professor Bernt Sigve Aadnøy. The research was funded by IGP through BRU21 – NTNU's Research and Innovation Program in Digital and Automation Solutions for the Oil and Gas Industry.

This thesis is divided into two parts: the first part consists of five chapters that give an overview of motivation, background, methods, summaries, and conclusions of the content that comprises the second part, which is three scientific articles contained in the appendices. The article in Appendix A is peer-reviewed and published in a conference proceedings journal. The article in Appendix B is submitted for publication. The article in Appendix C is published in a peer-reviewed journal.

Acknowledgements

I would like to thank my supervisors Alexey Pavlov and Bernt Sigve Aadnøy. I would also like to acknowledge the following list of people for providing support, encouragement and/or help during the research period:

- Noralf Vedvik
- Steffen Wærnes Moen
- Terje Bjerkan
- Håkon Myhren
- Thiago Lima Silva
- Sonja Moi
- Jan Einar Gravdal
- Sigve Hovda
- Bård Fjellså
- Andreas Teigland
- Brage Strand Kristoffersen
- The BRU21 team
- Family and friends

I also want to express my gratitude to my parents and Nina for their constant encouragement, their patience and unwavering support and love.

Table of Contents

Nomenclature

Abbreviations

ADR	Autodriller
ASME	American Society of Mechanical Engineers
BRU21	Better Resource Utilization in the 21st Century
BY	Bourgoyne-Young
DOC	Depth of Cut
DOT	Drill-off Test
ES	Extremum Seeking
HPF	High Pass Filter
HSE	Health, Safety and Environment
KF	Kalman Filter
LS	Least-Squares
LPF	Low Pass Filter
MSE	Mechanical Specific Energy
MPD	Managed Pressure Drilling
NCS	Norwegian Continental Shelf
PDC	Polycrystalline Diamond Compact
PI	Proportional-Integral
PID	Proportional-Integral-Derivative
ROP	Rate of Penetration
RPM	Revolutions per Minute
SF	Safety Factor
SNR	Signal to Noise Ratio
SPE	Society of Petroleum Engineers
SPP	Standpipe Pressure
WOB	Weight on Bit

Parameters

a	Least-squares slope	(m/hr/kg) or (m/hr/rpm)
A	Amplitude of excitation signal	(kg) or (rpm)
b	Least-squares intercept	(m/hr)
e	Error between requested and measured WOB	(kg)
γ	Adaptation gain	($kg^2 \cdot hr/m/s$)
J	Performance function	(m/hr) or (MPa)
K_D	Derivative gain in autodriller	(m/kg)
K_I	Integral gain in autodriller	($m/s^2/kg$)
K_P	Proportional gain in autodriller	(m/s/kg)
μ	Penalty parameter in J	(m/hr/kg)
P	Period of excitation signal	(s)
ρ	Tuning parameter in Eq. (3.10)	(-)
$\boldsymbol{r}$	Vector containing drilling parameters	(-)
ROP_{limit}	Limiting ROP value	(m/hr)
t	Time	(s)
T	Torque	(Nm)
T_{avg}	Average torque value in buffer	(Nm)
T_{limit}	Limiting torque value	(Nm)
u	Manipulated variable, WOB or RPM	(kg) or (rpm)
$\bar{u}$	Base value, WOB or RPM	(kg) or (rpm)
v	Spool rate of drawworks drum	(m/s)

List of figures

List of tables

1 Introduction

1.1 Motivation

Drilling a well for exploration or production of petroleum resources is a costly and complicated procedure. On the Norwegian Continental Shelf (NCS), it is estimated that approximately 50 percent of field development costs are related to drilling and well activities, with 80 percent of these costs being related to time [1]. There is in other words a great potential for cost reduction by drilling safer, faster and with less Non-Productive Time (NPT). Reducing the time spent on drilling will not only save costs, it also provides the benefit of lowering the environmental impact of drilling operations. One of the key enablers to achieve this potential is drilling automation systems, which can aid the driller and deliver consistency by performing tasks such as providing data analysis and visualization, envelope control, and automatic optimization of drilling variables. The focus of this thesis is on a method for automated drilling optimization, employed to seek out and maintain the optimal values for the mechanical input variables; Weight on Bit (WOB) and drillstring rotational speed (Revolutions per Minute - RPM), to achieve safe and high efficiency drilling.

1.2 Thesis objective and research outcome

The main goal of this thesis is to contribute towards automatic solutions for safe and efficient well construction. This goal is carried out by investigating a data-driven optimization method called Extremum Seeking (ES) for the purpose of automated drilling optimization through manipulation of the mechanical variables WOB and RPM. The overall research objective is summarized in Figure 1.1.

The ES algorithm is chosen for analysis because of its beneficial properties which satisfy the criteria given in Figure 1.1, as well as the methods proven track-record from other industries. The ES methodology employed in this thesis is a product of modifications proposed by the authors, as well as different algorithms and tools found in the literature, which are assembled to make the routine better suited for drilling applications. The articles resulting from this study investigate the ES algorithm's ability

to obtain drilling with optimal WOB and RPM in simulations and experiments. The studies indicate a potential for significant improvement in drilling efficiency from applying the ES method for real-time drilling optimization.

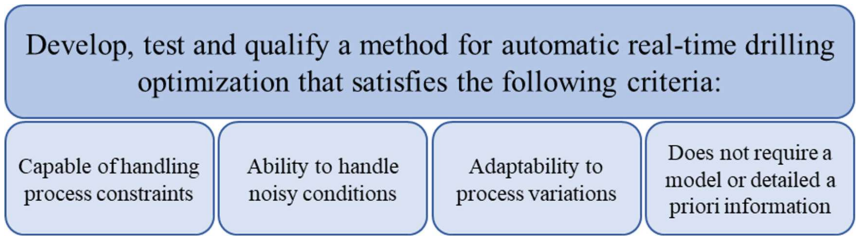

Figure 1.1 – Research objective.

1.3 Contributions

Publications

As part of this thesis, I have been the lead author on three scientific papers. The articles are summarized in Section 4 and given as full texts in the appendices. In the role of lead author, I performed all simulations, modeling, experiments, and analysis, wrote the manuscripts, and implemented revisions based on feedback from the co-authors and journal reviewers. The co-authors contributed with supervision, ideas, scientific discussions, and gave feedback on the paper manuscripts.

- **Article 1**, "Micro-Testing While Drilling for Rate of Penetration Optimization"
  Magnus Nystad, Alexey Pavlov

  Published in Proceedings of the ASME 2020 39th International Conference on Ocean, Offshore and Arctic Engineering, OMAE2020, December 2020.

- **Article 2**, "Micro-Testing While Drilling for Rate of Penetration Optimization: Experiments and Simulations"
  Magnus Nystad, Bernt Sigve Aadnøy, Alexey Pavlov

  Submitted to Journal of Offshore Mechanics and Arctic Engineering, March 2021.

- **Article 3**, “Real-Time Minimization of Mechanical Specific Energy with Multivariable Extremum Seeking”
  Magnus Nystad, Bernt Sigve Aadnøy, Alexey Pavlov

  Published in Energies, Special Issue: Drilling Technologies for the Next Generations, February 2021.

Conferences and Presentations

- **OG21 forum**, Popular science presentation: “Real-Time Analysis of Drilling Data to Improve the Drilling Process”, 8th of November 2017, Oslo, Norway.
- **OMAE 2020**, Technical Presentation, “Micro-Testing While Drilling for Rate of Penetration Optimization”, 4th of August 2020, Virtual, Online.

Knowledge sharing

As a part of the BRU21 program within the recently created field of petroleum cybernetics at IGP, I have contributed at internal meetings and workshops with presentations, supervised two international master’s students and worked as a teaching assistant in the course PG8406 - Petroleum Cybernetics.

1.4 Thesis outline

The first part of the thesis is structured as follows:

- **Section 1** provides motivation, research objective and outcome as well as an overview of scientific contributions made by the author.
- **Section 2** presents the background for the task of drilling safely and efficiently and gives a review of drilling optimization approaches in the literature.
- **Section 3** details the classical extremum seeking algorithm and how it was modified by the authors, followed by an overview of the drilling models and experimental setup employed in the articles.
- **Section 4** gives a summary of the articles contained in the appendices.
- **Section 5** rounds off the thesis by providing conclusions and directions for further research.

2 Background

2.1 Drilling equipment, measurements and control

The overall goal of drilling a petroleum well is to generate a high-quality wellbore which can be used as a conduit between the reservoir and the production facilities, to extract hydrocarbons from the subsurface. Figure 2.1 shows a schematic of a draw-works based drilling rig, which is the most common drilling apparatus used for well construction. To retain generality, the riser system employed in offshore drilling operations is omitted in this figure. The following sections give a brief overview of key elements on the drilling rig, relevant measurements and the control logic used to regulate the WOB.

2.1.1 Hydraulic system

During on-bottom drilling, a drilling fluid (mud) is continuously circulated through the system by a pump at the surface. The mud is pumped through the standpipe and into the hollow drill string as facilitated by a hydraulic swivel in the top drive assembly which allows for circulation while the top drive is rotating. At the bottom of the drill string, the mud is ejected at high velocity through nozzles at the bit into the annulus. The rock excavations are transported by the mud through the annulus to the surface, where the mud is processed to remove cuttings and prepared for re-injection into the well.

Apart from transporting cuttings out of the hole, the mud provides several other important functions in the drilling process. The drilling fluid cools and lubricates the bit, and most significantly, provides pressure support in open hole sections to stabilize the hole (to avoid formation collapse) and evade influx of formation fluids (commonly referred to as a kick). This principle is illustrated in the lower right corner of Figure 2.1, which shows nominal curves for pore-, annular-, and fracture pressures versus depth in the open hole interval. The mud must maintain a wellbore pressure above the pore pressure to act as the primary barrier of the well against unwanted kicks. At the same time, the annular pressure should be kept below the formation fracture pressure, to avoid fluid losses. This upper and lower bound on the annular pressure is often referred to as a pressure window. Maintaining wellbore pressures within this window can pose significant challenges. As an added safety measure against fluid influx, a Blowout

Preventer (BOP) at the top of the wellbore acts as the well's secondary barrier against kicks. The annular pressure is influenced by properties such as mud rheology and density (which might be altered though interaction with the formation), the amount of cuttings in suspension (which increases the mud density), as well as the mud velocity controlled by the pump rate. The depth to which a section can be drilled is often determined by the pressure window. Additional instrumentation can be installed on the rig to facilitate drilling through narrow pressure windows through different forms of Managed Pressure Drilling (MPD) [2], but these methods are not considered further here. When reaching a point where the hole cannot be further propagated without violating the pressure constraints, a casing string is set to isolate the open formation from the drilling fluid and a smaller diameter bit (and possibly a different mud) is used to drill the next section.

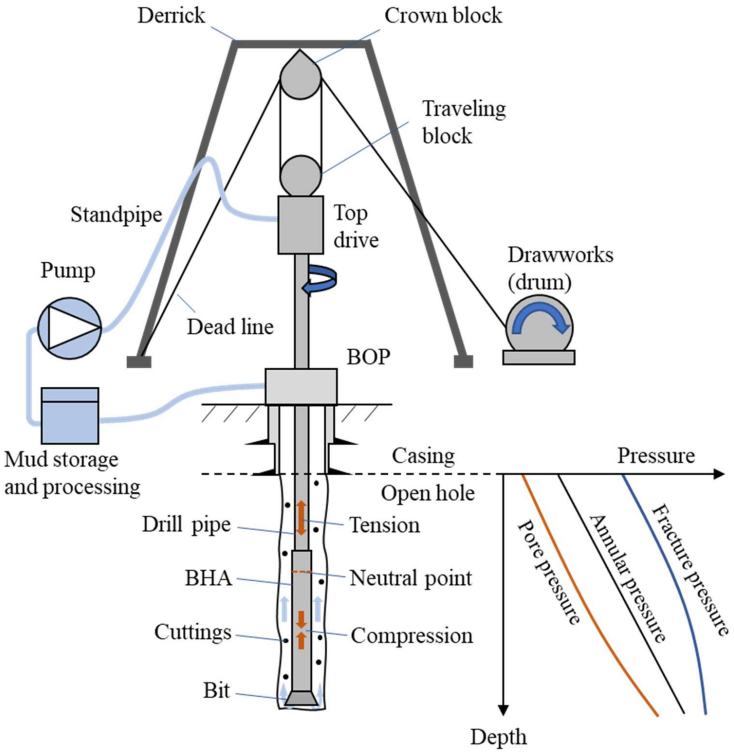

Figure 2.1 – Drilling rig schematic with key elements and pressure window, inspired by [3].

2.1.2 Mechanical system

To excavate rock, often several kilometers from the rig, a drill string is used. The string transmits the drilling fluid from the pumps, as well as rotational energy from the top drive (or alternatively, from a rotary table). The drill string is comprised of drill pipes, which make up the majority of its length, and a Bottom Hole Assembly (BHA), which contains components such as drill collars, stabilizers, reamers, subs, downhole motors, directional drilling and measurement tools, as well as the drill bit. The WOB used to engage the bit cutters/teeth with the formation is provided by the drill collars. A section of heavy-weight drill pipe is often used at the intersection between the drill pipe and the BHA to reduce drill string fatigue and to supply additional WOB if needed.

The drill string is lowered into the progressing borehole from a derrick (or a similarly functioning mast). The top of the string is attached to the top drive, which slides vertically along dolly guide rails (not shown in Figure 2.1). The position and velocity of the top of the string is controlled by a block and tackle system functioning through a wire rope being spooled in and out of the drawworks. In addition to the drawworks drum, this system consists of the crown block suspended from the derrick and the traveling block, between which wire rope is strung and subsequently anchored at the end of the dead line. As the bit progresses and the current length of drill string is lowered into the hole by the drawworks system, a connection is made with new joints of drill pipe that are added to the string (often in triplets, referred to as a stand) and further drilling can commence.

2.1.3 Commonly available measurements

To monitor and control the drilling process, measurements of relevant parameters are performed at different locations on the drilling rig, with the possible addition of measurements from downhole sensors sent to the surface through mud-pulse telemetry or wired drill pipe. Wired pipe also facilitates the inclusion of measurements performed along the string, in addition to sensors placed in the BHA. Because the drilling action itself happens at distances often several kilometers from the rig, it is common practice to rely in indirect measurements and calculation of even of some of the key factors, such as the ROP and WOB. The following list of available measurements that can be utilized by a driller or possibly an automated drilling system is modified from [4] and supplemented with additional information. It should be noted that the list is not exhaustive, but it

includes relevant measurements available on most rigs performing conventional drilling operations, with more details provided on measurements pertinent to the application of extremum seeking. Typical sampling rates vary by supplier, with 1 Hz or more being the standard and some vendors providing rates in the range of 10 Hz for critical values such as the traveling block position [5]. The factors commonly derived from the measurements are given in parentheses:

- Hook load (WOB) – Represents the combined weight of the top drive, traveling block and the buoyant weight of the drill string submerged in mud. The measurements are commonly performed by a sensor that measure tension or displacement in the dead line [5], from which an estimate of the WOB can be produced by subtracting measured hook load from a recorded (zeroed) off-bottom rotating hook load. The WOB calculated from this method can be made inaccurate from downhole phenomena such as mechanical and hydraulic drag forces along the string and hydraulic lift force from the nozzles [6]. Surface effects related to additional length of drill pipe being subject to buoyancy as compared to when the weight was zeroed [5,6], variations in the weight exerted by the mud hose attached to the top drive and sheave friction can also affect the calculated WOB [7]. Remedial actions to correct the estimated WOB can be performed based on the models provided in [6,7]. Another approach would be to apply the proximity principle of performing measurements as close as possible to the quantity of investigation [8]. Some or all of the aforementioned sources of inaccuracy could be alleviated by performing measurements with load pins beneath the traveling block [5], placing a measurement sub beneath the top drive [9] or by utilizing direct downhole measurements [10].
- Block position (ROP, bit position and well depth) – Signifies the elevation of the traveling block above some datum such as the rig floor. This quantity is commonly estimated from the angle of the drawworks drum (as measured by an incremental encoder) and its radius, which depends on the amount of wire rope currently on the drum. The calculated position is sometimes supplemented by proximity sensors placed on the dolly guide rails. Bit and well depth are calculated from the block position and tally description. Current industry practice is to use the time derivative of the estimated block position as the ROP [11]. This will on average provide a good estimate, but in a shorter timeframe it can cause inaccuracies. Several factors should be accounted for to improve the calculated

depth and ROP from the hook position [11]: elasticity of the drill line, thermal drill string expansion, elongation of the drill string caused by gravitational pull (which varies with applied WOB and jet force at the bit), hydrostatic pressure shortening, and ballooning effects. A method for estimating ROP from noisy block measurements with a Kalman filter is described in Appendix A. This method is extended to account for drill string elasticity in Appendix B, based on the formulation in [11].

- Surface torque (torque on bit) – the rotational force required to rotate the drill string at the surface can be extracted from the variable frequency drive with dynamic accuracy of about 2% for Alternating Current (AC) machinery [5]. This is the most common motor type in top drives. For Direct Current (DC) rigs, the torque can be estimated from the current passing through a magnetic field on its way to the motor. This technique can cause significant inaccuracies if this measurement is not routinely calibrated [5]. In some optimization applications (such as in Appendix C), the bit torque is needed. The bit torque can be calculated based on the surface value from a torque and drag model utilizing the latest known rotational friction factor [12]. Still, this calculation can be erroneous if the modeled friction factor is not known exactly, and it might be necessary to include downhole sensors to obtain more accurate bit torque.
- Surface RPM (downhole RPM) – is read from the variable frequency drive on the common AC top drive systems. In cases where a rotary table is used, the measurements are usually handled by a proximity switch which counts time between revolutions [5]. On average, the downhole RPM will be equal to the top-side measurement, and the two quantities are used interchangeably. In cases where the drill string is subject to stick-slip, the downhole RPM is known to fluctuate between no rotation (full stick) and rotation at typically more than twice the surface RPM in the slip phase [13]. If a mud motor is used, the increase in downhole RPM is usually estimated from the flow rate and/or SPP.
- Standpipe Pressure – the SPP is measured from a pressure gauge located at the standpipe and represents the frictional pressure loss accumulated throughout the mud's flow path from the pump and back to the surface (assuming no backpressure is applied). Although not standardly utilized, additional information about the mud density and rheology can be extracted by placing several differential pressure transducers along the circulation path between the pump and the top drive [14].

- Pump rate – Volumetric flow rate at the pump, usually derived from counted piston strokes per unit of time. More accurate estimates of the pump rate can be obtained through accounting for fluid compressibility and pump efficiency, or through installation of additional sensors which are not standardly used and might be cost prohibitive [5].
- Casing pressure – annular pressure measured at the wellhead when the well is shut in, used for well control purposes [4].
- Mud measurements – quantities relevant for well control and monitoring are routinely measured as the mud flows through the return line (outlet), in the mud tanks/pits, and in the suction line of the pumps (inlet). At the outlet, this includes volume fraction of gas in the return flow, temperature, density (often manual), and flow rate, where the flow is usually estimated with a displacement paddle. More accurate measurements of flow rate and density are achieved on rigs utilizing equipment such as Coriolis flow meters. Mud pit fluid level and temperature are usually automatically measured, and supplemented with manual measurements of the mud's density, rheology, and gel properties performed at regular intervals [4]. At the inlet, the pit measurement is commonly employed as a proxy for temperature, and can be accompanied with flow measurements performed at the suction line [5]. A system replacing manual mud measurements with automatic ones are detailed in [15].

Deployment of any type of drilling automation system is dependent on reliably having access to some or all of the aforementioned measurements, to gauge downhole conditions and monitor the well. Data quality is therefore of high importance, and has spurred research on how to improve quality of data [16] as well as the communication protocols needed to efficiently handle the ever growing stream of measurements [17]. The advent of technologies such as wired drill pipe that can facilitate high bandwidth measurements from the subsurface is yet a valuable tool on the way to further understanding the drilling process and achieving automated operations. But still, some of the key variables such as the ROP cannot be gauged by downhole tools [11], and surface measurements remain the backbone of available information about the drilling process. The ES methods investigated in the appendices mainly requires access to commonly available surface measurements, but the availability of downhole data could in some cases make the analysis more accurate (e.g. measured downhole torque in Appendix C).

2.1.4 Controlling the WOB – autodriller functionality

There are three main variables that the driller or a control system can regulate in real-time to affect the cutting action at the bit: WOB, mud flow rate (Q) and RPM. The drillstring rotation (and resulting torque) is provided directly by the top drive. The mud flow rate is directly controlled by the pumps. The WOB, however, is controlled indirectly by a functionality commonly denoted as an autodriller (ADR). Referring back to Figure 2.1, where it is indicated that the drill pipes and part of the collars hang in tension, their buoyant weight carried by the hoisting apparatus. The neutral point in the BHA signifies the transition between tension and compression, and the (buoyant) weight of the collars below this point is what provides weight at the bit. Assuming that this situation represents a snapshot in time, the system is operating in equilibrium at some Q and RPM and with a traveling block velocity, v_{block}, which is equal to the ROP. The WOB will in this case be constant and correspond to the weight required to drill at the current ROP. If the block velocity is increased, the top of the string will transiently travel faster than the bit. This "pulse" will be sent at the speed of sound through the pipe, and shortly reach the subsurface components. If the ROP cannot promptly increase to match the new v_{block}, the neutral point will start to move upwards and additional WOB starts to accumulate. The elevated WOB will (presumably) result in higher ROP, possibly with some of the recently added weight being "drilled off", and after some time the system attains a new equilibrium where the ROP is equal to the new v_{block} at constant WOB.

The ADR seeks to leverage this relationship between v_{block} and the WOB to control the applied weight, or possibly other factors. The amount of WOB is regulated by a control system that seeks to minimize the "error" between setpoint for the WOB and the measured value, $e = WOB_{SP} - WOB_{measured}$. This is done by controlling the rate at which wire is spooled in and out of the drawworks drum, here denoted by v. Increasing the spool rate will cause the travelling block to move at higher velocity. A typical ADR uses some variant of Proportional-Integral-Derivative (PID) control on the form

$$v = K_P e + K_I \int e\, dt + K_D \dot{e}. \tag{2.1}$$

In Eq. (2.1), the "dot-accent" signifies a time derivative, and $K_{P,}$ $K_{I,}$ and K_D are tuning parameters that represent the controller's proportional, integral, and derivative gain, respectively. To intuitively understand Eq. (2.1), consider a situation where the WOB is below the setpoint, resulting in a positive e-value. The first term will increase the spool rate, v, proportionally to how far the current WOB is away from the requested value, which will increase the applied weight. The integral in the second term will continue to grow as long as the WOB is below the setpoint, resulting in larger and larger spool rates until the setpoint is achieved (eliminating any offset). The last term's function is to predict how the error is changing with time and accordingly regulate the spool rate to avoid overshooting (increasing the weight excessively above the setpoint).

This relatively simple controller can be used to track the requested WOB, or alternatively follow setpoints for differential pressure over a mud motor, torque, or the spool can be run in constant velocity mode [18]. The derivative term in Eq. (2.1) is often omitted in autodrillers, because it will exacerbate the noise present in the measured/estimated WOB [18]. The ADR performance is reliant on proper tuning of the gain parameters, which should be designed for robust behavior in different rock formations (which will alter the ROP-WOB relationship). Poor ADR tuning has been shown to produce unstable drilling and to induce stick-slip vibrations [18,19]. Rules for automatic ADR tuning is provided in [19]. It has also been pointed out that operating at the peak ROP (assuming a convex steady state ROP-WOB relationship) requires a controller that is able to balance a nonlinear system at the border between stable and unstable steady states, and more advanced control strategies might be beneficial [20].

2.2 Bit/rock interaction

Drilling is a complicated process with a multitude of factors affecting the ROP, such as personnel and rig efficiency, formation characteristics, mechanical and hydraulic factors, and drilling fluid properties [21]. These many and often interconnected effects, together with dynamics related to drillstring vibration, make accurate modeling of the drilling process a complex task. However, the general mechanics of the interaction between the bit and formation and well understood [22]. The ROP that is expected for a given WOB is largely determined by three mechanical factors: RPM, formation strength,

and bit aggressiveness. The general relationship between these factors is depicted in Figure 2.2 and is conceptually representative for both roller cone and Polycrystalline Diamond Compact (PDC) bits [22]. Figure 2.2 indicates that ROP as a function of WOB is expected to show a linear trend with a steeper slope for drilling with an aggressive bit as compared to a less aggressive bit, and the same behavior for soft rock versus hard rock and high RPM versus lower RPM. This is because the ROP is mainly a product of the Depth of Cut (DOC), as determined by the applied WOB, formation strength and bit aggressiveness, and the sliding distance of the cutters provided by the drillstring rotation. What is meant here by DOC, is the combined indentation depth from all bit cutters/teeth over some interval, e.g. one rotation of the bit. If the ROP does not respond in a straight-line trend to changes in WOB, this is caused by effects that interfere with the DOC [22].

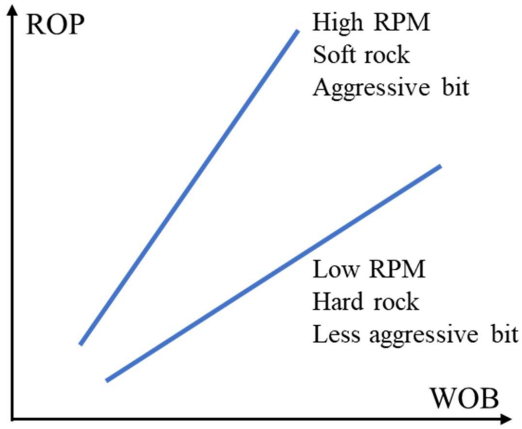

Figure 2.2 – Influence of mechanical drilling factors on ROP for an efficiently drilling bit, modified from [22].

Figure 2.3 depicts typical relationships between the ROP, WOB and RPM. The instantaneous ROP can conceptually be described by

$$ROP = f(WOB, RPM, \boldsymbol{r}), \tag{2.2}$$

where $\boldsymbol{r}$ is a vector containing all parameters other than the WOB and RPM which affect the ROP, such as flow rate, bit condition, bottomhole pressure and formation properties. The nonlinear function f is not known explicitly, but for any set of values contained in $\boldsymbol{r}$

it is expected that the ROP as a function of varying WOB or RPM (with the other variable constant) exhibits several characteristic drilling regimes. Figure 2.3a shows a nominal relationship between the ROP and the applied WOB, where it is assumed that the RPM and the factors in $\boldsymbol{r}$ are constant. The ROP-WOB relationship is characterized by three distinct phases [22-24]:

1) Inefficient drilling caused by low WOB, where the exerted weight is inadequate to obtain an acceptable DOC and the bit is not fully engaging with the formation.
2) Some threshold DOC has been achieved and the bit is fully engaged with the rock. This facilitates that all added WOB is translated to increases in ROP in a straight-line fashion at high efficiency (with a slope mainly determined by the factors in Figure 2.2).
3) At some point, effects which cause the DOC to be lower than the expected straight-line response will occur. These effects are commonly referred to as bit foundering and include inadequate cleaning at the bit and vibrations such as stick-slip or whirl.

The transition between the last two regions in Figure 2.3a is referred to as the founder point, and it is drilling at the WOB corresponding to this point (or slightly below) that is mainly desired. In this way, possible detrimental effects that cause bit foundering as well as the bit wear resulting from a large increase in WOB for a small increase in ROP can be avoided. The locations of the different phases in the ROP-WOB relationship depicted in Figure 2.3a are subject to change as parameters in $\boldsymbol{r}$ or the RPM vary, but the general shape of the three regions is expected to remain. A change in formation properties or an increase in RPM could alter the WOB at which foundering occurs, but WOB at or slightly lower than the foundering value would still correspond to the most efficient drilling and values above the foundering value would still constitute inefficient drilling. The shape of the third region depends on what type of effect is causing it. Contingent on the cause of founder, its onset could be delayed (increasing the ROP that can be achieved before foundering occurs) by manipulation of drilling parameters, e.g. increasing the flow rate if cuttings accumulation at the bit is the issue, or increasing the RPM if stick-slip is the culprit. Reengineering of the drilling equipment could also be performed to delay the onset of founder [23,25], but such considerations are beyond the scope of this thesis.

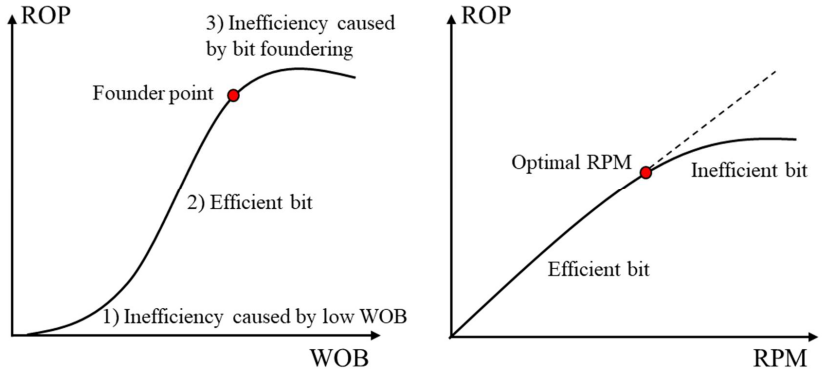

Figure 2.3 – Nominal relationships between ROP and mechanical input variables. (**a**) ROP as a function of applied WOB (at constant RPM), modified from [22,23]. (b) ROP as a function of RPM (at constant WOB), modified from [26,27].

Figure 2.3b depicts a nominal relationship between the ROP and RPM, for constant WOB and static values for the parameters in $\boldsymbol{r}$. The ROP is expected to increase linearly with increasing RPM up to some threshold value, where the efficiency declines. Typical causes of this deterioration are inadequate hole cleaning [26,27] and drillstring vibrations [22] which limit the DOC. The ROP-RPM relation in Figure 2.3b follows from the DOC concept, as the expected ROP scales linearly with the sliding distance of the bit (RPM) multiplied with the DOC. As was the case for the ROP-WOB relationship, the RPM value which marks the transition between the bit operating efficiently and inefficiently is subject to change as parameters in $\boldsymbol{r}$ vary.

The curves shown in Figure 2.3 represent typical average responses in ROP for applied WOB and RPM [22,23,26,27]. Because of vibrations and inaccurate measurements, the recorded values of e.g. ROP versus WOB during a Drill-off Test (DOT) can at first inspection look more like a cloud of datapoints than the characteristic curve shown in Figure 2.3a, but through appropriate data filtering the underlying relationship is revealed. This concept is illustrated in Figure 2.4, which shows a DOT performed on the experimental rig described in Section 3.3.3 and Appendix B. The gray datapoints represent values for instantaneous ROP and WOB recorded at a frequency of

50 Hz. The high frequency measurements capture the vibrational nature of the bit/rock interaction, resulting in scattered datapoints. Additionally, the numerical differentiation performed to calculate the ROP from positional measurements amplifies any noise in the signal. The blue dataset is generated with a moving average filter over a window of 6 seconds (300 datapoints), which reveal clear phase 1 and 2 drilling tendencies in the data. It is this average relationship that is of interest for most drilling modeling and optimization applications (including the extremum seeking approach employed in this thesis). For full-scale operations, the time or depth window needed in the analysis to obtain the "underlaying" static ROP-WOB relationship depends on factors such as measurement accuracy, absolute value of the ROP, drill string length, as well as the transients needed by the system to achieve steady state (as discussed in Section 2.1.4).

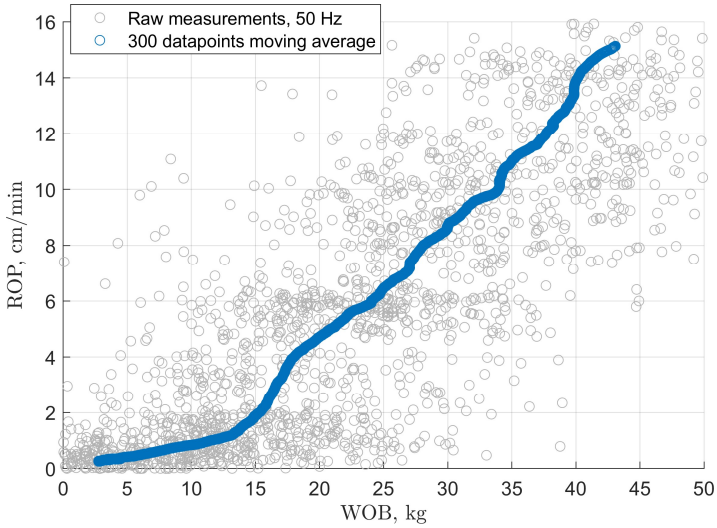

Figure 2.4 – DOT performed on experimental rig at RPM = 200.

The mud flow rate used when drilling will also impact the bit/rock interaction in several ways. A certain flow rate is needed to provide sufficient fluid velocity through the nozzles to effectively transport cuttings away from the bit. This facilitates that the bit can properly engage the formation. As ROP increases and more cuttings are produced, a higher flow rate is needed to avoid accumulation of cuttings. At the same time, higher flow rates will (to some extent) raise the bottomhole pressure. Elevated bottomhole

pressure can reduce the achieved ROP through two mechanisms; increased apparent rock strength and the chip hold-down effect [28]. The increase in apparent rock strength can be attributed to the confining pressure exerted on the formation by the mud, which can alter the failure mechanism of the rock. The chip hold-down effect stems from differential pressure between the wellbore- and pore pressure (at least in permeable formations). The dislodgement of recently cut rock is opposed by the differential pressure acting across the chip, generating the chip hold-down effect. The magnitude of these two effects depends on rock and bit properties (e.g. elevated differential pressure in low permeability rocks [29] and chip-hold down being more pronounced with drag bits [30]). However, the downhole pressure will be largely dictated by the mud density. The marginal decrease in ROP that could come about from increased flow rate through these pressure-related effects, can likely be offset by increased ROP from better hole cleaning which allows for higher WOB and RPM to be used. Additional factors to considered when determining appropriate mud flow rate are covered in Section 2.4.

2.3 Quantifying optimal drilling

Any real-time drilling optimization approach, manual or automated, needs some measure (objective function) that quantifies what constitutes optimal drilling. The driller or an automated algorithm uses this objective function to assess if the current values of WOB, RPM and possibly flow rate achieve objectives such as minimizing MSE [23], drilling cost [31], or maximizing ROP [32]. Other candidate objective formulations can include combinations of ROP and MSE, as well as additional terms to quantify detrimental effects such as stick-slip [33]. The theoretical foundation for the ROP-WOB-RPM relationships detailed in Section 2.2, dictates that the optimal operating conditions are found at the transitions between the bit operating efficiently and inefficiently. Operating at this point will result in the maximal dysfunction-free ROP, thereby achieving high drilling rates while at the same time avoiding excessive wear and tear on bit and downhole components [34].

Two objective formulations are utilized in the appendices to quantify efficient drilling conditions. In appendices A and B, the following formulation is employed to identify the optimal WOB to drill with,

$$J = ROP - \mu WOB. \tag{2.3}$$

The tuning parameter μ in Eq. (2.3) is a term which penalizes the use of excessive WOB, and was proposed in [35]. Its effect can be seen from Figure 2.5, which shows a drill-off curve generated with the drilling model detailed in appendix C, together with the objective function described by Eq. (2.3) with a μ-value of 0.001 m/hr/kg. Compared to the ROP-curve, the μ-parameter essentially shifts the extremum of the J-curve closer to the founder point. The exact behavior of this shift depends on the shape of the ROP-WOB relationship, but in general, a larger μ-value will correspond to a more conservative estimate of what the optimal WOB is. In the scenario depicted in Figure 2.5, the maximal ROP of 35.6 m/hr is found at a WOB of 16800 kg. Operating instead at the extremum dictated by Eq. (2.3) would result in a marginal decrease of 1 m/hr in ROP but drilling at 2 tonnes lower WOB, which would be beneficial for bit life. A second penalty term could be introduced to extend this methodology to also penalize excessive RPM, but this approach is not utilized in this thesis.

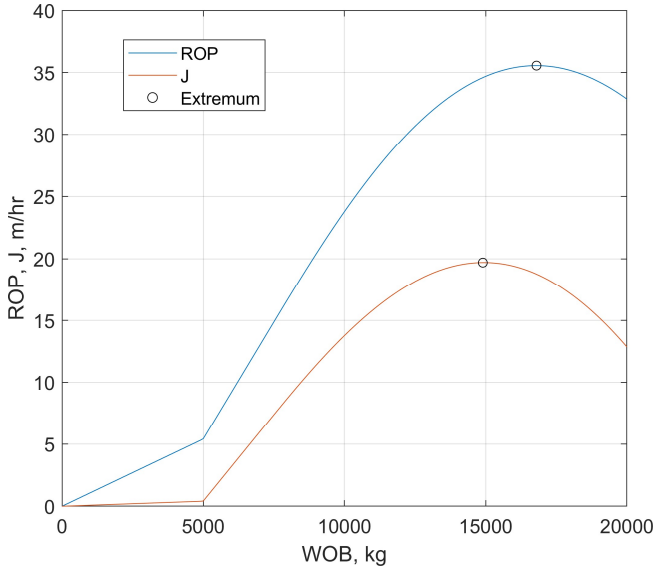

Figure 2.5 – Drill-off curve and objective function at constant RPM, with $\mu = 0.001$ m/hr/kg.

There are both pros and cons of using a formulation like Eq. (2.3) to quantify optimal drilling. On the one hand, it facilitates drilling at or closer to the founder point

than would be the case if one simply sought out maximal ROP. This behavior can extend bit life while still drilling at high ROP. On the other hand, it introduces an extra tuning parameter which has to be considered. If a gradient-based algorithm like the extremum seeking method was initiated in phase 1 drilling and a too high μ-value was utilized, it could result in the method requesting lower values of WOB rather than performing the wanted behavior of elevating the WOB in this situation. The μ-parameter can therefore in some cases dictate the ES method's domain of attraction. That is, where the algorithm can be initiated and still be able to seek out better operating conditions. For this reason, low μ-values should be used unless the driller has prior knowledge of the expected drilling conditions and is able to initiate the ES algorithm sufficiently close to the optimum.

Alternatively, a different objective function could be used. In Appendix C, the concept of MSE is utilized to identify the optimal WOB and RPM to drill with. This methodology is given in detail in the article and is not covered further here. The ROP/MSE ratio [33] could also be a potential candidate, as discussed in Section 5.2.

2.4 Drilling constraints

There are a multitude of factors that can affect the drilling efficiency. For an efficient bit that drills with the expected DOC, the ROP will increase linearly with increasing WOB and RPM, as shown in Figure 2.3, unless a dysfunction reduces the bit efficiency or a constraint limits the application of additional input energy [22,23,25]. The factors that influence ROP, and therefore to some extent the drilling efficiency, can in general be grouped into two categories [25]:

- *Bit limiters* – foundering effects that reduce the efficiency of energy transferal between the bit and the formation. Applying additional energy to the bit will in most cases result in less than proportional increases in ROP and can be damaging to the downhole equipment depending on the encountered foundering effect. A comprehensive overview of drilling dysfunctions and remedial actions that the driller can perform to mitigate them is provided in [22]. That overview includes effects related to bit and bottomhole balling, stick-slip, whirl, interfacial severity, and axial vibrations.
- *Non-bit limiters* – which constrain the amount of energy that can be applied through the controllable input variables when drilling. In the case when the input energy is

constrained before the onset of founder, the bit would still be able to drill efficiently at e.g. higher values of WOB and/or RPM, but because of a system constraint these parameters cannot be increased. One operator estimates that 60% of globally drilled footage occurs in a state where the ROP is constrained by non-bit limiters [25]. Table 2.1 gives an overview of non-bit limiters identified in the literature [23,36-39]. Some of these constraints are complex and depend on interplay between several effects. A prime example of this is in the case of a maximal ROP related to hole cleaning in deviated sections, which will be affected by the WOB and RPM which facilitate excavation at the bit. At the same time, hole cleaning can be aided by increased pump rate or drillstring rotation, which are both constrained by limiters of their own. These interconnected relationships dictate that several of the limiting factors in Table 2.1, especially those related to ROP and cuttings transport, might not be as straight-forward to implement as setting a maximal limit on the variable in question, unless a conservative value is used.

Table 2.1 – Non-bit limiters reported in the literature [23,36-39].

Parameter	Limiting property
WOB	• Allowable weight on bit or downhole tools • Available BHA weight (drill string buckling) • Maximal weight related to directional steerability
RPM	• Top drive limit (maximal RPM and maximal output power) • Allowable RPM specified by bit- or downhole motor design • RPM limit dictated by sampling rate of logging while drilling tools • Fatigue considerations in highly deviated wells drilled at low ROP • Maximal RPM related to directional steerability • Surface vibrations related to high RPM
Torque	• Drill string make-up torque • Maximal torque on bit or downhole tools • Top drive rating (maximal torque and output power)
ROP	• Cuttings concentration suspended in mud – increases fluid density which can cause high downhole pressures that exceed the fracture pressure • Formation of high cuttings bed in deviated sections – causing increased pressure, torque and drag, or ultimately a full pack-off • Directional targeting control • Solids handling capacity at surface • Limited ROP in laminated formations, to reduce bit damage from hard layers
Q	• Maximal pump pressure (dictated by the pump or other equipment) • Maximal pump flow rate capacity/available pump power • Maximal flow rate related to maintaining the annular pressure window • Minimal flow rate required to transport cuttings and clean the bit

2.5 Current state of drilling optimization

A substantial part of offshore field development costs originates from drilling, with most of these costs being related to time [1]. There is a great potential for reducing cost and environmental footprint by drilling safer, faster and with less NPT. One of the main drivers for realizing this potential is drilling automation systems, which can facilitate optimized and repeatable drilling operations. The evolution of automated and mechanized drilling, as well as the benefits brought by advancements in this field, has been traced in [40]. A timeline of breakthroughs in drilling optimization aided by rig automation systems and computerized data analytics has been detailed in [32]. The current state of drilling automation mainly consists of separate functionalities that can aid the driller by performing tasks like providing envelope control [41,42], fault detection [43,44], vibration mitigation [45,46] or selection of WOB, RPM and pump rate to drill with [37,38]. Systems that provide some or all of the aforementioned tasks in an integrated framework are also documented in the literature [47,48] and are routinely employed in the field. The focus of this thesis, and therefore of this overview section, is on methods for obtaining drilling with optimal values for WOB and RPM, and the models and techniques used to achieve this goal.

The main objective of optimizing drilling operations is to safely deliver a high-quality wellbore in a cost-effective manner [49]. In the context of real-time optimization, this is typically achieved by selecting the best suited WOB and RPM to obtain high drilling efficiency given the current downhole conditions and operational constraints. This ensures high drilling rates without excessive wear and tear on downhole components [34]. The WOB and RPM are selected for drilling optimization because they can be adjusted in real-time as the process is ongoing. A third variable, the mud flow rate, can also be adjusted in real-time to impact the drilling efficiency. Yet, because of its influence on well control, flow rate is often determined based on hole cleaning and HSE considerations rather than from the perspective of real-time optimization [39].

As detailed in Section 2.2, the task of drilling optimally (from a mechanical standpoint) consists of identifying and steering the drilling operation to the last point on the linear ROP-WOB and ROP-RPM relationships, as long as this is permissible given the constraints in Table 2.1 [23]. As downhole conditions are altered through effects such

as changes in formation, pore pressure or bit degradation, the optimal WOB and RPM combination(s) change, and the employed optimization approach must adapt to the new conditions to retain efficient drilling. The values for optimal WOB and RPM predicted by the chosen optimization routine can be displayed as suggestions for the driller, directly communicated to the rig's control system and executed with closed-loop, or some middle ground between the two [17]. The degree of human interaction in this process depends on the trust placed in the optimization system. As trust in such systems increase through field tests and demonstration of robust constraint handling, they could potentially bring about further increases in drilling efficiency by being allowed to autonomously perform optimization actions faster, as well as more frequently and precisely, than a driller would be able to. This outlook is echoed in [37], where it is stated that "The main benefits of a drilling optimization system are gained when it is integrated into a drilling control system such that the optimum decisions are automatically enforced".

The methods used for drilling optimization can broadly be grouped into classical model-based methods, data-driven methods, and hybrids between these two. The classical model-based approach uses models derived from physical principles, such as the one detailed by Detournay et al. [24], empirical correlations, as is the case in the Bourgoyne-Young (BY) model [50], or a combination of analytical and empirical terms as proposed by Warren [51]. Parameters in the chosen model is tuned to best fit relevant data from current or offset operations, and the calibrated model can subsequently be employed to predict optimal values for WOB, RPM and possibly mud flow rate. The data-driven method can in many cases be viewed as a reverse procedure of the model-based approach; where relevant data is used to construct a model, which can thereafter be used to forecast optimal values for controllable variables [52].

The classical model-based technique is well exemplified by the methods described in [32,36,38]. In [32], a multiple linear regression technique was used to fit the eight tuning parameters in the BY model to historical drilling data, and model predictions showed how the WOB and RPM could be changed to potentially drill at higher ROP. That study was performed on offline data, but the workflow was designed for real-time use [32]. In [36,38], the Detournay model was fit to recent drilling data and used for optimization of WOB and RPM. A multitude of constraints were identified and included in the model to limit the WOB and RPM suggested by the optimization routine to safe

values [36]. Field tests of this optimization system resulted in significant increases in ROP, as well as a reduction in downhole tool failures, with the largest ROP gains obtained when the system was run in closed-loop control [36]. The closed-loop results were attributed to the removal of the human element in following recommended WOB and RPM changes as frequently as the system dictated, as well as through improvements in the drilling engineering capabilities in the organization [36].

An important component in any drilling optimization approach, is determining what data should be used for model tuning (or model training, in the case of data-driven methods). For the optimization approach to be effective, the data needs to be representative of the current downhole conditions to yield accurate predictions [32,52], e.g. from the same formation and with the current state of bit wear. The dataset used for tuning/training also needs varied samples of the input variables (WOB, RPM) and the output (ROP) for any meaningful information to be extracted, a topic that is revisited later in this review.

In the optimization approach described in [36,38], a changepoint algorithm was utilized to determine what data was relevant for model tuning. A strategy based on particle filtering was proposed in [53] to tune the Detournay ROP model (with a possible inclusion of dynamic effects) to a window of recent drilling data. This statistical approach provides the advantage of quantifying the uncertainties in the modeled parameters and thus how much recommendations from the calibrated model can be trusted [53]. Using a multiple linear regression technique over a sliding window of recent measurements to tune the BY model in real-time, together with a predictive control strategy to implement optimal values for WOB and RPM, was investigated in [21]. A similar sliding window strategy was studied in [54] to tune a model combining terms from the BY and Warren ROP models for optimization purposes. It was however pointed out in that study, that the model-based approach suffers from existing models not being very accurate in predicting ROP [54]. An investigation of different ROP models fit to field data showed mixed results with some models providing good predictions in some instances, while showing poorer performance in other situations [55], which puts in question the reliability of available ROP models.

A potential drawback to the classical model-based approach is that it forces historical data to fit into the framework of a model which might not be able to accurately

describe the relation between the ROP and the input variables. This shortcoming stems from the sequentially linear and non-linear relationship in the ROP response to input WOB and RPM (as shown in Figure 2.3), which cannot be adequately captured by a closed-form model for all input values [56]. A remedy for this could be to replace or augment the classical models with data-driven models utilizing Machine Learning (ML) techniques. Studies comparing classical models and data-driven ML models have found that ML methods yielded better ROP predictions than their classical counterparts, when the same dataset was used to tune/train both approaches [52,56]. In [56], this result is largely attributed to the flexibility in the model form of ML methods, which permit segmentation of the drilling operational space to account for different phases in the ROP response. It should be pointed out that the Detournay model [24] was not amongst the classical models investigated in [52,56]. The Detournay model relies on separating the ROP response to WOB into three linear drilling phases and is therefore not subject to the closed-form model problem pointed out in [56]. This property could explain the success of the field trials of the "Detournay-based" optimization system in [36,38], as well as the choice of this particular ROP model as the foundation in other real-time optimization approaches [37,53,57]. Other classical drilling models could conceptually be employed with the same segmentation principle (using different model coefficients for different drilling phases). This could potentially increase model accuracy, but it would also complicate the tuning procedure.

Different ML methods have their distinct advantages and drawbacks [58], the interested reader is referred to the extensive reviews on ML methods and their use for drilling applications provided in [58-60]. At large, ML methods are able to account for (possibly non-linear) relations between model inputs and outputs without knowing these relationships in advance. The ML techniques also provide flexibility in the amount of input variables that are employed to provide predictions, a property which can be used to include additional information (if available) into the generated models. Selection of which inputs (features) to use in the ML model, referred to as feature engineering, can in itself be turned into an optimization problem that can be solved by combinations of drilling engineering knowledge and ML techniques [59,61]. In a review of ML methods used for ROP prediction, the authors in [59] found that the most common inputs used in ML models conform to the inputs and parameters commonly employed in the classical model-

based approach. This observation is quite intuitive since the variables and parameters in the classical models are included because of their physical influence on the drilling process.

The superior predictive capabilities of purely ML based approaches comes with some drawbacks. The unknown functional form of many ML methods makes them computationally expensive, which could preclude their use in real-time. The selection of data-driven/ML methods that can be applied in real-time is therefore a tradeoff between predictive capability and computational cost, where more advanced models will give better predictions but suffer from longer computational times and vice versa [62]. Of the 53 papers detailing ML methods for ROP prediction that were reviewed in [59], only three considered modeling while drilling. These three approaches [52,56,61] used recent drilling data (in an offline setting) to train ML models that were employed for ROP prediction, with the models being re-trained as new data "became available" in [56,61]. In [61], the ML generated model was used to simulate how WOB, RPM and mud flow rate could be optimized in real-time to improve drilling rate.

In addition to potential computational cost limitations, many ML methods also suffer from black-box properties which reduce the model's interpretability and therefore reduce trust in the model [58,63]. A potential remedy to the black-box property is to use hybrids methods that integrate both classical models and data-driven/ML algorithms for optimized solutions [58]. In [63], a hybrid method employing an ensemble of physics-based models was found to yield better ROP predictions than deterministic models alone, while retaining model interpretability. The particle filter approach to model tuning investigated in [37,53] can also be placed in the hybrid category, since it leverages a combination of statistical inference with a classical model. Other hybrid strategies employ a two-step approach [57,64]. The authors in [57] studied how to automatically minimize MSE when drilling through layered materials with a lab-scale rig. The first step consisted of using recent drilling data fit to the Detournay model to find an initial estimate of the optimal WOB. The second step was carried out by using a data-driven (golden search) algorithm while drilling, which varied the WOB in the neighborhood of the first-step estimate to identify WOB values which would further reduce the MSE [57]. In [64], an initial estimate of optimal WOB, RPM and mud flow rate was generated from a ML method trained from historical data. While drilling ahead, variations in WOB and RPM

were proposed to the driller according to a random search algorithm, to identify possible drilling conditions which would further increase ROP and reduce MSE [64].

Both data-driven and classical models need data that is representative of the current downhole conditions, as well as varied samples of the WOB and RPM (and possibly flow rate), to tune/train the models. The need for varied input samples (from drilling phases 1 – 3 in the case of WOB) can be illustrated by referring back to Figure 2.4, which shows drilling in phase 1 and 2 for ROP as a function of WOB. Any type of model fit to this dataset would not be able to predict the onset of foundering effects accurately and therefore what the optimal WOB is, without additional information (which might not be available). Performing variations in controllable variables such as WOB and RPM to gauge their effect on ROP and obtain information about the current downhole conditions and the location of the different drilling phases is perhaps the oldest form of drilling optimization. Designated testing procedures such as the drill-off test [65] and five-point test [31] have routinely been used to explore how the ROP or MSE responds to various combinations of WOB and RPM [22,23,33,66]. The prevalence of testing as a means of drilling optimization is stated in [67] as: "No credible optimization of drilling rate can be complete without some sort of drill-off testing designed to empirically test the effect of RPM, WOB, and other drilling parameters on ROP being conducted". The data collected from the designated testing procedures can be used for model tuning/training [32,62], or a "response surface" can be generated directly from the data to locate the optimal operating conditions [33]. A potential downside of the type of "one-time-testing" provided by e.g. drill-off tests is that the procedure can be time-consuming when testing a multitude of WOB and RPM combinations to find an operational sweet-spot [67]. In addition to time consumption, the results are valid only for the current downhole conditions, and as soon as conditions change the test has to be repeated.

An alternative to optimization based on pre-calculated models or on "one-time testing" are approaches employing "testing on the fly". In these approaches, the relation between the WOB and/or RPM (and possibly mud flow rate) and an objective function is explored by performing tests while drilling ahead and selecting more optimal WOB and RPM based on the obtained information. As downhole conditions change, the repeated tests can identify how e.g. WOB and RPM should be adjusted to drill more efficiently, given the new circumstances. In [48], the authors describe tests in the form of modulations

in applied WOB and RPM and observing the ROP response. The gathered information could be used to provide recommendations for the driller or for closed-loop optimization [48]. Field trials of advisory systems that can suggest variations in the applied WOB and RPM while drilling ahead to search for conditions that yield minimal MSE have been described in [68,69]. In [37], a hybrid optimization routine is detailed that provides stepwise updated setpoints (in advisory or closed-loop mode) for WOB, RPM and mud flow rate based on models continuously updated from the newly collected data. The second optimization step in the hybrid approaches [57,64] described a few paragraphs ago also employ the "testing on the fly" methodology.

In recent years, several authors have investigated a data-driven "testing on the fly" method called Extremum Seeking (ES) for drilling optimization, which is the topic of this thesis. This method has low computational cost, which makes it applicable for real-time optimization. It relies on continuous testing and optimization based on the test results and is described in detail in Section 3 as well as in the appendices. The method can briefly be explained by an example of WOB optimization: while drilling ahead, the ES algorithm continuously executes small variations in the WOB. A sliding window of recent data containing test results are used to generate a local linear model of how some objective function relates to the varied WOB. Small adjustments to the WOB are continuously performed based on the local linear model with closed-loop control, in the direction that will optimize the objective. In this way, the gradient-based search is used to iteratively drive the WOB to its optimal value where the objective is maximized (or minimized).

The ES method was first investigated for drilling purposes in [70], where it was employed to find the optimal driving frequency of an ultrasonic drilling apparatus designed for rock excavation in low-gravity environments. Later, Banks [71] investigated ES on a lab-scale drilling rig for the purpose of benchmarking drill bits. High frequency oscillations in imposed DOC was applied in to minimize an objective function related to MSE in real-time. The experiments showed that the ES algorithm was able to track operating conditions that resulted in minimal MSE drilling [71]. In [35], it was demonstrated in simulations that the ES method could be utilized to seek out WOB that resulted in drilling at the founder point in an unconstrained environment. An optimization system employing ES to optimize applied WOB and RPM was recently field tested [39]. Over a period of 2 years, the field tests resulted in ROP improvements of 7.2% and 8%

in vertical and lateral sections, respectively, with higher ROP gains obtained in the last year of the system rollout. This optimization system also includes modules for handling of dysfunction related to stick-slip, interfacial severity, downhole motor stalling and autodriller limitations [39]. It is conjectured in [72] that the improvements in ROP documented in [39] do not live up to the full potential of the ES algorithm, with a possible explanation being that the ES algorithm can "get stuck" in phase 3 drilling when encountering transient foundering effects related to bit cleaning/bit balling. However, no explicit data to back up this claim is provided in [72], and the hypothesis remains unvalidated.

2.5.1 On relating the content of this thesis to the state-of-the-art

As this overview of the state-of-the-art in drilling optimization has (hopefully) shown, research on drilling more efficiently, and therefore safer and with less environmental footprint, is a rich topic of investigation that spans a multitude of methods and approaches that each come with their potential strengths and weaknesses. The advantage of the ES method (and other "testing on the fly" techniques) is that it functions by continuously performing tests that extract information of the downhole conditions. The ES method can therefore perform optimization actions based on the most up-to-date information available. In the ES approach, the tests should be designed to not disturb the overall process, as discussed in Section 3.1.4. Drilling models (classical or ML-based) are still a valuable tool that can be combined with the ES algorithm or other "testing on the fly" methods. Models can e.g. be used to provide the initial starting point for the ES algorithm's search for optimal drilling, or the test data can be used for model tuning. These topics are discussed in Section 5, together with potential drawbacks to applying the ES algorithm for drilling optimization and how these can possibly be remedied.

Drilling optimization with the ES algorithm was chosen as the topic of this thesis because of the algorithm's proven track record from other industries, as well as beneficial properties related to the method's robustness to noise, relatively straight-forward tuning and the limited a priori knowledge of downhole conditions needed to apply the algorithm. During the period of research documented in this thesis, two independent studies were published by other groups of researchers on ES for drilling optimization, as documented in [35,39]. Although the idea of applying ES for drilling optimization is not new, the

papers constituting the core of this thesis and contained in the appendices fill a gap in the published literature. The contributions of the papers include several modifications of the classical ES method to make it more applicable to drilling and easier to tune, as well as proposals for several constraint handling techniques to ensure safe operations. Furthermore, the ES algorithm's performance is tested in a variety of scenarios in both simulations and experiments, and the papers incorporate practical aspects such as handling of the noisy conditions prevalent in drilling operations. Lastly, the papers contain tuning considerations and guidelines for applying the ES method, and all relevant details of the employed algorithm(s) are included to make the results reproducible (as opposed to the study documented in [39]).

3 Methods and materials

Section 3.1 introduces the classical Extremum Seeking (ES) algorithm and how it can be utilized to optimize a plant with limited a priori process knowledge. Then, an overview of modifications to the classical ES method that makes it more well-suited for drilling optimization, as well as different approaches for constraint handling, are detailed in Section 3.2. Lastly, the models and lab-setup used in second part of this thesis are described in Section 3.3.

3.1 The classical extremum seeking algorithm

Extremum Seeking is an adaptive control algorithm that can be employed to optimize a process in real-time. It is essentially a perturb and observe method, where the controllable input variable(s) to be optimized are systematically varied and the measured system response to these variations are used to automatically perform optimization actions. This methodology does not rely on an underlying model and has guaranteed convergence and stability under certain well-defined conditions, which makes ES a particularly useful approach for optimizing complex systems [73] such as the drilling process. Because of its relatively simple implementation, ES has previously been employed successfully in a variety of engineering systems ranging from yield optimization in bioprocesses to jet engine stability control and many others [73,74]. The ES methodology has also been studied for petroleum applications such as optimization of injection rates in gas lifted wells [75,76] and optimal injection of dilutants in oil-producers [77], in addition to selection of WOB [35,78,79], WOB and RPM combinations [39,80] and traveling block velocity [71] to drill more optimally.

The ES algorithm is a gradient ascent (or descent) method which requires a process with well-defined steady-state characteristics, so that for a given constant input, the system settles to a constant output within a reasonable time frame. It also needs the existence of a unique extremum in the measured output, which corresponds to some value in the input variable(s) within the operational envelope (if operating at the extremum is to be achieved). These conditions will be briefly elaborated on in the following. For a more comprehensive review of ES stability, convergence and underlying assumptions,

the interested reader is referred to [74,81] and the references therein. It should also be noted that with ES being a gradient based method, it is inherently a local optimizer. This implies that the starting point where the ES algorithm is initiated will determine which optima is sought out by the algorithm if several extremal points are present in the static map to be optimized. However, for drilling applications, as explained in Section 2.2, it is expected that there exists a unique optimum or an optimal region to operate in which the ES algorithm can be used to seek out. Care should still be taken to initialize the ES algorithm as close as possible to the optimal point, if prior process information is available to facilitate this, as this will make the method converge faster to the optimal region.

The ES method provides a whole range of algorithms and tools available for various applications, starting with the fundamental ES controllers described in e.g. [73,74,81]. The overview given here generally traces a combination of the algorithm explanations provided in [73] and [74]. In the following, a single variable version of the classical ES algorithm is explored for a generic drilling example where some objective function related to the drilling efficiency, J, is to be maximized. The same analysis can with minor modifications be adjusted to account for multiple manipulated input variables. A block diagram of the classical filter-based ES algorithm is shown in Figure 3.1, where the Laplace variable, s, in the adaptation block represents integral action. Let the manipulated input variable be denoted by u, which for this example could signify the WOB (although the same logic could be applied with the RPM). It is assumed that the measured process output represents a static map dependent on the input, $J = J(u)$. This assumption will be revisited in Section 3.1.4.

The overall goal of the ES algorithm is to perturb the input, u, measure how this affects the objective, J, and automatically implement how u should be adjusted based on the extracted information. This process can be split into three main components:

- *The excitation signal*, which introduces a variation in the input of the system.
- *Gradient estimation,* used to quantify how the system reacts to the excitation.
- *Adaptation,* which adjusts the input variable based on the estimated gradient.

The role of these components and how they interact can be explained by performing a loop through the block diagram in Figure 3.1, representing a single iteration of the ES algorithm.

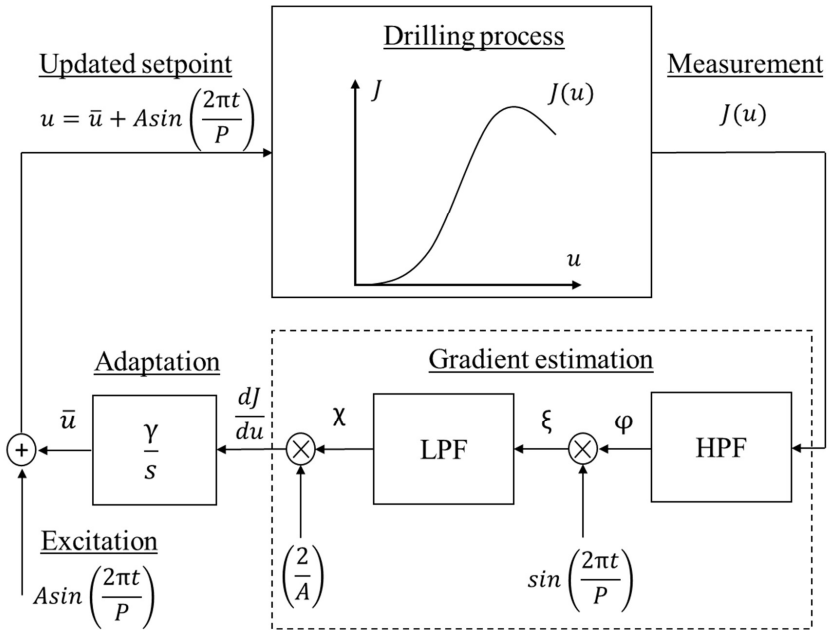

Figure 3.1 – The classical extremum seeking algorithm.

3.1.1 The excitation signal

Starting out in the lower left corner of Figure 3.1, drilling is commenced at an initial guess of the optimal input value, $\bar{u}$. While drilling ahead, the input is perturbed by a sinusoidal oscillation around this best guess value, by sending updated setpoints for u to the control system on the rig according to

$$u(t) = \bar{u}(t) + Asin\left(\frac{2\pi t}{P}\right). \tag{3.1}$$

In Eq. (3.1), A and P are the amplitude and period of the excitation signal, respectively. How the drilling process responds to this perturbation is captured by real-time measurements of the objective function, J, and passed over to the gradient estimation scheme.

3.1.2 Gradient estimation

The recorded values of the objective function are passed through several filters and a correlation block, to extract a local linear model of $J(u)$ from the processed signal. This procedure is based on the assumption that the measured values of the objective function can be described by a first order Taylor expansion around the (approximately) stationary point, $\bar{u}$,

$$J(u) = J\left(\bar{u}(t) + Asin\left(\frac{2\pi t}{P}\right)\right) = J(\bar{u}) + \left.\frac{dJ}{du}\right|_{u=\bar{u}} Asin\left(\frac{2\pi t}{P}\right) + O(A^2). \tag{3.2}$$

Further assuming that the amplitude is relatively small and/or that the underlying static map is quite linear inside the investigated region (which has been explored by the input excitation), the error term, O, can reasonably be neglected. The signal approximated by Eq. (3.2) is subsequently sent through a High Pass Filter (HPF) designed to allow the excitation frequency to pass while attenuating the static component, $J(\bar{u})$. The resulting signal can be expressed as

$$\varphi \approx \left.\frac{dJ}{du}\right|_{u=\bar{u}} Asin\left(\frac{2\pi t}{P}\right). \tag{3.3}$$

The filtered signal, φ, is subsequently multiplied with a sinusoidal term with the same period as the perturbation. This is done to correlate any changes in J with the corresponding variation in the input signal, e.g. if an increase in J correlates with an increase in u. An underlying assumption in this correlation procedure is that the variable u follows the prescribed sinusoidal excitation. The resulting signal, ξ, can be expressed with the aid of a trigonometric identity as

$$\xi \approx \left.\frac{dJ}{du}\right|_{u=\bar{u}} Asin^2\left(\frac{2\pi t}{P}\right) = \left.\frac{dJ}{du}\right|_{u=\bar{u}} \frac{A}{2}\left(1 - \cos\left(\frac{4\pi t}{P}\right)\right). \tag{3.4}$$

Processing ξ with a Low Pass Filter (LPF) tuned to diminish the oscillatory component of Eq. (3.4), the attenuated signal can be approximated by

$$\chi \approx \left.\frac{dJ}{du}\right|_{u=\bar{u}} \frac{A}{2}. \tag{3.5}$$

The final step is composed of multiplying the signal described by Eq. (3.5) with a factor equal to $2/A$, to obtain an estimate of the sought gradient.

3.1.3 Adaptation

The calculated gradient is used by the ES method to determine the direction and magnitude which the base value, $\bar{u}$, should be adjusted to increase the objective function. This is done by passing the signal through an integration block, which calculates an updated $\bar{u}$-value from

$$\dot{\bar{u}} = \gamma \frac{dJ}{du}\Big|_{u=\bar{u}}. \tag{3.6}$$

In Eq. (3.6), γ is the adaptation gain, which is a tuning parameter that determines the learning dynamics of the algorithm. That is, how fast the ES scheme should vary $\bar{u}$ as a response to the estimated gradient. If e.g. a large positive gradient is estimated, this is interpreted by the algorithm as a situation where there is a substantial potential for improvement which can be obtained by increasing the input, and the input should be adjusted accordingly. For a given γ-value, the incremental change in $\bar{u}$ will be proportional to the gradient, scaling the step size to the improvement potential recognized by the algorithm. The updated $\bar{u}$-value found from Eq. (3.6) is subsequently used as the starting point for a new iteration of the ES algorithm. Repeating this process will incrementally drive the input towards its optimal value.

3.1.4 Time scales and tuning considerations

The ES scheme outlined in the previous section relies on the assumption that there is an underlying static relationship, $J(u)$, which can be locally mapped by the excited input signal. In drilling, this static map is in practice dependent on multiple properties such as the characteristics of the formation being drilled and the current state of bit wear. The governing function could therefore more correctly be expressed as $J(u, \boldsymbol{r})$, where $\boldsymbol{r}$ is a vector containing all relevant parameters and properties that affect the process, other than the actuation signal u. An underlying assumption in the ES scheme is that the parameters contained in $\boldsymbol{r}$ are constant (within the relevant time frame) or slowly varying

compared to the time scale of the algorithm's learning dynamics. From this vantage point, the objective is only dependent on the manipulated variable, u.

Most processes, including drilling, will have dynamic periods where e.g. a variation in u (WOB or RPM) will not immediately be translated to a measurable variation in J (ROP or MSE). In extremum seeking, process dynamics as well as slow process variations are handled by the principle of time scale separation. There are three relevant time scales involved in the ES method: fast, intermediate, and slow. What constitutes e.g. fast or slow dynamics is relative and depends on ES tuning and on the dynamics of the process being optimized. For drilling applications, the time scales can be summarized as:

- *Fast* – system dynamics. This time scale represents transient behavior experienced when changing the WOB and/or RPM. The rig's control system will need some time to attain the updated setpoint, and the measured system response (often related to the ROP) will need additional time to settle to a measurable, stable value which can be related to the updated WOB and/or RPM.
- *Intermediate* – the excitation signal period. The periodic excitations in WOB and/or RPM are required to be slow enough so that the system dynamics are negligible compared to the variations in the process inputs. This allows the ES algorithm to "see" the static map, $J(u)$, without too much interference from process dynamics. The amount of measurement noise can also dictate the extent of the intermediate time scale, as longer excitation periods might be needed to obtain valid measurements of the objective.
- *Slow* – learning dynamics. The adaptation in $\bar{u}$ has to be slow compared to the intermediate time scale to extract meaningful derivative estimates. This property can be deduced from the approximation detailed in Eq. (3.2) and the subsequent signal processing, which relies on $\bar{u}$ being a fixed quantity and the excitation signal varying u around this point. At the same time, the learning dynamics need to happen fast enough with respect to process disturbances, be they abrupt (e.g. the time between changes in drilled formation) or gradual (e.g. from bit degradation), for the ES method to successfully adapt to changes in the underlaying static map, $J(u)$.

The main task when tuning the single-variable classical ES algorithm consists of finding suitable values for five parameters that will make the method adhere to the time

scale separation principles described above. At the same time, a well-tuned ES algorithm strives to converge to the optimum as rapidly as is practically possible, which is a competing interest when considering the slow adaptation required to separate the intermediate and slow time scales. As is common in optimization, simultaneously achieving these objectives might not be feasible, and requires a weigh-off between fast algorithm performance and robustness. In the following, some general tuning considerations for applying ES for real-time drilling optimization are given. Tuning guidelines for the multivariable case are covered in Appendix C. See also [82] for a general discussion on tuning of the classical single-variable ES algorithm.

The relevant tuning parameters are the adaptation gain, γ, the amplitude and period of the excitation signal, A and P, as well as one or more tuning parameter for each of the filters. Optimizing multiple inputs simultaneously will scale up the amount of required tuning parameters, but the guidelines given below will still be relevant:

- *The excitation amplitude's* main task is to elicit a measurable response in the output, J, for gradient estimation. To accomplish this, the amplitude needs to be large enough to obtain a good Signal to Noise Ratio (SNR), as well as be large enough to be realized within the resolution of the control system on the rig. At the same time, the amplitude should not be too large, as this can disturb the overall process and cause the estimated gradient to be inaccurate, as seen in the error term in Eq. (3.2). Recommended values for amplitudes in the WOB signal will typically lie in the interval 200 – 500 kg, and for the RPM in the interval 2 – 5 rpm. Determining amplitude values also depends on the chosen objective function, as well as engineering knowledge of e.g. the expected WOB to be used in the current section. An amplitude of 500 kg might be excessive for a formation expected to be drilled with WOB around 5 tonnes, but suitable for a non-responsive formation to be drilled with weights around 15 tonnes.
- *The excitation period's* lower bound is dictated by separation between the fast and intermediate time scales and is largely determined by a combination of the system dynamics and measurement resolution. In general, the period should be selected as low as possible while still allowing for the system dynamics to be neglectable [83] and retaining an acceptable SNR. Longer periods necessarily include more data in the gradient estimation, which increases the SNR. At the same time, an excessive period will make

the algorithm less responsive to changes in $J(u)$, which would increase the algorithm's response time to e.g. a change in formation. Long wells with complex geometries and the responsiveness of the rig's control system might also dictate that longer periods be used, as they could induce longer transients in the system's response to excitations. An additional effect to consider for the WOB excitation period, is that of induced stick-slip. As reported in [18], any significant WOB variation can cause enough torque variation to induce stick-slip vibrations. This problem can arise if the WOB is varied at a frequency close to the drill string's natural torsional frequency, which typically corresponds to a period of 3 – 20 seconds dependent on drill string length and design [18]. Instigation of stick-slip should therefore be avoided by keeping the WOB excitation period well outside of this interval, together with moderate amplitude values which will reduce torque oscillations. Based on these considerations, recommended period values lie in the interval 1 – 4 minutes.

- *The adaptation gain* is an important tuning parameter, which determines how rapidly the controlled input, u, is allowed to adapt as a response to the estimated gradient. The selection of γ-value is a weigh-off between speed of convergence and robustness. Overly large γ will make the algorithm susceptible to noise and disturbances, since the algorithm will respond to these disruptions by aggressively making changes to u. Additionally, large γ-values might fail to uphold the time scale separation principle, which could result in the entire feedback loop becoming unstable [82]. This time scale separation issue can be mediated by utilizing a Least-Squares (LS) method for gradient estimation [84], as will be elaborated on in Section 3.2.2. HSE considerations dictate that ES algorithms used for drilling optimization should avoid too aggressive tuning, in addition to being used in conjunction with robust constraint handling techniques.
- *Filter parameters* refers in the classical ES algorithm to the time constant in the HPF and LPF in Figure 3.1, which dictates which signal frequencies are allowed to pass and which frequencies are attenuated. The ideal signal processing described in Eqs. (3.3) and (3.5) cannot be fully realized, but the filters should be designed to retain as much of the sought signal while attenuating the "unwanted" components. The classical extremum seeking method is commonly studied through average analysis, where it can be shown that the algorithm performs as it should as long as the filters on average are able to extract

a good estimate of the gradient [74]. For single variable drilling optimization, the authors in [35] recommend a time constant equal to the excitation period in the HPF and a time constant of 3 times the excitation period in the LPF.

3.2 Customizing the extremum seeking algorithm for drilling

The purpose of this section is to give a description of and motivation for the modifications to the classical ES algorithm that are utilized in the second part of this thesis. These modifications are comprised of altering the shape of the excitation signal, using a least-squares method to estimate the gradient as well as the inclusion of several constraint handling techniques in the algorithm. There are many variants of the ES method with different algorithms and tools which can make it better suited for a given application. Tan et al. [74] broadly splits the ES methods into two categories: 1) gradient based ES techniques utilizing a continuous excitation signal, and 2) ES algorithms that use a (repeated) series of probing inputs, that exploit ideas and recipes from numerical optimization methods. The focus of this thesis is on a variant from the former category, based on the classical ES approach detailed in Section 3.1.

Within gradient based ES methods, there are many changes to the classical scheme (as depicted in Fig. 3.1) proposed in the literature. A phase shift can be included in the correlation signal, to account for known delays caused by system dynamics or the HPF [81]. The HPF can be replaced with a band pass filter to attenuate high frequency noise [85]. One can remove the HPF [82] or both filters, at the possible expense of algorithm performance [74]. Second order derivatives can be included in the analysis to potentially increase convergence speed over curved static maps [86]. Augmenting the integral action in the adaptation block with proportional action can speed up algorithm convergence, if the objective gradient can be directly measured [87]. Sliding mode control has been employed in ES to smoothen the adaptation rate in u [88], a topic which is further explored in Appendix C. Known process dynamics can be used to abolish the need for time scale separation between the fast and intermediate scales [89]. Replacing the filter-based gradient estimation with a Least-Squares method removes the requirement of separating the intermediate and slow time scales [84], and can in some cases alleviate the need for the excitation signal altogether [90]. A variant of the LS gradient estimation

technique is described in Section 3.2.2. The shape of the excitation signal can also play a vital role in the performance of the ES algorithm [91], which brings us to the first modification made to the classical ES method in our work.

3.2.1 A square wave excitation signal

Tan, Nešić and Mareels [91] studied different excitation signal shapes and found that for a given adaptation gain and amplitude, a square wave signal improved the convergence rate of the ES algorithm. This result can be intuitively understood by performing a loop through the ES scheme in Figure 3.1 with an excitation signal on the form

$$u(t) = \bar{u}(t) + A \cdot sgn\left(sin\left(\frac{2\pi t}{P}\right)\right). \tag{3.7}$$

In Eq. (3.7), sgn is the signum function which takes on a value of 1 when the argument is positive, a value of 0 when the argument is zero and a value of -1 when the argument is negative. Repeating the analysis in Section 3.1 with the square wave signal, which has twice the signal power of the sinusoidal shape [91], the resulting version of Eq. (3.5) would appear without the factor $1/2$, causing adaptation proportional to twice the value of the estimated gradient. This property in itself bears limited practical consequence, as one could simply double the adaptation gain with a sinusoidal dither and obtain similar convergence properties. However, when the measured values of J are noisy, as is the case for drilling optimization, the increased signal power of the square wave will increase the SNR (assuming that the noise is additive). For a given amplitude, this translates to the maximal SNR that can be obtained, from which a more accurate estimate of the objective gradient can be calculated.

The main advantage of the square wave excitation signal as compared to the sinusoidal shape, is that the sinusoidal excitation requires about 40% larger amplitude to obtain the same signal power as the square signal. This is relevant because the amplitude should be designed to not disturb the overall process, as discussed in Section 3.1.4, which can be achieved by selecting a square wave and a smaller amplitude without losing information from the signal. However, the discrete nature of the square wave in the "transition periods" when the signum function changes sign will cause transients in the

applied input, as the rig's control system strives to follow the changed setpoint. These transients can inherently be handled by replacing the filter-based gradient estimation with a least-squares technique, which uses measurements of the applied input rather than assuming that the input follows the provided setpoint. The data stemming from these transients will not necessarily correspond to the underlaying static map, $J(u)$, but the symmetry of the excitation will cause most of the transient effects to cancel out. Still, models can be used to account for transient effects such as drill string elongation when the WOB is altered (as is done in Appendix B), to make the analysis more accurate.

3.2.2 Least-squares gradient estimation

One of the main limitations of the ES technique is the need for time scale separation, which can cause prohibitively slow convergence of the method [84,89]. For the drilling process with its slow dynamics, time scale separation necessitates long excitation periods and consequently low adaptation gain. In this case, the optimal WOB and/or RPM sought by the ES algorithm can likely change (e.g. through a change in lithology) before the optimum can be achieved, causing the ES algorithm to constantly chase elusive optimal operating conditions.

Chioua et al. [84] evaluated ES with a recursive least-squares method for gradient estimation and found that this technique allows for more aggressive tuning of the adaptation gain and faster convergence. This result stems from the LS gradient estimation not requiring the base value, $\bar{u}$, to be approximately constant, which relaxes the need for separation between the intermediate and slow time scales. Figure 3.2 depicts the customized ES algorithm used in the appendices, where the ongoing drilling process is perturbed by square wave oscillations in the input. The most recent measurements of the objective function and the input are stored in buffers containing one period of the excitation signal, P. These buffers are used to estimate the gradient from

$$\int_{t-P}^{t} \big(J(\tau) - (au(\tau) + b)\big)^2 \mathrm{d}\tau \rightarrow \min_{a,b}, \tag{3.8}$$

$$\left.\frac{\partial J}{\partial u}\right|_{u=\bar{u}} \approx \mathrm{a}. \tag{3.9}$$

In Eq. (3.8), a and b are the least-squares slope and intercept, respectively. The slope parameter is used as an estimated gradient of the objective function. As seen from Figure 3.2, the estimated gradient is passed to the adaptation block to update the input base value and a new setpoint for u is provided by adding the square wave excitation. As new measurements of J and u become available, the new measurements are incorporated in the analysis and the oldest measurements contained in the buffers are discarded. The formulation in Eq. (3.8) is based on the technique proposed in [90], where a fixed window of historical data was used to estimate the gradient, as opposed to the forgetting factor used to limit the amount of evaluated data in [84]. In our approach, only the minimal amount of data needed to evaluate the gradient, one period of the excitation signal, is utilized in the algorithm. This LS formulation results in only three tuning parameters needed to employ (the unconstrained version of) our method: the amplitude and period of the excitation, as well as the adaptation gain.

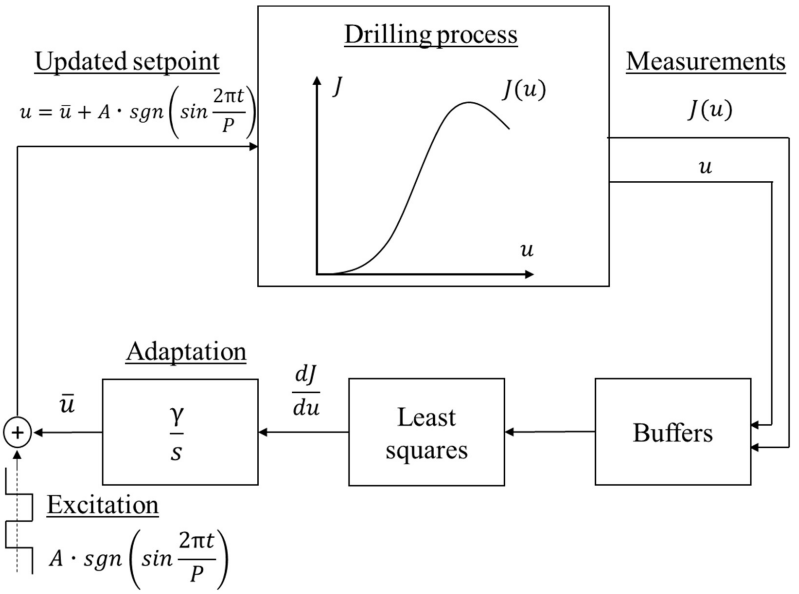

Figure 3.2 – Extremum seeking scheme with least-squares gradient estimation.

In drilling, the WOB and RPM enacted by the rig's control system might deviate from their requested setpoints, see e.g. [39]. Apart from the aforementioned advantages, a benefit of the LS method is that this technique uses actual measurements of the process input, rather than assuming that the input follows the prescribed setpoints. This makes the LS method account for divergence from the setpoints in the analysis, resulting in more representative gradient estimates. For the multivariable ES case, the LS method also has beneficial properties when it comes to estimating e.g. a gradient related to WOB while the RPM is varied. This property is explored in Appendix C.

Zengin and Fidan [92] compared the classical filter-based ES scheme to a recursive LS method and found that in addition to faster convergence, the LS method also showed beneficial properties with respect to handling measurement noise. The LS technique for gradient estimation is robust to noise and sensor bias, since much of the noise is filtered out over the least-squares window, and any sensor bias is captured by the b-parameter (which is not used by the algorithm). Furthermore, the integral action in the adaptation block acts as a LPF to limit abrupt variations in the adaptation rate. However, since the measurements on the rig are notoriously noisy, it can still be beneficial to filter the data before it is used for gradient estimation. If filtering is performed, all relevant data should be processed with filters that result in an equal time delay. This will synchronize the data so that e.g. a given WOB measurement will be correlated with the corresponding ROP response. This technique is discussed in Appendix B, where a Kalman Filter (KF) is used to estimate the instantaneous ROP from noisy block measurements, and a LPF is used to remove excessive WOB measurement noise.

3.2.3 Constraint handling

An important component of a practically relevant optimization method is handling of operational constraints. Since the ES method inherently needs full control over e.g. the WOB while drilling, it is integral that the algorithm does not steer the WOB to values which violate process limitations. A distinction can be made between constraints that are known a-priori and constraints related to process output values that are not known in advance. In the former category, a maximal WOB associated with e.g. a buckling criterion can be enforced by rejecting adaptation proposed by the algorithm past a certain WOB value with a logic criterion such as: $if\ (\overline{WOB} + A + SafetyFactor) \geq WOB_{limit}$,

$disallow\ \dot{WOB} > 0$. Similar logic could be used to compel the algorithm to avoid high RPM values associated with e.g. top-side vibrations.

In the latter category, where a process output, e.g. a maximal ROP related to hole cleaning should not be exceeded, the WOB and RPM that produce too high ROP is not known in advance and a different approach is needed. In the second part of this thesis, three strategies for this type of output constraint handling in combination with the ES algorithm are investigated and explained in detail. A presentation of these strategies and their rationale is also given in the following. The techniques are exemplified for cases of limiting ROP and torque values, but the methods are generic and could be used to account for other process limitations as well, given certain assumptions.

The modified objective function approach

This is the type of constraint handling often employed in ES algorithms, see e.g. [93-95], and involves including a barrier term in the objective function. The barrier term will be zero if the constraint is not violated, and conversely take on non-zero increasing values if a process output exceeds a certain limit (in the case of a minimization problem, such as finding the minimal MSE to drill with. In a maximization problem, the barrier term will necessarily make the objective decrease). This functionality disincentivizes the ES scheme from making further adjustments in the direction which makes the modified objective function grow. In Appendix C, rather than minimizing the MSE, the following function is used to quantify optimal conditions that avoid drilling with too high ROP:

$$J = MSE \cdot \left(1 + \rho \frac{\max(0, ROP - ROP_{limit})}{ROP_{limit}}\right) \tag{3.10}$$

In Eq. (3.10), max is a function which outputs the largest of the input arguments and ρ is a tuning parameter that determines how much the function increases when drilling with ROP higher than the allowable value. A formulation similar to Eq. (3.10) has previously been used to quantify drilling with stick-slip in a drilling surveillance system [33].

Different constraining parameters can be additively included in Eq. (3.10), in a similar fashion as the ROP term, to penalize the presence of e.g. measured vibrations or high torque, which makes the technique very versatile. In appendix C, this constraint handling method is used in combination with a saturation function which limits the

allowable adaptation in the inputs, to ensure slow and steady behavior. A downside of this approach is that if a sudden change in operating conditions, e.g. entering a more drillable formation, makes the ROP increase by some margin above the threshold, the time it takes for the ES algorithm to steer the applied WOB and/or RPM to better values is dictated by the rather slow adaptation rate of the algorithm. A more prudent approach would then be to employ a separate control loop with the ability to modify the inputs more rapidly.

Reactive constraint handling

To be able to swiftly reduce e.g. the applied WOB if the measured torque is suddenly above its permissible value, a reactive control loop was introduced in the ES scheme. This technique could also be used on other limiting parameters, if they satisfy the premise that the constrained output is correlated (in known direction) with the adjusted input variable. Another possible use of this technique could be for observed stick-slip vibrations which would be met with a reduction in WOB (or through minor modifications of the method, an increase in RPM or a combination of the two)

This method relies on a penalty variable which is zero when the constraint is not violated, and proportional to the amount of violation if the limit has been exceeded. If the torque is deemed too high, a PI controller with the penalty variable as input is used to reduce the applied WOB until the torque is again within permissible bounds, at which point the integral term in the controller is reset to "forget" any previous torque-transgressions. The rationale behind this method is that it allows faster adjustment of the WOB than would be enacted by a robustly tuned ES algorithm through the adaptation block. It can be argued that constraint handling through the modified objective function, with a high ρ-value, could obtain similarly rapid adjustments in the WOB. However, use of Eq. (3.10) relies on an estimated gradient. If the high torque values arose from e.g. a change in lithology at a time when the excitation signal was in a "low position", this could lead the ES algorithm to relate low WOB with high torque (for a limited time). This would result in increasing WOB for some time (when a reduction was needed) before more data became available for analysis. This behavior is avoided with the reactive constraint handling technique and justifies its use. It can be noted that as the name implies, this method is only able to adjust the WOB to lower the torque after some limit has been

violated. This necessitates that a threshold lower than the system's actual limitation is used.

Predictive constraint handling

The changes in the drilling process caused by varying the WOB and RPM can be a good source of information about the current system conditions and how other drilling parameters are affected by the varying inputs. The same LS methodology that was used in Eqs. (3.8) and (3.9) can also be utilized to extract a gradient of other drilling parameters and how they vary in relation to the excited inputs. Using again the example of a limiting torque value, a gradient of $\partial \mathrm{T}/dWOB$ can be calculated from the past P seconds of drilling data. This estimate is used to predict how the torque will vary if the WOB is increased further, and to stop WOB-adaptation if operations are sufficiently close to the limiting torque value, according to

$$\gamma = \begin{cases} \gamma, & if\ \left(T_{avg} + A\frac{\partial \mathrm{T}}{\partial \mathrm{WOB}}SF\right) < T_{limit} \\ 0, & if\ \left(T_{avg} + A\frac{\partial \mathrm{T}}{\partial \mathrm{WOB}}SF\right) \geq T_{limit}\ and\ \frac{\partial \mathrm{J}}{dWOB} > 0 \end{cases}. \tag{3.11}$$

In Eq. (3.11), T_{avg} is the average torque value from the past P seconds and SF is a safety factor with a value greater than one. The product $A \cdot dT/dWOB$ is a projection of how much the torque will grow if the WOB is increased by A kg. By setting SF to a value of e.g. 3, Eq. (3.11) seeks to stop adaptation if the $\overline{WOB}$-value is $3A$ kg away from the critical WOB which would make the torque exceed its limit. This allows the ES algorithm to continue performing excitations without violating the torque-restriction, as well as allowing for some error in the estimated torque gradient. The positive objective gradient condition in Eq. (3.11) is included to avoid a situation where the ES algorithm wants to reduce the WOB to drill more efficiently but is precluded from doing so because it is currently close to the maximal allowable torque.

The formulation in Eq. (3.11) relies on three assumptions: 1) that T_{avg} approximately represents the torque when drilling with a weight of $\overline{WOB}$ kg, which is close to the average weight during the past P seconds. 2) That the torque is mainly a (positively correlated) function of WOB, as is commonly assumed in the literature

[24,96]. 3) that the algorithm is initiated at conditions where the constraint is not violated, since the method is only able to stop adaptation, not navigate away from detrimental conditions. For this reason, the predictive method should be used in combination with the reactive technique. The first assumption essentially reintroduces the need for separation between the slow and intermediate time scales, since it requires relatively slow adaptation to be valid. This problem is mediated by introducing the safety factor, which can make the adaptation stop before the constraint is violated even when more aggressive gain is used and assumption 1 is not completely satisfied.

3.3 Drilling models and experimental setup

In the appendices, the ES algorithm is studied in three different simulation/experimental settings to investigate the method's applicability to drilling optimization. Section 3.3.1 gives a brief introduction to OpenLab, a high-fidelity drilling simulator employed in Articles 1 and 2. In Section 3.3.2, a qualitative drilling model developed by the authors for use in Article 3 is described. The experimental setup utilized in Article 2 is detailed in Section 3.3.3.

3.3.1 OpenLab

OpenLab is a high-fidelity drilling simulator developed by the Norwegian Research Centre (NORCE) in collaboration with the University of Stavanger. The simulator consists of a set of integrated numerical models covering different aspects of the drilling process, including torque and drag effects, cuttings transport, multi-phase flow and heat transfer [97]. This simulator has since 2017 been available to the public, with the stated purpose of facilitating and accelerating development and testing of real-time drilling automation systems [98], which makes it an excellent environment for testing and qualifying the ES algorithm in realistic scenarios.

Simulations in OpenLab are performed by first defining a configuration, where the designer can specify properties such as well-path, hole sections and casing program, the drilling fluid program, drillstring components, drilling window in terms of pore and fracture pressures, formation strength(s) as well as the top-side equipment used. From a defined configuration, the models on the OpenLab platform are run by supplying the

simulator with setpoints for input variables such as the desired flow rate, RPM and WOB (or hook velocity, when run in ROP-mode). The setpoints are translated to actions on the drill-floor with built in functionalities which simulates the actuation of the relevant rig equipment [99,100]. The proposed optimization method was investigated in simulations run through a Matlab client. Figure 3.3 shows a typical OpenLab desktop for a sample simulation of single variable ES applied to find the optimal WOB to drill with.

Although OpenLab provides a high-fidelity environment to test automated optimization routines, one weakness of this simulation platform must be pointed out. The location of the founder point, as a function of WOB and RPM, is in the current OpenLab version hardcoded. This means that e.g. in a scenario where one drills into a new formation, the optimal WOB and RPM stays fixed, which is not what is expected from drilling theory (see Section 2.2). One of the most beneficial properties of the ES algorithm is that it can track optimal operating conditions as they change (if they do not change too frequently or quickly). To be able to study this property, the authors developed a drilling model which qualitatively accounts for drilling dysfunctions and allows for a study of the ES algorithm in scenarios where the optimal operating conditions change.

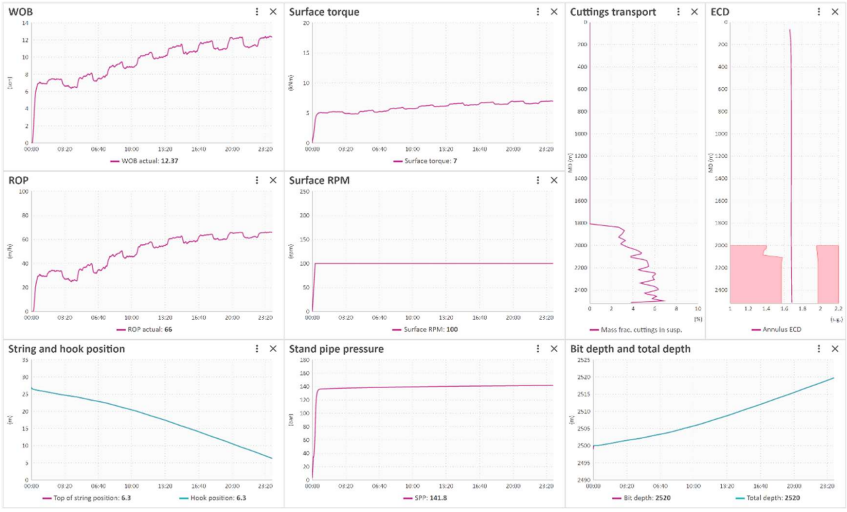

Figure 3.3 – Sample simulation of single variable extremum seeking in OpenLab.

3.3.2 A qualitative drilling model

The theoretical foundation for the qualitative drilling model, henceforth referred to as the *extended model*, is detailed in Appendix C, and briefly summarized here. The extended model utilizes as a "base model" the rate-independent interface laws proposed by Detournay et al. [24], which define static relationships between the WOB, RPM, bit Torque and ROP from bit and formation properties. It is expected that for a given BHA configuration drilling through some rock formation, that certain combinations of WOB and RPM can result in detrimental dysfunctions such as stick-slip or whirl. The locations of these dysfunction zones in the WOB-RPM plane are heavily affected by bit and BHA characteristics, as well as mechanical rock properties [101].

To account for these phenomena in a qualitative way, the extended model utilizes a penalty function which reduces the modeled ROP when drilling with WOB/RPM combinations in zones that are being affected by dysfunctions (as defined by the user prior to simulations). The penalty functionality is set up to reduce the ROP as a function of how far into the dysfunction region the operating point is. In this way, drilling "further into" any of the deleterious regions (as seen by moving outwards from the green region in Figure 3.4) will result in a penalized ROP output that deviates further and further from the expected straight-line behavior predicted by the Detournay model. The methodology is illustrated in Figures 3.4 and 3.5. Figure 3.4 shows contours of the (dysfunction-free) ROP response calculated from the Detournay model for combinations of WOB and RPM, as well as generically placed zones that are affected by dysfunctions (based on the dysfunction zone placements in [38,101,102]). Because the Detournay model does not explicitly account for deviations from phase II drilling, the ROP is seen to monotonically increase for all values of applied WOB and RPM.

Figure 3.5 depicts the ROP calculated from the extended model after ROP reductions have been imposed on drilling in the dysfunction zones, for the same scenario as in Figure 3.4. In Figure 3.5, the ROP now resembles a hill where there is a region of WOB/RPM combinations that result in maximal ROP, resembling the "heatmaps" generated from field data in [33]. It can be noted from Figures 3.4 and 3.5 that the regions which are not affected by the dysfunctions are identical (e.g. the shaded region in Figure 3.4), since the Detournay-modeled ROP is used in both these cases.

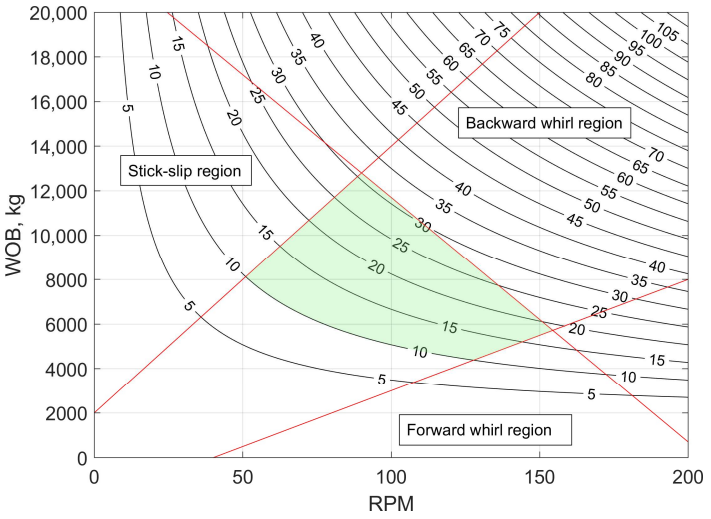

Figure 3.4 – Contour map of ROP (m/hr) response for combinations of WOB and RPM in the Detournay model, together with dysfunction zones and an optimal region (green).

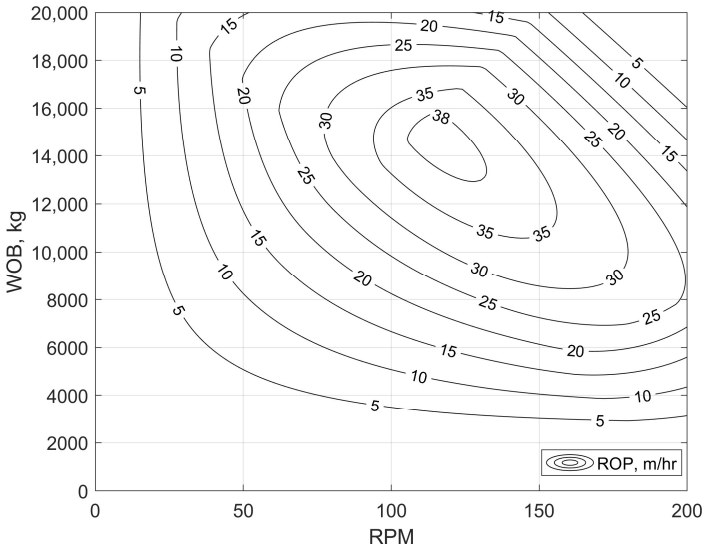

Figure 3.5 – Contour plot of ROP as a function of WOB and RPM with the extended model.

Altering the location(s) of the dysfunction zones in the WOB-RPM plane for different formations allows for simulations which can capture effects such as drilling hard formations being more prone to whirl vibrations [103]. A tuning parameter in the extended model is used to determine how much different dysfunctions affect the output, so that e.g. whirl can have a stronger negative impact on the ROP than stick-slip [22] or stick-slip effects on ROP being more pronounced in hard formations [104]. The extended model is not meant as a predictive tool, but rather as a representation of a steady state drilling response which qualitatively replicates field observations of reduced ROP and increased MSE when drilling with dysfunctions [22,23,101]. The use of the extended model as a part of the drilling plant (as applied in Appendix C) is depicted in Figure 3.6. The plant receives setpoints for WOB and RPM, which are translated to applied values according to a discrete first order system response that emulates actuation on the rig floor. The exerted WOB and RPM are used to calculate an "ideal" ROP response from the Detournay model, which is passed through a penalty layer that reduces the output ROP if the current operating point is in a zone of dysfunction.

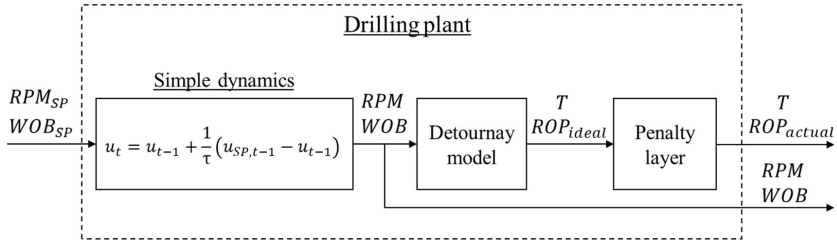

Figure 3.6 – Block diagram of the plant in Article 3.

3.3.3 Experimental setup

The experimental rig used in Appendix B was built to compete in the annual Drillbotics competition [105] hosted by the Society of Petroleum Engineers (SPE), allowing students and researchers to get hands-on experience with drilling automation technologies. The miniature rig is designed to work in an analogous fashion as a full-scale rig. It consists of a steel framework with integrated motors, sensors, hydraulic circulation system and other functionalities that are needed to drill through rock samples. A more

detailed description than the one provided here of the miniature rig and its use for other drilling automation applications can be found in [106-108]. Figure 3.7 shows the experimental drilling rig together with a schematic that highlights key components.

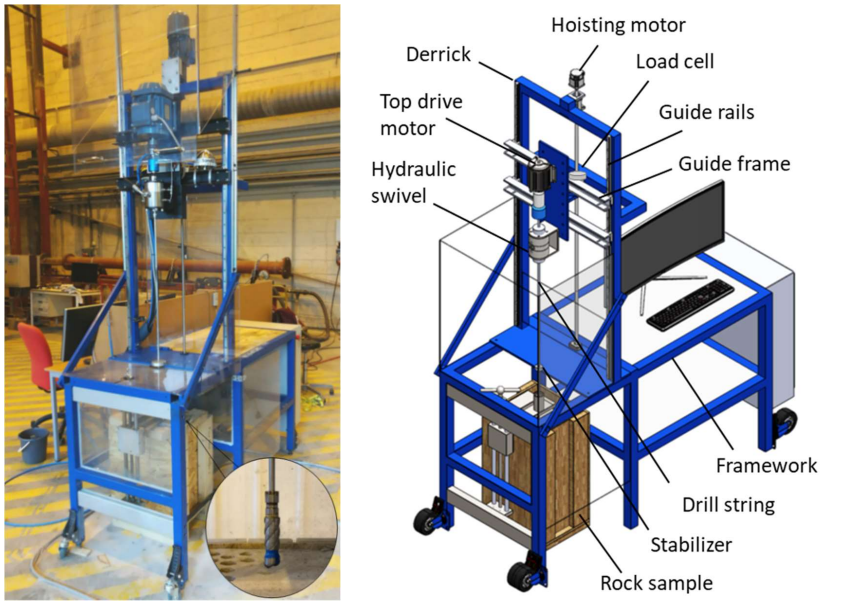

Figure 3.7 – The experimental rig used in Article 2, figures modified from [108]. (**a**) Rig photo, highlighting the BHA. (**b**) Rig schematic with key components.

At the top of the derrick, approximately 2.85 m above floor level, a hoisting motor provides rotational energy which is translated to vertical movement of the top drive assembly and drill string through a ball screw system. The top drive assembly is comprised of a motor to provide drill string rotation and a hydraulic swivel to facilitate circulation of drilling fluid while rotating. These components are mounted on a frame which slides along guide rails to ensure that all movement of the top drive and drill string is vertical, similar to the functionality of a full-scale top drive system. Fresh water from a standard water outlet is circulated through the drill string to transport cuttings out of the annulus and to cool and lubricate the bit. The drill string has a length of approximately

0,9 m and is made up of a hollow steel drill pipe, connection joints, a stabilizer sub, and a generic two-wing PDC bit with an outer diameter of 2,8 cm. Because of the reduced scale of the drilling rig, adequate WOB cannot be applied through high-weight drill string components as is done in full-scale operations. Instead, WOB is exerted by the top drive assembly pushing down on the drill string, placing the entire string in compression. The drill pipe is passed through a radial ball bearing stabilizer on the "rig floor" to mitigate buckling, by reducing the effective length of the string.

A load cell located at the hoisting system's nut bracket provides measurements of the total load from the bit and from the weight of the guide frame and top drive, which is converted to WOB by subtracting the weight of the mechanical components. Internal sensors in the top drive and hoisting motor supply measurements of drillstring rotational speed, (surface) torque, and the guide frame position. From the position measurement, an estimate of the ROP is calculated with a Kalman Filter by approximating the downhole ROP as the surface velocity of the traveling block (guide frame), as described in Appendix A. Because of the reduced scale of the system, the drill string elasticity can be reasonably neglected. The rig's control system is implemented in LabVIEW, where all communication with the motors and sensors is done with a 50 Hz update frequency. The top drive and hoisting motors are controlled by supplying them with requested setpoints for RPM and hoisting velocity, respectively, which are translated to the apposite motor and rotational rates by factory tuned internal PID controllers. To run experiments with WOB control, a PID autodriller was implemented in LabVIEW to convert requested WOB setpoints to the appropriate velocity setpoints for the hoisting motor.

The lab-scale drilling rig was used to investigate single variable ES with the WOB as the manipulated variable, as described in Appendix B. The maximal amount of WOB that could be applied without the top drive motor stalling out (at torque values of 7.2 Nm) was approximately 50 kg in the two investigated concrete formations. Within this interval, we were not able to repeatedly induce "natural" foundering effects without the top drive stalling (e.g. by decreasing the flow rate to facilitate cuttings accumulation around the bit at high enough ROP). For this reason, a simulation layer was employed in the experiments. This effect was used to simulate a reduction in ROP (as read by the rig's control system) when drilling at rates higher than some threshold ROP value which typically occurred within the allowable WOB range. The shape of the simulated ROP

response was designed to mimic the curves provided in [22,23], and allowed for experiments where the ES algorithms performance could be studied in the presence of (simulated) drilling dysfunctions.

4 Article summaries

4.1 Article 1: Micro-Testing While Drilling for Rate of Penetration Optimization

This paper investigates a data-driven optimization strategy called Extremum Seeking for attaining drilling at the optimal WOB. The method's main facilitator is a continuous series of micro-tests which vary the WOB while drilling ahead. The information gathered from these tests is used to automatically adjust the WOB based on a local linear model constructed from the test results. The studied ES method is a product of different algorithms and tools found in the literature, which are assembled to make the routine better suited for drilling application. This includes a least-squares method to calculate the local model as well as the use of a square wave excitation signal to maximize the obtained test information. Emphasis is placed on avoiding violation of operational constraints, as well as practical considerations related to estimation of instantaneous ROP and handling of noisy measurements. To ensure that the WOB is not steered to values which might be detrimental, a combination of two generic constraint handling techniques is proposed by the authors and demonstrated for an example of a limiting torque value that prevents drilling at the founder point. The effectiveness of constrained optimization algorithm is exhibited with simulations on a high-fidelity drilling simulator.

Paper highlights

- A modified version of the Extremum Seeking optimization method is proposed and employed to achieve drilling at the WOB which corresponds to maximal dysfunction-free ROP, with limited a priori information.
- The optimization routine is augmented with two novel strategies for constraint handling, to ensure safe operations.
- The proposed algorithm's ability to optimize the applied WOB while adhering to process constraints is demonstrated in simulation scenarios on a high-fidelity drilling simulator for instances with and without measurement noise.

4.2 Article 2: Micro-Testing While Drilling for Rate of Penetration Optimization: Experiments and Simulations

This paper is an extension of Article 1. The performance of the single-variable extremum seeking algorithm and constraint handling techniques used to optimize the WOB in Article 1 is here studied on a lab-scale drilling rig. The experimental setup is designed to work in an analogous fashion to a full-scale rig, with a hydraulic system to remove cuttings, a top drive providing bit rotation and a "traveling block" that controls the bit velocity (and indirectly the WOB). The scaled rig captures the vibrations and noisy nature of the drilling process, which makes it a well-suited arena for studying the drilling optimization algorithm under conditions mimicking those in the field. However, the foundering tendencies reported in field operations could not be replicated in the lab and had to be added through a simulation layer. The ES method was experimentally tested in different scenarios, including initiating the algorithm above and below the optimal WOB value, drilling through a change in formation as well as in constrained situations where the torque had to be kept below a threshold value. A study of the ES method was also performed on a high-fidelity simulator to qualify the experimental results for field conditions, where the algorithm only had access to noisy top-side measurements. In both experiments and simulations, the algorithm demonstrated the sought behavior of navigating to the optimal WOB and avoiding constraint violations, without requiring detailed prior process information.

Paper highlights

- A constrained data-driven optimization method used for obtaining drilling with optimal WOB is explained in detail.
- The proposed optimization strategy is tested in a series of experiments on a lab-scale drilling rig.
- The experimental results are supplemented with simulations on a high-fidelity drilling simulator, to study the optimization method for full-scale operations.
- In both experiments and simulations, the algorithm demonstrated the ability to seek out the optimal WOB while avoiding violation of constraints, resulting in safe and efficient drilling.

4.3 Article 3: Real-Time Minimization of Mechanical Specific Energy with Multivariable Extremum Seeking

In this paper, a constrained multivariable extremum seeking algorithm is employed to simultaneously optimize the WOB and RPM by minimizing the MSE. A drilling model that includes vibrational effects in an existing model from the literature is proposed and used to study the optimization approach. The modified drilling model does not capture the dynamics of drilling dysfunction effects, but it does qualitatively represent steady state drilling responses that are documented from field operations, which is what is needed to study the average behavior of the algorithm. Emphasis is placed on algorithm design and tuning for application of the algorithm in drilling operations, as well as different constraint handling techniques that ensure safe operations. An in-depth analysis of MSE as a tool to increase drilling efficiency and how it can be employed as an objective function in automated drilling optimization routines is also provided. This methodology involves programming the ES algorithm to interpret a flat MSE-response to varying WOB and/or RPM as a scenario where the relevant input should be increased to improve the drilling efficiency. The simulations show the method's ability to simultaneously optimize the WOB and RPM while avoiding violation of drilling constraints.

Paper highlights

- A constrained multivariable extremum seeking algorithm that minimizes the MSE through manipulation of the applied WOB and RPM is given in detail, together with tuning guidelines that facilitate its use.
- A drilling model that qualitatively includes vibrational dysfunction effects is proposed by the authors and used to study the ES algorithm.
- Three constraint handling strategies to be used in conjunction with the optimization method are presented and employed in simulation scenarios.
- The simulations demonstrate the algorithm's ability to seek out and maintain drilling with minimal MSE, avoid violation of constraints and track variations in optimal operating conditions resulting from changes in the drilled formation.

5 Conclusions

5.1 Concluding remarks

The main goal of this thesis is to contribute towards automatic solutions for safe and efficient well construction. This goal is carried out by investigating a data-driven optimization method called Extremum Seeking for the purpose of automated drilling optimization through manipulation of the mechanical variables WOB and RPM. Drilling optimization with the ES algorithm is chosen as the topic of this thesis because of the algorithm's proven track record from other industries, as well as beneficial properties related to the method's robustness to noise, relatively straight-forward tuning and the limited a priori knowledge of downhole conditions needed to apply the algorithm. The ES methodology employed in the appendices is a product of modifications proposed by the authors, as well as different algorithms and tools found in the literature, which are assembled to make the routine better suited for drilling applications.

In Appendix A, a single variable ES algorithm is presented and the method's ability to seek out the optimal WOB to drill with while adhering to process constraints is demonstrated in simulation scenarios on a high-fidelity drilling simulator. In Appendix B, the single variable constrained ES algorithm from Appendix A is investigated with experiments on a lab-scale drilling rig, as well as in simulations. In Appendix C, a constrained ES algorithm that minimizes MSE while drilling by simultaneously optimizing applied WOB and RPM is detailed, and its performance is studied in simulation scenarios. In the simulations and experiments detailed in the appendices, the proposed ES algorithm demonstrates the capability of avoiding violation of process constraints while seeking out optimal drilling conditions with limited a priori information. The algorithm also exhibits the ability to adapt to downhole changes and seek out new optimal conditions when drilling into new rock formations. Overall, the three studies indicate a potential for significant improvement in drilling efficiency from applying the ES algorithm for real-time drilling optimization.

The advantage of a data-driven "testing on the fly" method like the ES approach, is that it functions by continuously performing tests that extract information of the downhole conditions. It can therefore perform optimization actions based on the most up-

to-date information available and does not require detailed prior knowledge of the downhole conditions to be applied. This property is very beneficial for drilling optimization, since the detailed knowledge of downhole conditions needed to accurately model the bit/rock interaction might not be directly measurable or available in real-time, which is a limiting factor for some model-based approaches.

There are some possible drawbacks to applying the ES algorithm for drilling optimization. The method needs full control of the applied WOB and/or RPM while drilling and could in its search for optimal drilling potentially steer these values to regions that could lead to unsafe operations. Robust constraint handling should therefore be integrated into the algorithm, as detailed in Section 3.2.3 and the appendices. As theorized in [72], the ES algorithm could possibly fail to seek out the optimum in the presence of transient foundering effects. This hypothesis is not investigated in this thesis and remains unanswered. Additionally, the choice of objective function used in the method could limit the region of where the algorithm can be initiated and still successfully converge to the optimal WOB and/or RPM, as discussed in Section 2.3. Steps that could be taken to avoid or mediate these potentially detrimental properties are described below.

5.2 Topics for further research

There are several interesting directions for further studies which would build on the results of this thesis:

- Further research could be performed based on the ES method's inherent nature of relating measurements of drilling parameters to known variations in the WOB and/or RPM induced by the excitation signal(s). If available, additional measured or calculated parameters such as the magnitude of different forms of vibrations could be related to the input variations. This modeling could be performed with the simple linear relationship extracted by the least-squares technique in the ES algorithm, or by more advanced models. Knowing how downhole vibrations vary as a function of WOB and/or RPM could be utilized for optimization, constraint handling or be displayed as useful information for the driller
- Two different functions were investigated to quantify optimal drilling in this work: a formulation related to ROP in appendices A and B and MSE in Appendix C. Application

of both of these formulations require a tuning parameter to alter the objective function so that its extremum is at or close to the founder point. A candidate objective function that potentially does not require this tuning parameter is the ROP/MSE ratio, which should be the topic of an additional study. This objective function also has the beneficial property that it is monotonically increasing for phase 1 and 2 drilling (at least according to the drilling model detailed in appendix C). This implies that an ES algorithm employing this objective could be initiated also in phase 1 drilling without the risk of the algorithm erroneously reducing the WOB in this scenario. It is possible that the ROP/MSE ratio was used in the ES approach described in [39], but the limited amount of algorithmic details given in that paper obfuscates what objective function was used.

- The ES algorithm can be used as a stand-alone method for optimization as long as it is initiated within the domain of attraction of the selected objective function (see Section 2.3). However, the most efficient drilling is (logically enough) obtained when the method is initiated with a "good guess" of the optimal conditions, as the method will converge to the optimum more rapidly. Using a model-based approach to provide the starting point for the ES algorithm would formalize the initialization process, by incorporating any a priori knowledge of the drilling conditions into the analysis through the model. This approach would be conceptually similar to the methodology used in [57].
- The proposed ES method should be tested in facilities that are able to capture the dynamics of bit foundering, either in the field or a more advanced testing site than the experimental setup used in Appendix B. Such a study would be needed to confirm that the ES algorithm is able to provide stabile drilling at or sufficiently close to the founder point, a property that was questioned in [72].
- The mud flow rate could be included as a third manipulated variable in the ES algorithm. This approach would necessitate rigorous constraint handling and monitoring of the well, so that the ES algorithm would not steer the flow rate to values that would interfere with adequate hole cleaning and well integrity. Manipulating the flow rate would potentially require additional terms in the used objective function, to account for changes in the well that happen at a slower time scale (e.g. accumulation of a cuttings bed in deviated sections), since such effects would not be adequately captured by formulations related to instantaneous ROP or MSE.

Bibliography

[1] *NTNU Strategy for Oil and Gas.* Technical report (Trondheim, Norway: 2017).

[2] Rehm, B., Schubert, J., Haghshenas, A., Paknejad, A.S., and Hughes, J. *Managed pressure drilling.* Elsevier, 2013.

[3] Willersrud, A., 2015, "Model-Based Diagnosis of Drilling Incidents." PhD Thesis, NTNU, Trondheim, Norway.

[4] Gravdal, J.E., 2011, "Kick Management in Managed Pressure Drilling Using Well Flow Models and Downhole Pressure Measurements." PhD Thesis, UiS, Stavanger, Norway.

[5] Florence, F., and Iversen, F.P., "Real-time models for drilling process automation: Equations and applications." Paper presented at the IADC/SPE Drilling Conference and Exhibition, 2010.

[6] Kyllingstad, Å., and Thoresen, K.E., "Improving Surface WOB Accuracy." Paper presented at the IADC/SPE Drilling Conference and Exhibition, 2018. doi:10.2118/189601-MS.

[7] Cayeux, E., Skadsem, H.J., and Kluge, R., "Accuracy and Correction of Hook Load Measurements During Drilling Operations." Paper presented at the SPE/IADC Drilling Conference and Exhibition, 2015. doi:10.2118/173035-MS.

[8] Cayeux, E., Daireaux, B., Dvergsnes, E.W.W., and Florence, F., 2014, "Toward Drilling Automation: On the Necessity of Using Sensors That Relate to Physical Models," *SPE Drilling & Completion,* 29, no. 02, pp. 236-55. doi:10.2118/163440-PA.

[9] Lesso, B., Ignova, M., Zeineddine, F., Burks, J., and Welch, B., "Testing the Combination of High Frequency Surface and Downhole Drilling Mechanics and Dynamics Data under a Variety of Drilling Conditions." Paper presented at the SPE/IADC Drilling Conference and Exhibition, 2011. doi:10.2118/140347-ms.

[10] Hareland, G., Wu, A., and Lei, L., "The Field Tests for Measurement of Downhole Weight on Bit(DWOB) and the Calibration of a Real-time DWOB Model." Paper presented at the International Petroleum Technology Conference, 2014. doi:10.2523/iptc-17503-ms.

[11] Kyllingstad, Å., and Thoresen, K.E., "Improving Accuracy of Well Depth and ROP." Paper presented at the SPE/IADC International Drilling Conference and Exhibition, 2019. doi:10.2118/194098-ms.

[12] Cayeux, E., and Skadsem, H.J., "Estimation of weight and torque on bit: Assessment of uncertainties, correction and calibration methods." Paper presented at the ASME 2014 33rd International Conference on Ocean, Offshore and Arctic Engineering, 2014.

[13] Cayeux, E., Ambrus, A., Øy, L., Helleland, A., Brundtland, S., Nevøy, H., and Morys, M., 2021, "Analysis of Torsional Stick-Slip Situations from Recorded Downhole Rotational Speed Measurements," *SPE Drilling & Completion*, pp. 1-15.

[14] Carlsen, L.A., Nygaard, G., and Time, R., 2012, "Utilizing instrumented stand pipe for monitoring drilling fluid dynamics for improving automated drilling operations," *IFAC Proceedings Volumes,* 45, no. 8, pp. 217-22.

[15] Magalhães, S., Calçada, L.A., Scheid, C., Paraíso, E., Moraes, G., Valim, E., Almeida, H., *et al.*, "Field Results of a Real Time Drilling Fluid Monitoring System." Paper presented at the SPE Latin American and Caribbean Petroleum Engineering Conference, 2020. doi:10.2118/199101-ms.

[16] Ashok, P., Ambrus, A., Ramos, D., Lutteringer, J., Behounek, M., Yang, Y.L., Thetford, T., and Weaver, T., "A Step by Step Approach to Improving Data Quality in Drilling Operations: Field Trials in North America." Paper presented at the SPE Intelligent Energy International Conference and Exhibition, 2016. doi:10.2118/181076-ms.

[17] Macpherson, J.D., de Wardt, J.P., Florence, F., Chapman, C.D., Zamora, M., Laing, M.L., and Iversen, F.P., 2013, "Drilling-Systems Automation: Current State, Initiatives, and Potential Impact," *SPE Drilling & Completion,* 28, no. 04, pp. 296-308. doi:10.2118/166263-pa.

[18] Pastusek, P., Owens, M., Barrette, D., Wilkins, V., Bolzan, A., Ryan, J., Akyabi, K., Reichle, M., and Pais, D., "Drill rig control systems: Debugging, tuning, and long term needs." Paper presented at the SPE Annual Technical Conference and Exhibition, 2016.

[19] Badgwell, T., Pastusek, P., and Kumaran, K., "Auto-Driller Automatic Tuning." Paper presented at the SPE Annual Technical Conference and Exhibition, 2018.

[20] Nikolaou, M., Misra, P., Tam, V.H., and Bailey III, A.D., 2005, "Complexity in semiconductor manufacturing, activity of antimicrobial agents, and drilling of hydrocarbon wells: Common themes and case studies," *Computers & chemical engineering,* 29, no. 11-12, pp. 2266-89.

[21] Sui, D., Nybø, R., and Azizi, V., "Real-time optimization of rate of penetration during drilling operation." Paper presented at the 2013 10th IEEE International Conference on Control and Automation (ICCA), 12-14 June 2013. doi:10.1109/ICCA.2013.6564893.

[22] Dupriest, F., Hutchison, I., Oort, E.v., and Armstrong, N. *The IADC Drilling Manual - Drilling Practices.* 12th ed.: International Association of Drilling Contractors, 2014.

[23] Dupriest, F.E., and Koederitz, W.L., "Maximizing Drill Rates with Real-Time Surveillance of Mechanical Specific Energy." Paper presented at the the SPE/IADC Drilling Conference, Amsterdam, The Netherlands, 23-25 February 2005. doi:10.2118/92194-MS.

[24] Detournay, E., Richard, T., and Shepherd, M., 2008, "Drilling response of drag bits: Theory and experiment," *International Journal of Rock Mechanics and Mining Sciences,* 45, no. 8, pp. pp. 1347-60. doi:10.1016/j.ijrmms.2008.01.010.

[25] Dupriest, F.E. "Comprehensive Drill Rate Management Process To Maximize ROP." the SPE Annual Technical Conference and Exhibition, San Antonio, Texas, USA, Society of Petroleum Engineers, SPE, 24-27 September 2006 2006. doi:10.2118/102210-MS.

[26] Bourgoyne, A.T., Millheim, K.K., Chenevert, M.E., and Young, F.S. *Applied drilling engineering.* Vol. 2: Society of Petroleum Engineers Richardson, TX, 1986.

[27] Maurer, W., 1962, "The" perfect-cleaning" theory of rotary drilling," *Journal of Petroleum Technology,* 14, no. 11, pp. 1,270-1,74.

[28] Garnier, A., and Van Lingen, N., 1959, "Phenomena affecting drilling rates at depth," *Transactions of the AIME,* 216, no. 01, pp. 232-39.

[29] Warren, T.M., and Smith, M.B., 1985, "Bottomhole Stress Factors Affecting Drilling Rate at Depth," *Journal of Petroleum Technology,* 37, no. 08, pp. 1523-33. doi:10.2118/13381-PA.

[30] Caenn, R., Darley, H.C., and Gray, G.R. "Drilling Problems Related to Drilling Fluids." Chap. 10 In *Composition and Properties of Drilling and Completion Fluids*: Gulf professional publishing, 2011.

[31] Young, F.S., Jr., 1969, "Computerized Drilling Control," *Journal of Petroleum Technology,* 21, no. 04, pp. pp. 483-96. doi:10.2118/2241-PA.

[32] Eren, T., and Ozbayoglu, M.E., "Real Time Optimization of Drilling Parameters During Drilling Operations." Paper presented at the SPE Oil and Gas India Conference and Exhibition, Mumbai, India, 20-22 January 2010. doi:10.2118/129126-MS.

[33] Payette, G.S., Spivey, B.J., Wang, L., Bailey, J.R., Sanderson, D., Kong, R., Pawson, M., and Eddy, A., "A Real-Time Well-Site Based Surveillance and Optimization Platform for Drilling: Technology, Basic Workflows and Field Results." Paper presented at the the SPE/IADC Drilling Conference and Exhibition, The Hague, The Netherlands, 14-16 March 2017 2017. doi:10.2118/184615-ms.

[34] Koederitz, W.L., and Weis, J. "A Real-Time Implementation of MSE." the AADE National Technical Conference and Exhibition, Houston, Texas, USA, 5-7 April 2005 2005.

[35] Aarsnes, U.J.F., Aamo, O.M., and Krstic, M., "Extremum Seeking for Real-time Optimal Drilling Control." Paper presented at the the American Control Conference (ACC), Philadelphia, PA, USA, 10-12 July 2019.

[36] Chapman, C.D., Sanchez, J.L., De Leon Perez, R., and Yu, H., "Automated Closed-Loop Drilling with ROP Optimization Algorithm Significantly Reduces Drilling Time and Improves Downhole Tool Reliability." Paper presented at the the IADC/SPE Drilling Conference and Exhibition, San Diego, California, USA, 6-8 March 2012. doi:10.2118/151736-MS.

[37] Daireaux, B., Ambrus, A., Carlsen, L.A., Mihai, R., Gjerstad, K., and Balov, M., "Development, Testing and Validation of an Adaptive Drilling Optimization System." Paper presented at the SPE/IADC International Drilling Conference and Exhibition, 2021. doi:10.2118/204083-ms.

[38] Dunlop, J., Isangulov, R., Aldred, W.D., Sanchez, H.A., Flores, J.L.S., Herdoiza, J.A., Belaskie, J., and Luppens, C. "Increased Rate of Penetration Through Automation." the SPE/IADC Drilling Conference and Exhibition, Amsterdam, The Netherlands, Society of Petroleum Engineers, SPE, 1-3 March 2011 2011. doi:10.2118/139897-MS.

[39] Lai, S.W., Ng, J., Eddy, A., Khromov, S., Paslawski, D., van Beurden, R., Olesen, L., Payette, G.S., and Spivey, B.J., 2020, "Large-Scale Deployment of a Closed-Loop Drilling Optimization System: Implementation and Field Results," *SPE Drilling & Completion,* Preprint, pp. doi:10.2118/199601-PA.

[40] Eustes, A.W. "The Evolution of Automation in Drilling." the SPE Annual Technical Conference and Exhibition, Anaheim, California, USA, Society of Petroleum Engineers, SPE, 11-14 November 2007 2007. doi:10.2118/111125-MS.

[41] Chmela, B., Gibson, N., Abrahamsen, E., and Bergerud, R. "Safer Tripping Through Drilling Automation." the IADC/SPE Drilling Conference and Exhibition, Fort

Worth, Texas, USA, Society of Petroleum Engineers, 4-6 March 2014 2014. doi:10.2118/168018-MS.

[42] Iversen, F.P., Cayeux, E., Dvergsnes, E.W., Ervik, R., Welmer, M., and Balov, M.K., 2009, "Offshore Field Test of a New System for Model Integrated Closed-Loop Drilling Control," *SPE Drilling & Completion,* 24, no. 04, pp. 518-30. doi:10.2118/112744-PA.

[43] Gulsrud, T.O., Nybø, R., and Bjørkevoll, K.S., "Statistical Method for Detection of Poor Hole Cleaning and Stuck Pipe." Paper presented at the SPE Offshore Europe Oil and Gas Conference and Exhibition, Aberdeen, UK, 8-11 September 2009. doi:10.2118/123374-MS.

[44] Tarr, B.A., Ladendorf, D.W., Sanchez, D., and Milner, G.M., 2016, "Next-Generation Kick Detection During Connections: Influx Detection at Pumps Stop (IDAPS) Software," *SPE Drilling & Completion,* 31, no. 04, pp. pp. 250-60. doi:10.2118/178821-PA.

[45] Kyllingstad, A., and Nessjøen, P.J. "A New Stick-Slip Prevention System." the SPE/IADC Drilling Conference and Exhibition, Amsterdam, The Netherlands, Society of Petroleum Engineers, SPE, 17-19 March 2009 2009. doi:10.2118/119660-MS.

[46] Runia, D.J., Dwars, S., and Stulemeijer, I.P., "A Brief History of the Shell "Soft Torque Rotary System" and Some Recent Case Studies." Paper presented at the SPE/IADC Drilling Conference, Amsterdam, The Netherlands, 5-7 March 2013. doi:10.2118/163548-ms.

[47] Rommetveit, R., Bjorkevoll, K.S., Odegaard, S.I., Herbert, M.C., Halsey, G.W., and Kluge, R., "eDrilling used on ekofisk for real-time drilling supervision, simulation, 3D visualization and diagnosis." Paper presented at the Intelligent Energy Conference and Exhibition, 2008.

[48] Rommetveit, R., Bjørkevoll, K.S., Halsey, G.W., Larsen, H.F., Merlo, A., Nossaman, L.N., Sweep, M.N., Silseth, K.M., and Ødegaard, S.I. "Drilltronics: An Integrated System for Real-Time Optimization of the Drilling Process." the IADC/SPE Drilling Conference, Dallas, Texas, USA, Society of Petroleum Engineers, SPE, 2-4 March 2004 2004. doi:10.2118/87124-MS.

[49] Lyons, W.C., and Plisga, G.J. *Standard handbook of petroleum and natural gas engineering.* Elsevier, 2011.

[50] Bourgoyne, A.T., Jr., and Young, F.S., Jr., 1974, "A Multiple Regression Approach to Optimal Drilling and Abnormal Pressure Detection," *Society of Petroleum Engineers Journal,* 14, no. 04, pp. 371-84. doi:10.2118/4238-PA.

[51] Warren, T.M., 1987, "Penetration Rate Performance of Roller Cone Bits," *SPE Drilling Engineering,* 2, no. 01, pp. pp. 9-18. doi:10.2118/13259-PA.

[52] Hegde, C., Daigle, H., Millwater, H., and Gray, K., 2017, "Analysis of Rate of Penetration (ROP) Prediction in Drilling Using Physics-Based and Data-Driven Models," *Journal of Petroleum Science and Engineering,* 159, pp. 295-306. doi:10.1016/j.petrol.2017.09.020.

[53] Ambrus, A., Daireaux, B., Carlsen, L.A., Mihai, R.G., Karimi Balov, M., and Bergerud, R., "Statistical Determination of Bit-Rock Interaction and Drill String Mechanics for Automatic Drilling Optimization." Paper presented at the International Conference on Offshore Mechanics and Arctic Engineering, 2020.

[54] Sui, D., and Aadnoy, B., 2016, "Rate of Penetration Optimization using Moving Horizon Estimation," *Modeling, Identification and Control: A Norwegian Research Bulletin,* 37, pp. 149-58. doi:10.4173/mic.2016.3.1.

[55] Bataee, M., Kamyab, M., and Ashena, R. "Investigation of Various ROP Models and Optimization of Drilling Parameters for PDC and Roller-cone Bits in Shadegan Oil Field." the International Oil and Gas Conference and Exhibition in China, Beijing, China, Society of Petroleum Engineers, SPE, 8-10 June 2010. doi:10.2118/130932-MS.

[56] Soares, C., and Gray, K., 2019, "Real-time predictive capabilities of analytical and machine learning rate of penetration (ROP) models," *Journal of Petroleum Science and Engineering,* 172, pp. 934-59.

[57] Spencer, S.J., Mazumdar, A., Jiann-Cherng, S., Foris, A., and Buerger, S.P., "Estimation and Control for Efficient Autonomous Drilling Through Layered Materials." Paper presented at the 2017 American Control Conference (ACC), 24-26 May 2017. doi:10.23919/ACC.2017.7962950.

[58] Noshi, C.I., and Schubert, J.J., "The role of machine learning in drilling operations; a review." Paper presented at the SPE/AAPG Eastern Regional Meeting, 2018.

[59] Barbosa, L.F.F., Nascimento, A., Mathias, M.H., and de Carvalho Jr, J.A., 2019, "Machine learning methods applied to drilling rate of penetration prediction and optimization-A review," *Journal of Petroleum Science and Engineering,* 183, pp. 106332.

[60] Bello, O., Holzmann, J., Yaqoob, T., and Teodoriu, C., 2015, "Application of artificial intelligence methods in drilling system design and operations: a review of the state of the art," *Journal of Artificial Intelligence and Soft Computing Research,* 5, no. 2, pp. 121-39.

[61] Hegde, C., and Gray, K., 2017, "Use of machine learning and data analytics to increase drilling efficiency for nearby wells," *Journal of Natural Gas Science and Engineering,* 40, pp. 327-35.

[62] Hegde, C., Daigle, H., and Gray, K.E., 2018, "Performance Comparison of Algorithms for Real-Time Rate-of-Penetration Optimization in Drilling Using Data-Driven Models," *SPE Journal,* 23, no. 05, pp. 1706-22. doi:10.2118/191141-PA.

[63] Hegde, C., Soares, C., and Gray, K., "Rate of penetration (ROP) modeling using hybrid models: deterministic and machine learning." Paper presented at the Unconventional Resources Technology Conference, Houston, Texas, 23-25 July 2018, 2018.

[64] Alali, A.M., Abughaban, M.F., Aman, B.M., and Ravela, S., 2021, "Hybrid data driven drilling and rate of penetration optimization," *Journal of Petroleum Science and Engineering,* 200, pp. 108075.

[65] Lubinski, A., 1958, "Proposal for future tests," *The Petroleum Engineer (Jan 1958)*, pp. 50-52.

[66] Israel, R., McCrae, D., Sperry, N., Gorham, B., Thompson, J., Raese, K., Pink, S., and Coit, A., "Delivering Drilling Automation II–Novel Automation Platform and Wired Drill Pipe Deployed on Arctic Drilling Operations." Paper presented at the SPE Annual Technical Conference and Exhibition, 2018.

[67] Ramsey, M.S. *Practical Wellbore Hydraulics and Hole Cleaning: Unlock Faster, More Efficient, and Trouble-free Drilling Operations.* Gulf Professional Publishing, 2019.
[68] Chang, D.-L., Payette, G.S., Pais, D., Wang, L., Bailey, J.R., and Mitchell, N.D. "Field Trial Results of a Drilling Advisory System." the International Petroleum Technology Conference, IPTC, Doha, Qatar, 19-22 January 2014. doi:10.2523/IPTC-17216-MS.
[69] Koederitz, W.L., and Johnson, W.E., "Real-Time Optimization of Drilling Parameters by Autonomous Empirical Methods." Paper presented at the SPE/IADC Drilling Conference and Exhibition, 1-3 March 2009 2011. doi:10.2118/139849-MS.
[70] Aldrich, J., Sherrit, S., Bao, X., Bar-Cohen, Y., Badescu, M., and Chang, Z., "Extremum-seeking control for an ultrasonic/sonic driller/corer (USDC) driven at high power." Paper presented at the Smart Structures and Materials 2006: Modeling, Signal Processing, and Control, 2006.
[71] Banks, S., "Minimizing the Mechanical Specific Energy While Drilling Using Extremum Seeking Control." Paper presented at the the 11th International Conference on Vibration Problems, Lisbon, Portugal, 9-12 September 2013, Corpus ID: 214789826.
[72] Aarsnes, U.J.F., Ambrus, A., Di Meglio, F., and Gerbaud, L., 2021, "A phenomenological transient model of bit foundering," *Journal of Petroleum Science and Engineering,* 199, pp. 108299.
[73] Brunton, S.L., and Kutz, J.N. "Adaptive Extremum-Seeking Control." Chap. 10.3 In *Data-driven science and engineering: Machine learning, dynamical systems, and control*. Cambridge, UK: Cambridge University Press, 2019.
[74] Tan, Y., Moase, W.H., Manzie, C., Nešić, D., and Mareels, I.M., "Extremum seeking from 1922 to 2010." Paper presented at the the 29th Chinese Control Conference, 29-31 July 2010.
[75] Peixoto, A.J., Pereira-Dias, D., Xaud, A.F.S., and Secchi, A.R., 2015, "Modelling and Extremum Seeking Control of Gas Lifted Oil Wells," *IFAC-PapersOnLine,* 48, no. 6, pp. 21-26. doi:10.1016/j.ifacol.2015.08.004.
[76] Silva, T.L., and Pavlov, A., 2020, "Dither signals optimization in constrained multi-agent extremum seeking control," *IFAC-PapersOnLine,* 53, no. 2, pp. 1633-39.
[77] Pavlov, A., and Fjalestad, K. "Method and system for the optimisation of the addition of diluent to an oil well comprising a downhole pump." Google Patents, 2019.
[78] Nystad, M., and Pavlov, A., "Micro-Testing While Drilling for Rate of Penetration Optimization." Paper presented at the the International Conference on Offshore Mechanics and Arctic Engineering, Virtual, Online, 3-7 August 2020.
[79] Nystad, M., Aadnøy, B.S., and Pavlov, A., 2021, "Micro-Testing While Drilling for Rate of Penetration Optimization: Experiments and Simulations," *Submitted to Journal of Offshore Mechanics and Arctic Engineering*, pp.
[80] ———. 2021, "Real-Time Minimization of Mechanical Specific Energy with Multivariable Extremum Seeking," *Energies,* 14, no. 5, pp. 1298.
[81] Ariyur, K.B., and Krstić, M. *Real-Time Optimization by Extremum Seeking Control.* Wiley Online Library, 2003. doi:doi:10.1002/0471669784

[82] Tran, Q.N., Scholten, J., Ozkan, L., and Backx, A., 2014, "A model-free approach for auto-tuning of model predictive control," *IFAC Proceedings Volumes,* 47, no. 3, pp. 2189-94.
[83] Krstić, M., 2000, "Performance improvement and limitations in extremum seeking control," *Systems & Control Letters,* 39, no. 5, pp. 313-26.
[84] Chioua, M., Srinivasan, B., Guay, M., and Perrier, M., 2016, "Performance improvement of extremum seeking control using recursive least square estimation with forgetting factor," *IFAC-PapersOnLine,* 49, no. 7, pp. 424-29.
[85] Wang, H.-H., Yeung, S., and Krstic, M., 2000, "Experimental application of extremum seeking on an axial-flow compressor," *IEEE Transactions on Control Systems Technology,* 8, no. 2, pp. 300-09.
[86] Moase, W.H., Manzie, C., and Brear, M.J., 2010, "Newton-like extremum-seeking for the control of thermoacoustic instability," *IEEE Transactions on Automatic Control,* 55, no. 9, pp. 2094-105.
[87] Guay, M., 2016, "A perturbation-based proportional integral extremum-seeking control approach," *IEEE Transactions on Automatic Control,* 61, no. 11, pp. 3370-81.
[88] Yau, H.-T., Lin, C.-J., and Wu, C.-H., 2013, "Sliding Mode Extremum Seeking Control Scheme Based on PSO for Maximum Power Point Tracking in Photovoltaic Systems," *International Journal of Photoenergy,* 2013, pp. doi:10.1155/2013/527948.
[89] Krishnamoorthy, D., and Skogestad, S. "A fast and robust extremum seeking scheme using transient measurements." Submitted to Automatica, 2019.
[90] Hunnekens, B., Haring, M.A., van de Wouw, N., and Nijmeijer, H., "A dither-free extremum-seeking control approach using 1st-order least-squares fits for gradient estimation." Paper presented at the 53rd IEEE conference on decision and control, 2014.
[91] Tan, Y., Nešić, D., and Mareels, I., 2008, "On the Choice of Dither in Extremum Seeking Systems: A Case Study," *Automatica,* 44, no. 5, pp. 1446-50. doi:10.1016/j.automatica.2007.10.016.
[92] Zengin, N., and Fidan, B. "Adaptive extremum seeking using recursive least squares." arXiv preprint arXiv:2003.03891, 2020.
[93] Guay, M., Moshksar, E., and Dochain, D., 2015, "A constrained extremum-seeking control approach," *International Journal of Robust and Nonlinear Control,* 25, no. 16, pp. 3132-53.
[94] Hazeleger, L., Nešić, D., and van de Wouw, N., "Sampled-data extremum-seeking control for optimization of constrained dynamical systems using barrier function methods." Paper presented at the 2019 IEEE 58th Conference on Decision and Control (CDC), 2019.
[95] Tan, Y., Li, Y., and Mareels, I.M., 2013, "Extremum seeking for constrained inputs," *IEEE Transactions on Automatic Control,* 58, no. 9, pp. 2405-10.
[96] Pessier, R.C., and Fear, M.J., "Quantifying Common Drilling Problems With Mechanical Specific Energy and a Bit-Specific Coefficient of Sliding Friction." Paper presented at the the SPE Annual Technical Conference and Exhibition, Washington, DC, USA, 4-7 October 1992 1992. doi:10.2118/24584-ms.
[97] Ewald, R., Gravdal, J.E., Sui, D., and Shor, R., "Web Enabled High Fidelity Drilling Computer Model with User-Friendly Interface for Education, Research and

Innovation." Paper presented at the Proceedings of The 59th Conference on Simulation and Modelling (SIMS 59), 26-28 September 2018, Oslo Metropolitan University, Norway, 2018.
[98] Gravdal, J.E., Sui, D., Nagy, A., Saadallah, N., and Ewald, R., "A Hybrid Test Environment for Verification of Drilling Automation Systems." Paper presented at the SPE/IADC International Drilling Conference and Exhibition, 2021.
[99] Saadallah, N., Gravdal, J.E., Ewald, R., Moi, S., Ambrus, A., Daireaux, B., Sivertsen, S., *et al.*, "OpenLab: Design and applications of a modern drilling digitalization infrastructure." Paper presented at the SPE Norway One Day Seminar, 2019.
[100] Gravdal, J.E., Ewald, R., Saadallah, N., Moi, S., Sui, D., and Shor, R., "A New Approach to Development and Validation of Artificial Intelligence Systems for Drilling." Paper presented at the 2020 15th IEEE Conference on Industrial Electronics and Applications (ICIEA), 2020.
[101] Wu, S.X., Paez, L., Partin, U., and Agnihotri, M., "Decoupling Stick-Slip and Whirl to Achieve Breakthrough in Drilling Performance." Paper presented at the the IADC/SPE Drilling Conference and Exhibition, New Orleans, Louisiana, USA, 2-4 Februrary 2010 2010. doi:10.2118/128767-ms.
[102] Vogel, S.K., and Creegan, A.P., "Case Study for Real Time Stick/Slip Mitigation to Improve Drilling Performance." Paper presented at the the SPE/IADC Middle East Drilling Technology Conference and Exhibition, Abu Dhabi, UAE, 26-28 January 2016 2016. doi:10.2118/178176-ms.
[103] Dykstra, M.W., Chen, D.C.-K., Warren, T.M., and Azar, J.J., 1996, "Drillstring Component Mass Imbalance: A Major Source of Downhole Vibrations," *SPE Drilling & Completion,* 11, no. 04, pp. 234-41. doi:10.2118/29350-PA.
[104] Brett, J.F., 1992, "The genesis of bit-induced torsional drillstring vibrations," *SPE Drilling Engineering,* 7, no. 03, pp. 168-74.
[105] "Drillbotics Competition." 2021, https://drillbotics.com/.
[106] Arnø, M., Thuve, A., Knoop, S., Hovda, S., Pavlov, A., and Florence, F., "Design and Implementation of a Miniature Autonomous Drilling Rig for Drillbotics 2018." Paper presented at the SPE/IADC International Drilling Conference and Exhibition, 5-7 March 2019 2019. doi:10.2118/194226-MS.
[107] Egeland, R.L., Lescoeur, A., Olsen, M., Vasantharajan, M., Hovda, S., and Pavlov, A., 2018. "Miniature Robotic Drilling Rig for Research and Education in Drilling Automation." Paper presented at the IEEE Conference on Control Technology and Applications (CCTA), 21-24 August 2018. doi:10.1109/CCTA.2018.8511506.
[108] Handeland, A.S., 2018, "Design and Optimization of a Miniature Autonomous Drillig Rig - Contributions to the Drillbotics Competition 2018." MSc, Norwegian University of Science and Technology. doi:11250/2559474.

Appendix A – Article 1

Micro-Testing While Drilling for Rate of Penetration Optimization

Magnus Nystad, Alexey Pavlov

This paper was presented at ASME 2020 39th International Conference on Ocean, Offshore and Arctic Engineering, August 3-7, 2020, Virtual, Online, and published in the conference proceedings. doi: 10.1115/OMAE2020-18838.

MICRO-TESTING WHILE DRILLING FOR RATE OF PENETRATION OPTIMIZATION

Magnus Nystad[1], Alexey Pavlov
Norwegian University of Science and Technology
Trondheim, Norway

ABSTRACT

The Rate of Penetration (ROP) is one of the key parameters related to the efficiency of the drilling process. Within the confines of operational limits, the drilling parameters affecting the ROP should be optimized to drill more efficiently and safely, to reduce the overall cost of constructing the well. In this study, a data-driven optimization method called Extremum Seeking is employed to automatically find and maintain the optimal Weight on Bit (WOB) which maximizes the ROP. To avoid violation of constraints, the algorithm is adjusted with a combination of a predictive and a reactive approach. This method of constraint handling is demonstrated for a maximal limit imposed on the surface torque, but the method is generic and can be applied on various drilling parameters. The proposed optimization scheme has been tested on a high-fidelity drilling simulator. The simulated scenarios show the method's ability to steer the system to the optimum and to handle constraints and noisy data.

Keywords: Data-Driven, ROP, Drilling Optimization, Micro-Testing, Constraint Handling, Extremum Seeking

INTRODUCTION

A substantial part of offshore field development costs originates from drilling, with most of these costs being related to time. There is a great potential for cost reduction by drilling safer, faster and with less non-productive time, which is why drilling optimization has been the subject of research for more than six decades, a process which has been traced by Eren and Ozbayoglu [1]. Methods used for real-time drilling optimization often focus on tuning physics-based models of the drilling process to fit available data from current or offset operations. The tuned models are used to predict how the drilling process will react to different values of the controllable parameters such as WOB, drill string rotational speed (RPM) and flow rate. Based on this prediction, the models can be used to provide estimates of the optimal drilling parameters, which can be supplied to the driller as suggestions or directly fed to the control system on the rig in a closed loop [1-5]. Field tests of an ROP optimization algorithm using physics-based models have shown good results, with the largest increases in ROP obtained when the algorithm was run in closed loop [2,3] and a reduction in downhole tool failures when applying the optimization algorithm [3].

A potential drawback to real-time optimization with the physics-based models is that the analysis is based on a mathematical description of the drilling process, and the existing models might not be very accurate in predicting the ROP [5,6]. A possible remedy for model inaccuracies could be the use of data-driven modelling techniques, or a hybrid between data-driven and physics-based modelling methods. The latter approach was applied by Spencer et al. [7] in a study on how to automatically minimize Mechanical Specific Energy (MSE) when drilling through layered materials with a lab-scale rig. A physics-based drilling model was used to find an initial estimate of the optimal WOB. A data-driven algorithm was subsequently utilized while drilling to search the neighborhood of the initial estimate for WOB values which could further reduce the MSE. Hegde et al. [8] found that a data-driven model gave better ROP predictions compared to physics-based models when both approaches were using the same input parameters. The selection of which type of data-driven model that can be used for real-time optimization is a tradeoff between runtime and performance where more advanced models will give more accurate ROP predictions but suffer from longer computational time and vice versa [9]. A recent study investigated the application of a data-driven optimization strategy with low computational cost called Extremum Seeking (ES) to maximize the ROP [10]. Using simulated data, it was shown that ES can identify the WOB

[1] Contact author: magnus.nystad@ntnu.no

which maximizes the ROP and automatically steer the WOB to this optimal value in an unconstrained environment.

The drilling process is subject to a multitude of operational constraints which affect the safe operational space of the input parameters. Chapman et al. [3] gives a detailed list of factors that could directly limit the application of the controllable parameters such as a maximal WOB and RPM dictated by the drilling equipment, as well as listing more indirect factors related to torque, vibrations and hole cleaning which will limit certain combinations of input parameters. Dunlop et al. [2] further describe the implementation of these constraints for real-time drilling optimization. Factors limiting the amount of energy that can be applied to the drilling process through the controllable input parameters and factors which diminish the efficiency of the energy transferal between input parameters and ROP have also been investigated [11,12]. A solution for constraint handling in data-driven modelling is to limit the data used as the training set to values that do not violate constraints and not allowing the model to extrapolate results outside of this region [9].

The data used to tune or train the models used for real-time optimization, both physics-based and data-driven, needs to be representative of the current drilling conditions (e.g. from the same formation) to yield more accurate predictions [1,8]. A changepoint algorithm which determines what historical data is relevant for the task of ROP modelling and optimization has been implemented [2]. Using a sliding window of data containing a fixed amount of the most recent measurements to tune a physics-based drilling model has also been suggested [4,5]. In addition to using representative data, the models need a varied sample of input (e.g. WOB and RPM) and output parameters (e.g. ROP) within this dataset to generate a representative data-driven model [9] or to tune the parameters in a physics-based model. A drilling advisory system which suggests changes in input parameters to the driller for the purpose of exploring the parameter space and identifying the operational point which minimizes the MSE has been field tested with good results [13].

Extremum seeking has previously been implemented successfully in a variety of engineering systems ranging from yield optimization in bioprocesses to jet engine stability control and many others [14], as well as in the petroleum industry for gas lift [15,16] and has been investigated for the purpose of drilling optimization [10]. The ES algorithm is a gradient ascent (or descent) method which requires a process with well-defined steady-state characteristics, so that for a given constant input, the system settles to a constant output within a reasonable time. It also needs the existence of a unique extremum in the output which corresponds to some value in the input variable(s) within the operational envelope. A more thorough review of these conditions and convergence criteria can be found in Tan et al. [14] or Ariur and Krstić [17]. When the system conditions are satisfied, the ES algorithm will automatically seek and maintain the value of the optimal input variable(s), without knowing the details of the relationship between the system's input and output.

The method we employ in this study is an ES algorithm that searches for the WOB which optimizes the ROP by use of real-time drilling data. While drilling ahead, the ES algorithm prescribes a continuous series of micro-tests by sending commands for variations in the WOB to the autodriller. The micro-tests are performed by periodically varying the input WOB around some base value to gather information about the current drilling conditions, and the data generated from this procedure is the training data used by the ES algorithm. The magnitude and frequency of the WOB variations are determined before the start of drilling and should be designed to induce a measurable change in the ROP, without interfering much with the overall drilling process. The algorithm relates the changes in the output ROP to the corresponding variations in the input WOB and uses this information to estimate the gradient of the output in the local region which has been investigated by the micro-test procedure. A sliding window of recent data is used to estimate the current gradient by means of linear least-squares regression. The gradient is automatically used to determine the direction and magnitude in which the WOB base value should be changed to increase the ROP by providing the autodriller with updated setpoints for the WOB. By continuously repeating this procedure, the ES algorithm can navigate the system to its optimal point and keep the process at its optimum by continuing to probe for changes in the system conditions.

Hegde, Wallace and Gray [18] found that regression modelling methods gave acceptable ROP prediction, but the accuracy of the prediction suffers from the nonlinearity between the ROP and the regressors, among others the WOB. The gradient estimated by the ES algorithm is based on a relatively small region defined by the extent of the most recent variations in the WOB. In this local region the accuracy of a linear approximation of the nonlinear relationship between the ROP and the WOB will suffer less than when one considers a wider range of ROP and WOB values.

We focus in this study on the practical aspects related to using ES for drilling optimization. The ES algorithm is automatically making changes to the applied WOB to maximize the ROP. To ensure that the algorithm does not steer the WOB to values which will result in e.g. the torque exceeding its maximal limit, a combination of a predictive and a reactive constraint handling technique is proposed. The constraint handling is based on real-time measurements while drilling and is demonstrated for a maximal limit imposed on the surface torque, but the method is generic and can be applied on various drilling parameters. The proposed optimization scheme is able to handle the process and measurement noise inherent to the drilling process, which can have a strong effect on the algorithm performance. Compared to the classical filter-based ES scheme (see e.g. Aarsnes, Aamo and Krstić [10]), the proposed method is also adjusted to ensure easier tuning of the system by using a least-squares method to estimate the gradient, which reduces the number of tuning parameters in the algorithm.

The paper is organized in the following way: first, the background of the problem is given, before the ES algorithm is described. Then, a control strategy for handling drilling constraints is detailed, followed by a section containing details on instantaneous ROP estimation. The last two sections contain simulation results and conclusions.

BACKGROUND

Drilling is a complicated process with a multitude of factors affecting the ROP, such as personnel and rig efficiency, formation characteristics, mechanical and hydraulic factors, and drilling fluid properties [4]. These many and often interconnected effects make accurate modelling of the process in real-time a complex task, because many of the parameters needed to correctly model the situation are not measured directly and will change over time. However, the general mechanics of the interaction between the bit and formation are well understood [19]. The instantaneous ROP can be described by

$$ROP = f(WOB, \boldsymbol{r}), \tag{1}$$

where $\boldsymbol{r}$ is a vector containing all parameters other than the WOB which affect the ROP, such as RPM, flow rate, bit condition, bottomhole pressure and formation properties. The nonlinear function f which governs the relationship between the WOB, $\boldsymbol{r}$ and the ROP is not known explicitly, but for any set of values for the parameters contained in $\boldsymbol{r}$ it is assumed that f as a function of WOB inhibits several characteristic drilling regimes. Figure 1 shows a nominal relationship between the ROP and the applied WOB, where it is assumed that the values of the parameters in $\boldsymbol{r}$ are constant. The ROP-WOB relationship is characterized by three distinct phases: 1) Inefficient drilling caused by low WOB, where the depth of cut is inadequate, 2) efficient drilling where all added WOB is transferred to cutting action at the bit in a straight-line fashion, and 3) inefficient drilling caused by founder [11,19]. The locations of the different phases in the ROP-WOB relationship are subject to change as parameters in the vector $\boldsymbol{r}$ vary, but the general shape of the three regions is expected to remain. A change in formation properties or an increase in RPM could alter the WOB at which foundering occurs, but WOB lower than the foundering value would still correspond to efficient drilling and values above founder would constitute inefficient drilling. The shape of the third region depends on what type of inefficiency is causing it, which could be excessive vibrations or inadequate cleaning at the bit. Depending on the cause of founder, its onset could be delayed by manipulation of combinations of drilling parameters or reengineering of the system [11,12], but these approaches are beyond the scope of this paper.

The transition between the last two regions in Figure 1 is referred to as the founder point, and it is drilling at WOB which corresponds to this point or slightly below that is mainly desired. In this way, the possibly detrimental effects causing the founder as well as the bit wear resulting from a large increase in WOB for a small increase in ROP can be avoided. A convenient way of approaching this situation is to try and maximize not the ROP itself, but a performance function on the form

$$J = ROP - \mu WOB, \tag{2}$$

where μ is a tuning parameter which penalizes the use of excessive WOB [10]. As the ES optimization scheme outlined in the next section is driven by an estimated gradient of J with respect to the WOB, the algorithm seeks the optimum given by

$$\frac{\partial J}{\partial WOB} = \frac{\partial ROP}{\partial WOB} - \mu = 0. \tag{3}$$

From equation (3), the physical meaning of μ can be interpreted as a limiting value at which the ROP gradient is deemed too low to want to further change the WOB, even though the maximal ROP is not yet achieved. A larger value for μ will therefore correspond to a more conservative estimate of what the optimal operating point is.

In practice, the drilling process is subject to constraints which might limit how much WOB can be applied, so that drilling at the founder point may not be feasible. A multitude of constraints like this have been identified by Dupriest and Koederitz [11] and Chapman et al. [3], such as available BHA weight, solids handling capacity and top drive torque rating. A method of avoiding violation of limitations while searching for the founder point is outlined in the constraints handling section.

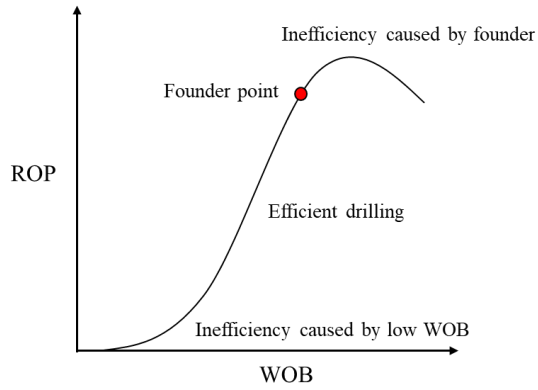

FIGURE 1: NOMINAL RELATIONSHIP BETWEEN ROP AND WOB, MODIFIED FROM DUPRIEST AND KOEDERITZ [11].

EXTREMUM SEEKING FOR ROP OPTIMIZATION

The variables that the driller or an algorithm can readily control from the rig floor to affect the ROP are the WOB, the RPM and the flow rate. In this paper, we consider the case of optimizing the ROP by means of controlling the WOB in a constrained ES approach, with constant RPM and flow rate. The method is illustrated in Figure 2, where a continuous excitation signal is applied to the WOB to investigate the steady-state characteristics of an output performance function defined by equation (2). Under the assumption that the ROP-WOB relationship is subject to the different drilling regimes outlined in the Background section, the drilling process has a unique optimal WOB at which foundering starts to occur and is well suited for optimization with ES.

Although drilling is a continuous process, the sampled measurements and the commands given to the control system on the rig are performed in discrete time. This motivates the notation used here: t is the current time, Δt is the time interval between both measurements of drilling parameters and updated setpoints provided to the autodriller (here assumed to be the same), so that $t + \Delta t$ signifies a value for the coming timestep.

The ES algorithm can be divided into three main components: 1) The excitation signal, which introduces a variation in the input of the system, 2) the gradient estimator, used to quantify how the system reacts to the excitation, and 3) the optimizer, which changes the input WOB based on the estimated gradient. These components are described in detail in the following sections.

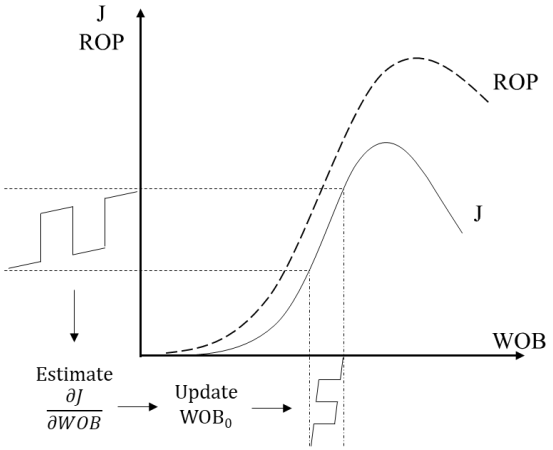

FIGURE 2: CONCEPT ILLUSTRATUION OF EXTREMUM SEEKING APPLIED TO DRILLING.

The Excitation Signal

Some best estimate of the optimal input value, WOB_0, is initially applied to the system. This estimate could be based on calculations from an available drilling model or experience from a similar offset well. While drilling ahead, the ES algorithm continuously explores the neighborhood of WOB_0 and how the system responds to small variations in the WOB by conducting a series of micro-tests. This is done by automatically varying the WOB-setpoint provided to the autodriller according to

$$WOB(t) = WOB_0(t) + d(t, A, P). \tag{4}$$

The last term in equation (4) is the excitation signal, which for any integer, n, is given by

$$d(t, A, P) = \begin{cases} A & t \in \left[nP, \left(n + \frac{1}{2}\right)P\right\rangle \\ -A & t \in \left[\left(n + \frac{1}{2}\right)P, (n+1)P\right\rangle \end{cases}. \tag{5}$$

This signal is a square wave with an amplitude of A kg and a period of P seconds, which oscillates symmetrically about WOB_0. For each period, the magnitude of A approximately determines the extent of the WOB-interval which is being investigated by the algorithm. A should be small enough to not detrimentally affect the overall drilling process, but at the same time be large enough to elicit a measurable change in the ROP which can be used for gradient estimation. The period of the excitation signal determines the amount of historical data used to estimate the gradient of the performance function and needs to be tuned accordingly. The parameter P should be designed large enough to generate a dataset that contains enough information so that it can be used for gradient estimation, while at the same time considering that a very large value for P will result in a lot of previous drilling data (which might no longer be representative of the current drilling conditions) being used for gradient estimation.

Gradient Estimation

The applied WOB and the resulting values of J calculated from equation (2) are stored in a buffer containing P seconds of history for these two parameters, denoted by WOB_B and J_B. At each update of measurements, the past values of J(t) and WOB(t) stored in the buffer are used to solve the 1st-order least-squares problem given by

$$\min_{a,b} \sum_{i=0}^{P-1} \left(J_B(t - i\Delta t) - (aWOB_B(t - i\Delta t) + b)\right)^2, \tag{6}$$

where a and b are the slope and intercept of the least-squares fit, respectively. These two parameters represent a linear approximation to how J has changed with the varying WOB for the past P seconds. The slope parameter a is used as an estimate of the gradient of the performance function at the current timestep,

$$\frac{\partial J}{\partial WOB}(\mathrm{t}) \approx a(t). \tag{7}$$

In this way, a sliding window of data corresponding to one full period of the excitation signal is used to estimate the current gradient of J. On average, this estimate corresponds to the formation which was drilled $P/2$ seconds earlier, as this is the center of the sliding window. The excitation signal is symmetric about the slowly varying WOB_0, so that equation (7) represents a gradient evaluated approximately at WOB_0.

This technique of gradient estimation is a variant of the method proposed by Hunnekens et al. [20], where least-squares estimation was used in an ES algorithm without an excitation signal. This way of calculating the gradient is robust with respect to noise and sensor bias, since much of the noise is filtered out over the least-squares window, and any sensor bias is captured by the b-parameter, which is not used by the algorithm. In addition to this, the method is easier to apply than the classical filter-based ES approach. This is because the least-squares

gradient estimation does not require any tuning apart from determining the amplitude and period of the excitation signal, while the classical ES approach needs to tune both the excitation signal parameters and the filters to obtain an estimated gradient.

Optimizer

From Figure 2 it can be seen that the performance function has a positive slope when drilling with a WOB to the left of the maximal value of *J*, and a negative slope for WOB values beyond this point. The gradient obtained from equations (6) and (7) can thus be used to determine how the WOB should be altered to increase the performance function, *J*. This is done by calculating an updated WOB_0 value for the coming timestep from

$$WOB_0(t + \Delta t) = WOB_0(t) + \gamma \frac{\partial J}{\partial WOB}(t)\Delta t, \qquad (8)$$

which will move the drilling system to a slightly higher value of *J*. The parameter γ is a gain which determines the *learning dynamics* of the algorithm. That is, how fast the ES scheme should vary WOB_0 as a response to the estimated gradient of *J*. The new WOB_0 value calculated from equation (8) is used to update the WOB which will be sent to the autodriller in the next timestep, as dictated by equation (4) evaluated at $t + \Delta t$. The algorithm will subsequently repeat the process of estimating a new gradient based on new measurements and adapting to the newest information. It is worth noting that this update takes place at each timestep, with γ tuned so that WOB_0 varies slowly compared to the variations in WOB caused by the excitation signal. In the constrained case, the WOB_0 value requested by the algorithm is calculated from equation (14).

A block diagram of the described optimization structure is shown in Figure 3. Each timestep constitutes a loop through this diagram, where the algorithm will vary the WOB according to equation (4), record and quantify the system response with equations (6) and (7) and use this information in equation (8) to update the WOB which should be applied to initiate a new iteration of the algorithm.

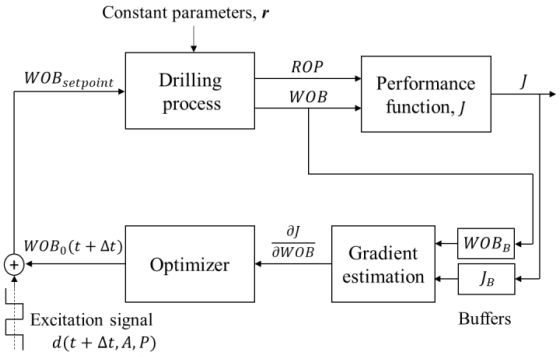

FIGURE 3: ES SCHEME FOR UNCONSTRAINED DRILLING OPTIMIZATION.

ROP OPTIMIZATION WITH CONSTRAINT HANDLING

The optimization algorithm proposed in the previous section will be able to steer the drilling system to the optimum dictated by the performance function. In practice, operating at this point might not be feasible. Some reasons for this could be that the required WOB might exceed the available BHA weight or allowable WOB, there could be a maximal ROP limit related to cuttings transport or handling of cuttings at the surface, or the torque generated at the bit or at the surface could exceed the allowable values. Two methods for making the ES algorithm avoid violation of this type of constraints while searching for the optimum is presented below. The methods are illustrated for a maximal limit imposed on the surface torque, but the techniques are generic and could also be used on other limiting parameters.

Predictive Constraint Handling

The changes in the drilling process caused by varying the WOB can be a good source of information about the current system conditions and how other drilling parameters are affected by the WOB. The same methodology as was used to extract an estimate of the gradient of *J* in equations (6) and (7) is also able to estimate gradients of other drilling parameters and how they vary with the changing WOB. By storing measured values of the surface torque in an additional buffer, T_B, containing *P* seconds of data, the gradient of the surface torque can be calculated from

$$\min_{\alpha,\beta} \sum_{i=0}^{P-1} \left(T_B(t - i\Delta t) - (\alpha WOB_B(t - i\Delta t) + \beta)\right)^2, \qquad (9)$$

$$\frac{\partial T}{\partial WOB}(t) \approx \alpha(t). \qquad (10)$$

The parameters α and β are the slope and intercept of the least-squares fit, respectively. The gradient estimate given by equations (9) and (10) can be used to predict how the surface torque will react to further changes in the WOB, and how to avoid violation of constraints based on this information.

The recorded surface torque is often plagued by noise, both from inaccurate measurements and process noise in the form of drillstring vibrations. Because of this, there is some uncertainty as to what the value of the surface torque is. To remedy this issue, the average value of the torque buffer, $T_{B,avg}$, is taken as the surface torque, which approximates the torque experienced by the system when drilling with a weight on bit of WOB_0. This averaging will reduce the amount of noise in the torque value used by the algorithm, but it will also introduce a time delay in the averaged torque value corresponding to half of the averaged period, the same delay that is inherently present in the gradient calculated in equations (9) and (10).

To avoid the WOB being steered to values which cause a violation of the allowable torque, T_{limit}, the gain parameter γ in equation (8) is calculated as

$$\gamma = \begin{cases} \gamma\,, & \left(T_{B,avg} + A\frac{\partial T}{\partial WOB}(t)SF\right) < T_{limit} \\ 0\,, & \left(T_{B,avg} + A\frac{\partial T}{\partial WOB}(t)SF\right) \geq T_{limit} \end{cases}, \quad (11)$$

where SF is a safety factor greater than 1. Because the algorithm varies the weight on bit about WOB_0 with a magnitude of *A* kg, equation (11) will stop the optimizer from exceeding the torque limit with a margin dictated by the SF parameter. This method also allows the excitation signal to continue the micro-testing for changes in the drilling conditions, even when the torque is close to the highest allowable value. The value for T_{limit} used in equation (11) should be lower than the maximal limit the drilling system can handle, as an added safety measure.

Reactive Constraint Handling

In some instances, the predictive constraint handling detailed in equation (11) might not be enough to ensure that the torque stays within the allowable boundaries. This could be caused by either very noisy measurements which makes the calculated torque gradient inaccurate, or abrupt changes in drilling conditions, such as a formation change, which alters the torque in a short span of time. To ensure safe operations, a reactive constraint handling technique is implemented using a variable which is equal to zero if the constraint is not violated and proportional to the violation if the torque limit is exceeded,

$$e(t) = \begin{cases} 0\,, & T_{avg} < T_{limit} \\ T_{avg}(t) - T_{limit}\,, & T_{avg} \geq T_{limit} \end{cases}. \quad (12)$$

T_{avg} is an average value spanning a few seconds of the most recent torque measurements, e.g. 5 seconds, to remove some of the measurement noise while still being representative of the current torque. This average parameter is introduced so that the constraint handling routine will not react to very short-term spikes in the measured surface torque. The value for T_{limit} should be lower than the actual system limit, because the reactive constraint handling will only start to affect the system when T_{avg} is larger than T_{limit}. The variable *e* from equation (12) is used to calculate a penalty variable, λ, by use of a discrete PI controller,

$$\lambda(t) = K_P e(t) + K_I \sum_{i=0}^{t} e(i)\Delta t. \quad (13)$$

K_P and K_I are the proportional and integral gains, respectively, which are the tuning parameters that determine how aggressively the controller should penalize torque values above the limit. The penalty term calculated from equation (13) is used to reduce the weight on bit demanded by the ES algorithm according to

$$WOB_{0,constrained}(t + \Delta t) = WOB_0(t + \Delta t) - \lambda(t). \quad (14)$$

The parameter $WOB_{0,constrained}$ is used in equation (4) to calculate the constrained WOB setpoint which is sent to the autodriller. The first term on the right-hand side of equation (14) is the unconstrained WOB_0 value found by the optimizer, equation (8), which is calculated independently of the reactive constraint handling. If the torque limit has not been violated, λ will be equal to zero and the constrained WOB_0 value will be equal to the WOB_0 found by the optimizer. If the torque limit is exceeded, the WOB demanded by the ES algorithm will be reduced until the torque is again below its limiting value, at which point λ will retain a value determined by the summation term in equation (13). How fast the reduction in WOB takes place once the constraint is violated is controlled by the gain parameters K_P and K_I in equation (13). They should be large enough to ensure that the penalty variable, λ, reduces the requested WOB faster than the adaptation gain, γ, is able to demand increases in the WOB.

PRACTICAL CONSIDERATIONS

Instantaneous ROP Estimation

The proposed optimization algorithm relies heavily on causing a change in the ROP by varying the WOB and being able to quantify this change. The ROP is not a directly measured parameter, but rather calculated as a derivative of the position of the travelling block or other surface equipment, possibly with a model to account for the elasticity of the drill string. This differentiation procedure will amplify any inaccuracies in the measured block position, making the calculated ROP imprecise. These inaccuracies could be caused by measurement noise, rig heave or unaccounted for elongation and shortening of the drilling line when the hook position is estimated from the drawworks. A common way of dealing with this issue is to use ROP values averaged over a certain time or depth increment, which will reduce the inaccuracy but cause a time-delay in the estimated ROP.

In this paper, the instantaneous ROP is approximated as the velocity of the travelling block. This is done by means of a Kalman Filter (KF), which is designed to account for process and measurement noise to yield a better ROP estimate. The KF is based on a linear state-space model which describes the relationship between the block position, h_{block}, and its derivative, the ROP, in consistent units as

$$\begin{bmatrix} h_{block} \\ ROP \end{bmatrix}(t + \Delta t) = \begin{bmatrix} 1 & -\Delta t \\ 0 & 1 \end{bmatrix}\begin{bmatrix} h_{block} \\ ROP \end{bmatrix}(t) + w(t). \quad (15)$$

The last term in equation (15) is the process noise, which represents any forces which affects the ROP and makes it non-constant, which in turn will affect the hook position. This could be a change in drilling conditions or variations in the input WOB, RPM or flow rate. The measurement of the block position is described by

$$y(t) = \begin{bmatrix} 1 & 0 \end{bmatrix}\begin{bmatrix} h_{block} \\ ROP \end{bmatrix}(t) + v(t). \quad (16)$$

In equation (16), *y* represents the measured block position, which is made inaccurate by the measurement noise, *v*.

The KF uses a combination of the h_{block} and ROP predicted by equation (15) and the measured *y* from equation (16) to yield

an estimate of what the true ROP is. This combination is done based on how much noise is affecting equations (15) and (16), where the KF will trust the ROP from equation (15) more if there is a lot of measurement noise compared to process noise, and vice versa. The values of *v* and *w* at any given time are not known by the filter, but some assumptions are made about them. The KF assumes that the disturbances are normally distributed variables which continuously affect the system, and that their distribution is described by

$$w \sim N(0, Q), \qquad Q = \begin{bmatrix} \frac{(\Delta t)^4}{4} & \frac{(\Delta t)^3}{2} \\ \frac{(\Delta t)^3}{2} & (\Delta t)^2 \end{bmatrix} \sigma_p^2, \qquad (17)$$

$$v \sim N(0, R), \qquad R = \sigma_m^2. \qquad (18)$$

In equations (17) and (18), Q and R are the covariance matrices of the process and measurement noise, respectively. The parameter σ_m is the standard deviation of the measurement noise and is presumed known from the specifications of the applied sensor or measurement technique. The standard deviation of the process noise, σ_m, is then the only unknown factor in equations (15) - (18) and is used as a tuning parameter for the KF. It should be noted that equations (15) and (17) can be derived from the 1st and 2nd equations of motion, where *w* captures the effect of a normally distributed acceleration affecting the system.

In practice, it is not expected that the process noise affecting the drilling rate and hook position is normally distributed and continuously affecting the system, as is assumed in equation (17). It is more likely that this noise is displayed as more discrete variations in the system caused by changing drilling conditions and the fluctuating WOB. Despite this, the Kalman filter will still be able to provide good estimates of the instantaneous ROP when properly tuned. A block diagram of the complete ES scheme with constraint handling and ROP estimation is shown in Figure 4.

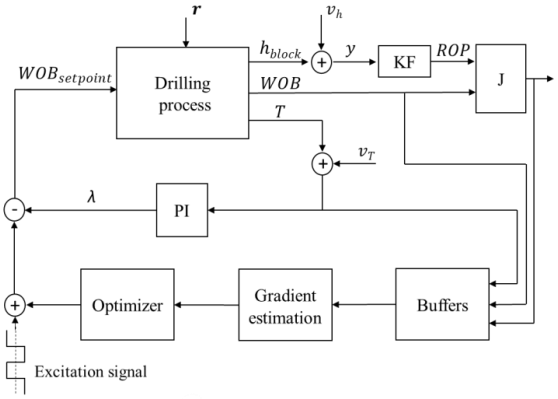

FIGURE 4: ES SCHEME FOR CONSTRAINED DRILLING OPTIMIZATION.

SIMULATION RESULTS

Drilling Simulator

The simulator used to study the proposed optimization technique is OpenLab, a high-fidelity drilling simulator developed by the Norwegian Research Centre (NORCE) in collaboration with the University of Stavanger. The simulator consists of a set of integrated numerical models covering different aspects of the drilling process, including torque and drag effects, cuttings transport, multi-phase flow and heat transfer [21]. The models on the OpenLab platform are run by supplying the simulator with setpoints for input variables, which the simulator translates to actions on the drill-floor with built-in functions which limits the allowable rate of changes according to equipment specifications [22].

To simulate the effects of measurement noise, an option to add white gaussian noise to the surface torque and block position was included in the system. These sources of noise are denoted by v_T and v_h, respectively, and can be seen in Figure 4. The noise parameters used in the simulations have been taken to match the noise from logged drilling operations.

Simulation Results

A series of simulations have been performed in OpenLab to investigate the applicability of the proposed optimization scheme. The simulations detailed here are all carried out in the 8.5" section of a vertical well, with drilling commencing at a depth of 2500 meters through a homogeneous formation. The system is set up to start the drilling of each new stand at an initial constant value of WOB for three minutes, followed by a full oscillation period of the excitation signal to estimate an initial gradient of *J*, before the ES algorithm starts the WOB-adaptation according to equation (14). Both RPM and flow rate are held constant throughout the runs, except when ramping up and down for connections every 27 meters. Parameters common for all the simulated scenarios are listed in Table 1. The value for μ used in the simulations signify that the optimum determined by *J* is reached when the ROP increases less than 5 m/hr for a 1000 kg increase in WOB. The simulations are all initiated at a conservative WOB value of 2000 kg, at which the ROP is 23 m/hr. The optimum point sought by the ES algorithm is found at 4700 kg of WOB and corresponds to a drilling speed of 43 m/hr, meaning that there is a potential increase in the ROP of 20 m/hr by drilling at the optimum WOB value.

TABLE 1: PARAMETERS COMMON FOR ALL SIMULATIONS.

Parameter	*Value*	*Unit*
A	200	kg
P	240	s
μ	0.005	m/hr/kg
Δt	1	s
K_p	0.5	kg/Nm
K_i	0.25	kg/Nm
SF	3	-
RPM	150	rpm
Q	2000	lpm
$WOB_0(t = 0)$	2000	kg

Simulations Without Measurement Noise

This section covers two simulated scenarios where three stands are drilled. The gain parameter γ in equation (8) is here set to a value of 400 $kg^2 \cdot hr/m/s$. No noise is added to the measurements, and the ROP used is the actual drilling rate reported by the simulator. The two simulation conditions are identical, with the exception of a limiting value for the surface torque of 5000 Nm which is imposed on the system in the second run. Figure 5 shows the resulting ROP, *J*, WOB and surface torque from these two simulations.

In simulation 1, the weight on bit is steered from 2000 kg to a WOB_0 value of about 4300 kg during the drilling of the first stand, before a connection takes place at approximately 2850 seconds. This adjustment in WOB results in an increase in ROP of 18 m/hr, which is 90% of the interval between the starting point and the optimum. The next two stands are spent drilling while the ES algorithm slowly makes the system converge to the optimal WOB value, at which the performance function is seen to flatten out and become constant.

The second simulation is initially identical to the first, before the increasing WOB causes the surface torque to become too close to the limiting value after 1400 seconds. At this point, the predictive constraint handling part of the algorithm stops the WOB-adaptation before the constraint is exceeded. Because the system is forced to drill with a WOB lower than the optimal value, the second simulation spends about 23 minutes more than the first to complete the three stands.

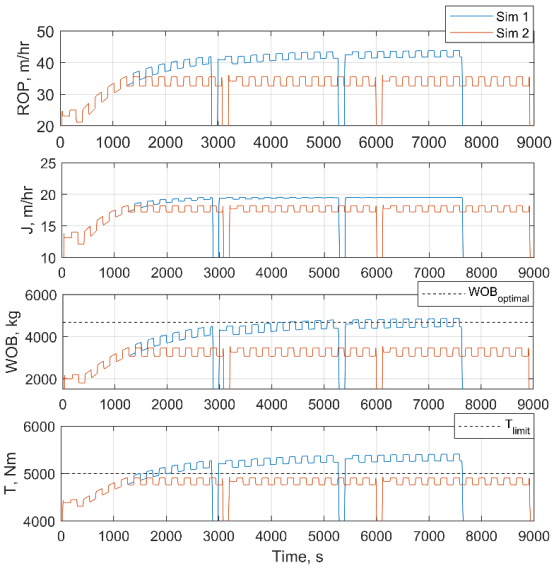

FIGURE 5: SIMULATIONS 1 AND 2, WHERE A TORQUE LIMIT IS IMPOSED ON THE SYSTEM IN SIMULATION 2.

Simulations with Measurement Noise

The results from simulations 3 and 4 are presented in Figure 6, where the latter run is limited by a maximal surface torque of 5000 Nm. Other than this, the scenarios are identical and are both performed with the parameters given in Table 2. A lower value of the adaptation gain, γ, is used in these simulations compared to the first two. The noise levels, v_h and v_T, are designed so that the measurements are disturbed by normally distributed random variables that take on values in the intervals $\pm$ 0.03 m and $\pm$ 500 Nm, respectively. The ROP used in the algorithm is estimated from noisy block measurements with the Kalman filter. The spikes seen in the estimated ROP at the start of each drilled stand in Figure 6 are caused by the KF, which overestimates the ROP initially, before it has more data to work with and is able to home in on the true ROP value. These ROP-spikes occur during the initiation of drilling where the weight on bit is held constant and are thus not used by the algorithm for adaptation of the WOB.

TABLE 2: PARAMETERS USED IN SIMULATIONS 3 AND 4.

Parameter	*Value*	*Unit*
v_h	$\sim N(0, 0.01)$	m
v_T	$\sim N(0, 167)$	Nm
σ_p	$3 \cdot 10^{-5}$	m/s^2
σ_m	10^{-2}	m
γ	250	$kg^2 \cdot hr/m/s$
T_{avg} interval	5	s

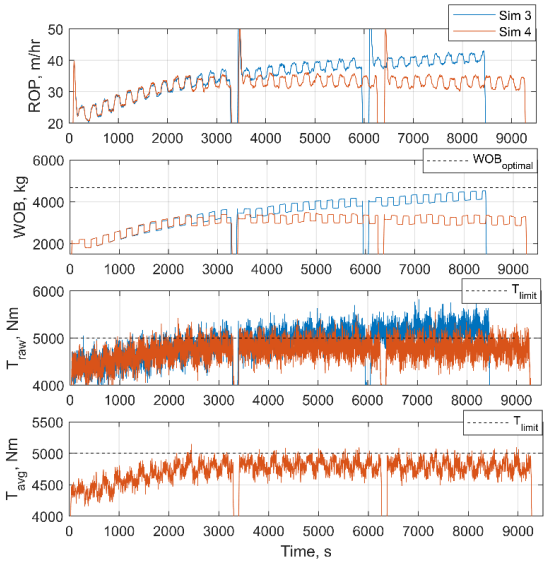

FIGURE 6: SIMULATIONS 3 AND 4, WHERE A TORQUE LIMIT IS IMPOSED ON THE SYSTEM IN SIMULATION 4.

Simulation 3 is from the second track in Figure 6 seen to be adapting towards the optimal WOB-value but is not able to reach it within the simulated interval. The fastest adaptation takes place during the drilling of the first stand, where he ROP is increased by about 12 m/hr from the initial value. This corresponds to 60% of the total ROP improvement sought by the algorithm in this scenario.

The third track in Figure 6 displays the "raw" noisy torque. This value is frequently seen to surpass the limiting torque, as the algorithm interprets it as very short-term fluctuations which it does not react to. The bottom track in Figure 6 shows the 5 second average torque value for simulation 4, which is used in equation (12) to determine when the torque is above the limit. After drilling for 2500 seconds and onwards, this T_{avg} value is seen to exceed the constraint for a short period of time on several occasions. Each time this occurs, a reduction in WOB takes place until the torque is again within its allowable values. As in simulation 2, the WOB in simulation 4 is not allowed to work its way further towards the optimum, which causes the drilling of the three stands to take more time.

Discussion of Results

Throughout the simulations, the ES algorithm is seen to adjust the WOB the fastest during the first drilled stand. This is caused by the adaptation being proportional to the gradient of the performance function. As the WOB closes in on its optimal value, this gradient will become smaller (see Figure 2). As can be observed in simulations 1 and 3, this property allows the ES algorithm to quickly modify the WOB to the neighborhood of the optimal value. After the initial fast adaptation, it slowly converges towards the optimum while continuously probing for any changes in drilling conditions. An important parameter which affects the adaptation rate of the algorithm is the gain parameter γ. On the one hand, it determines the rate of convergence of the WOB to the optimum. The larger it is, the faster is the convergence. On the other hand, higher values of γ will make the algorithm more sensitive to measurement and process noise, as the system makes larger adjustments even for small deviations caused by noise. Thus, finding a value for gamma which balances the convergence rate and sensitivity to noise is an important tuning task when using the ES algorithm.

The constraining torque value which is used in simulations 2 and 4 is only a fraction of what would be the allowable continuous torque of e.g. a top drive. The limitation is implemented to demonstrate the algorithm's ability to stay within constrictions in a practical manner while it searches for the optimum WOB, as is seen in the simulated scenarios. Simulation 4 demonstrates that when the constrained parameter (the torque) is very noisy, it can exceed the limit for short periods of time. This observation together with general HSE considerations necessitates that the maximal torque value implemented in the algorithm is lower than the actual system limitation.

The initial WOB_0 used in all the simulations is quite far from the optimal value. Even though the adaptation of the algorithm is faster when further away from the optimum, a more efficient optimization method in this scenario could be a hybrid between the data-driven and physics-based approaches, conceptually similar to what was done by Spencer et al. [7]. The information gathered from the initial WOB excitations could be used to roughly tune a physics-based drilling model, and the suggested optimal parameters provided by this model would be the starting point for the ES algorithm which would further home in on the founder point.

CONCLUSIONS

We present a data-driven optimization strategy which automatically seeks and maintains the optimal WOB maximizing the ROP. The algorithm does not require any model of the drilling process and utilizes continuous micro-testing of the drilling conditions to identify and implement adjustments of the WOB leading to higher ROP. The micro-testing procedure does not cause any significant perturbation to the drilling process and is run continuously to adapt to the current drilling environment. The algorithm has been tested on a high-fidelity drilling simulator where it demonstrated the ability to steer the WOB to values resulting in higher ROP both with and without the presence of noise in the data. The simulated scenarios show that the proposed optimization strategy is able to automatically search for and implement improvements in the ROP while adhering to process constraints, where the constraint handling was demonstrated with the example of a maximal limit imposed on the surface torque.

NOMENCLATURE

Parameters

a	Least-squares slope	(m/hr/kg)
α	Least-squares slope	(Nm/kg)
A	Amplitude of excitation signal	(kg)
b	Least-squares intercept	(m/hr)
β	Least-squares intercept	(Nm)
d	Excitation signal	(kg)
Δt	Time increment	(s)
e	Torque limitation variable	(Nm)
γ	Adaptation gain	($kg^2 \cdot hr/m/s$)
h_{block}	Height of travelling block	(m)
J	Performance function	(m/hr)
J_B	Buffer with past J values	(m/hr)
λ	Penalty variable	(kg)
μ	Parameter in J	(m/hr/kg)
N	Probability density function of the normal distribution	
P	Period of excitation signal	(s)
Q	Process noise covariance matrix	
r	Vector of drilling parameters	
R	Measurement noise covariance matrix	
σ_m	Measurement noise std. dev.	(m)
σ_p	Process noise standard deviation	(m/s^2)
t	Time	(s)
T	Torque	(Nm)
T_{avg}	5 second average torque value	(Nm)
T_B	Buffer with past torque values	(Nm)

$T_{B,avg}$	Average value of T_B	(Nm)
T_{limit}	Limiting torque value	(Nm)
v	Measurement noise	
v_h	Measurement noise in h_{block}	(m)
v_T	Torque measurement noise	(Nm)
w	Process noise	
WOB_0	Center WOB value in d	(kg)
$WOB_{0,constrained}$	Constrained WOB_0 value	(kg)
WOB_B	Buffer with past WOB values	(kg)
y	Measurement of h_{block}	(m)

Abbreviations

ES	Extremum Seeking	
KF	Kalman Filter	
MSE	Mechanical Specific Energy	
ROP	Rate of Penetration	(m/hr)
RPM	Revolutions per Minute	(rpm)
SF	Safety Factor	
WOB	Weight on Bit	(kg)

ACKNOWLEDGEMENTS

This research is a part of BRU21 – NTNU Research and Innovation Program on Digital and Automation Solutions for the Oil and Gas Industry (www.ntnu.edu/bru21).

REFERENCES

[1] Eren, T., and Ozbayoglu, M. E., 2010, "Real Time Optimization of Drilling Parameters During Drilling Operations", *Society of Petroleum Engineers*, doi:10.2118/129126-MS.

[2] Dunlop, J., Isangulov, R., Aldred, W. D., Sanchez, H. A., Flores, J. L. S., Herdoiza, J. A., Belaskie, J., and Luppens, C., 2011, "Increased Rate of Penetration Through Automation," *Society of Petroleum Engineers,* doi:10.2118/139897-MS.

[3] Chapman, C. D., Sanchez, J. L., De Leon Perez, R., and Yu, H., 2012, "Automated Closed-Loop Drilling with ROP Optimization Algorithm Significantly Reduces Drilling Time and Improves Downhole Tool Reliability," *Society of Petroleum Engineers,* doi:10.2118/151736-MS.

[4] Sui, D., Nybø, R., and Azizi, V., 2013, "Real-Time Optimization of Rate of Penetration During Drilling Operation," *10th IEEE International Conference of Control and Automation*, Hangzhou, China, pp. 357-362.

[5] Sui, D., Aadnøy, B. S., 2016, "Rate of Penetration Optimization Using Moving Horizon Estimation," *Modeling, Identification and Control,* **37**(3), pp. 149-158.

[6] Bataee, M., Kamyab, M., and Ashena, R., 2010, "Investigation of Various ROP Models and Optimization of Drilling Parameters for PDC and Roller-cone Bits in Shadegan Oil Field," *Society of Petroleum Engineers,* doi:10.2118/130932-MS.

[7] Spencer, J. S., Mazumdar, A., Su, J. C., Foris, A., and Buerger, S. P., 2017, "Estimation and Control for Efficient Autonomous Drilling Through Layered Materials," *American Control Conference*, Seattle, WA, pp. 176-182.

[8] Hegde, C., Daigle, H., Millwater, H., and Gray, K., 2017, "Analysis of Rate of Penetration (ROP) Prediction in Drilling Using Physics-Based and Data-Driven Models," *Journal of Petroleum Science and Engineering*, 159, pp. 295-306.

[9] Hegde, C., Daigle, H., and Gray, K. E., 2018, "Performance Comparison of Algorithms for Real-Time Rate-of-Penetration Optimization in Drilling Using Data-Driven Models," *Society of Petroleum Engineers,* doi:10.2118/191141-PA

[10] Aarsnes, U. J. F., Aamo, O. M., and Krstić, M., 2019, "Extremum Seeking for Real-time Optimal Drilling Control," *2019 American Control Conference,* Philadelphia, PA, USA, pp. 5222-5227.

[11] Dupriest, F. E., and Koederitz, W. L., 2005, "Maximizing Drill Rates with Real-Time Surveillance of Mechanical Specific Energy," *Society of Petroleum Engineers*, doi:10.2118/92194-MS.

[12] Dupriest, F. E., 2006, "Comprehensive Drill Rate Management Process to Maximize ROP," *Society of Petroleum Engineers,* doi:10.2118/102210-MS

[13] Chang, D. L., Payette, G. S., Pais, D., Wang, L., Bailey, J. R., and Mitchell, N. D., 2014, "Field Trial Results of a Drilling Advisory System," *International Petroleum Technology Conference*, doi:10.2523/IPTC-17216-MS

[14] Tan, Y., Moase, W. H., Manzie, C, Nešić D., and Mareels, I. M. Y., 2010, "Extremum seeking from 1922 to 2010," *Proceedings of the 29th Chinese Control Conference*, Beijing, pp. 14-26.

[15] Peixoto, A. J., Pereira-Dias, D., Xaud, A.F.S., and Secchi, A.R., 2015, "Modelling and Extremum Seeking Control of Gas Lifted Oil Wells," *IFAC-PapersOnLine,* **48**(6), pp. 21-26.

[16] Krishnamoorthy, D., Pavlov, A., and Li, Q., 2016, "Robust Extremum Seeking Control with application to Gas Lifted Oil Wells," *IFAC-PapersOnLine,* **49**(13), pp. 205-210.

[17] Ariur, K. B. and Krstić, M., 2003, Real-Time Optimization by Extremum-Seeking Control, *John Wiley & Sons.*

[18] Hegde, C. M., Wallace, S. P., and Gray, K. E., 2015, "Use of Regression and Bootstrapping in Drilling Inference and Prediction," *Society of Petroleum Engineers*, doi:10.2118/176791-MS

[19] "The IADC Drilling Manual," 2014, *International Association of Drilling Contractors,* 12th ed., Chap. DP.

[20] Hunnekens, B. G. B., Haring, M. A. M., van de Wouw, N., and Nijmeijer, H., 2014, "A Dither-Free Extremum-Seeking Control Approach Using 1st-Order Least-Squares Fits for Gradient Estimation," *53rd IEEE Conference on Decision and Control, Los Angeles, CA,* pp. 2697-2684.

[21] Ewald, R., Gravdal, J. E., Sui, D., and Shor, R., 2018, "Web enabled High Fidelity Drilling Computer Model with User-Friendly Interface for Education, Research and Innovation", *Proceedings of the 59th Conference on Simulation and Modelling,* Oslo, Norway, pp. 162-168.

[22] Saadallah, N., Gravdal, J. E., Ewald, R., Moi, S., Ambrus, A., Daireaux, B., … Odgaard, J., 2019, "OpenLab: Design and Applications of a Modern Drilling Digitalization Infrastructure," *Society of Petroleum Engineers*, doi:10.2118/195629-MS.

Appendix B – Article 2

Micro-Testing While Drilling for Rate of Penetration Optimization: Experiments and Simulations

Magnus Nystad, Bernt Sigve Aadnøy, Alexey Pavlov

This paper was submitted to ASME Journal of Offshore Mechanics and Arctic Engineering, March 2021, and is currently undergoing peer review.

Submitted to Journal of Offshore Mechanics and Arctic Engineering

Micro-Testing While Drilling for Rate of Penetration Optimization: Experiments and Simulations

Magnus Nystad[1]
Norwegian University of Science and Technology
Department of Geoscience and Petroleum, S.P. Andersens veg 15a, 7031 Trondheim
e-mail: magnus.nystad@ntnu.no

Bernt Sigve Aadnøy
Norwegian University of Science and Technology/University of Stavanger
Department of Geoscience and Petroleum, S.P. Andersens veg 15a, 7031 Trondheim/
Department of Energy and Petroleum Engineering, Kristine Bonnevies vei 22, 4021 Stavanger
e-mail: bernt.s.aadnoy@ntnu.no/bernt.aadnoy@uis.no

Alexey Pavlov
Norwegian University of Science and Technology
Department of Geoscience and Petroleum, S.P. Andersens veg 15a, 7031 Trondheim
e-mail: alexey.pavlov@ntnu.no

ABSTRACT

The Rate of Penetration (ROP) is one of the key parameters related to the efficiency of the drilling process. Within the confines of operational limits, the drilling parameters affecting the ROP should be optimized to drill more efficiently and safely, to reduce the overall cost of constructing the well. In this study, a data-driven optimization method called Extremum Seeking (ES) is employed to automatically find and maintain the optimal Weight on Bit (WOB) which maximizes the ROP. The ES algorithm is a model-free method which gathers information about the current downhole conditions by automatically performing small tests with the WOB and executing optimization actions based on the test results. In this paper, this optimization method is augmented with a combination of a predictive and a reactive constraint handling technique to adhere to operational limitations. These methods of constraint handling within ES application to drilling are demonstrated for a maximal limit imposed on the surface torque, but the methods are generic and can be applied on various drilling parameters. The proposed optimization scheme is tested with experiments on a downscaled drilling rig and simulations on a high-fidelity drilling simulator of a full-scale drilling operation. The experiments and simulations show the method's ability to steer the system to the optimum and to handle constraints and noisy data, resulting in safe and efficient drilling at high ROP.

[1] Corresponding author.

1. INTRODUCTION

A substantial part of offshore field development costs originates from drilling, with most of these costs being related to time. There is a great potential for cost reduction by drilling safer, faster and with less non-productive time. Methods used for real-time drilling optimization often focus on tuning physics-based models of the drilling process to fit available data from current or offset operations. The tuned models are used to predict how the drilling process will react to different values of the controllable parameters such as Weight on Bit (WOB), drill string rotational speed (RPM) and mud flow rate. Based on this prediction, the models can be used to provide estimates of the optimal drilling parameters, which can be supplied to the driller as suggestions or directly fed to the control system on the rig in a closed loop [1-4]. Field tests of a Rate of Penetration (ROP) optimization algorithm using physics-based models have shown good results, with the largest increases in ROP obtained when the algorithm was run in closed loop [1,2] and a reduction in downhole tool failures when applying the optimization system [2].

A potential drawback to real-time optimization with the physics-based models is that the analysis is based on a mathematical description of the drilling process, and the existing models might not be very accurate in predicting the ROP [4,5]. A possible remedy for model inaccuracies could be the use of data-driven modelling techniques, or a hybrid between data-driven and physics-based modelling methods. The latter approach was applied in a study on how to automatically minimize Mechanical Specific Energy (MSE) when drilling through layered materials with a lab-scale rig [6]. A physics-based drilling model was used to find an initial estimate of the optimal WOB. A data-driven algorithm was subsequently utilized while drilling to search the neighborhood of the initial estimate for WOB values which could further reduce the MSE. Hegde et al. [7] found that a data-driven model gave better ROP predictions compared to physics-based models when both approaches were using the same input parameters. The selection of which type of data-driven model that can be used for real-time optimization is a tradeoff between runtime and performance, where more advanced models will give more accurate ROP predictions but suffer from longer computational time and vice versa [8].

The data used to tune or train the models employed for real-time optimization, both physics-based and data-driven, needs to be representative of the current drilling conditions (e.g. from the same formation) to yield more accurate predictions [8,9]. A changepoint algorithm which determines what historical data is relevant for the task of ROP modelling and optimization has been implemented in [1]. Using a sliding window of data containing a fixed amount of the most recent measurements to tune a physics-based drilling model has also been suggested [3,4]. In addition to using representative data, the models need a varied sample of input (e.g. WOB and RPM) and output parameters (e.g. ROP) within this dataset to generate a representative data-driven model [8] or to tune the parameters in a physics-based model.

An important component of a practically relevant optimization method is handling of operational constraints. The drilling process is subject to a multitude of operational limitations which affect the safe operational space of the input parameters. Chapman et al. [2] give a detailed list of factors that could directly limit the application of the controllable parameters such as a maximal WOB and RPM dictated by the drilling equipment, as well as listing more indirect factors related to torque, vibrations and hole cleaning which will limit certain combinations of input parameters. Dunlop et al. [1] further describe the implementation of these constraints for real-time drilling optimization. Factors limiting the amount of energy that can be applied to the drilling process through the controllable input parameters and factors which diminish the efficiency of the energy transferal between input parameters and ROP have also been investigated [10,11]. A solution for constraint handling in data-driven modelling is to limit the data used as the training set to values that do not violate constraints and not allowing the model to extrapolate results outside of this region [8]. The downside of these types of constraint handling is that the limiting values for e.g. the WOB needs to be known in advance (e.g. based on a model), which can lead to conservative estimates which precludes drilling at peak efficiency.

In this paper, we apply a data-driven optimization method called Extremum Seeking (ES) [12] to the problem of seeking optimal WOB providing maximal dysfunction-free ROP under unknown and uncertain downhole conditions. The ES method does not require any a priori

model of the process to be optimized and has low computational cost. This makes it especially suitable for the considered real-time optimization of ROP(WOB). ES has previously been implemented successfully in a variety of engineering systems ranging from yield optimization in bioprocesses to jet engine stability control and many others [13]. In several recent studies, ES has been investigated for the purpose of drilling optimization. Banks [14] evaluated ES with induced high-frequency oscillations on a laboratory drill rig to benchmark different bits through MSE minimization. Simulation studies on single variable [15,16] and multivariable [17] ES have explored the method's potential for drilling applications. A closed-loop optimization system employing ES has been tested in the field with promising results [18].

The ES method, applied to the optimization of ROP(WOB), can be briefly described as follows. While drilling ahead, the ES algorithm prescribes a continuous series of micro-tests by sending commands for small variations in the WOB to the autodriller. The micro-tests are performed by periodically varying the input WOB around some base value to gather information about the current drilling conditions. The data generated from this procedure is the training data used by the ES algorithm to create a local linear model. The algorithm relates the changes in the output ROP to the corresponding variations in the input WOB and uses this information to estimate the gradient (linear model) of the ROP as a function of WOB in the local region investigated by the micro-test procedure. The gradient is then automatically used to determine the direction and magnitude in which the WOB base value should be changed to increase the ROP. By continuously repeating this procedure, the ES algorithm can navigate the system to its optimal point and keep the process at its optimum by continuing to probe for changes in the system conditions.

Although the idea of applying ES to drilling optimization is not new, the state-of-the-art literature lacks details on the practical application of ES in the inherently noisy drilling environment, as well as details on constraint handling techniques used to ensure safe application of the optimization method. In this paper we are addressing this gap by focusing on the practical aspects related to using ES for drilling optimization, with emphasis on handling process constraints, uncertain conditions, and noisy measurements. To do this, we

investigate the ES algorithm on a downscaled drilling rig which captures the vibrations and noisy behavior of the drilling process. The ES method is also tested with a high-fidelity drilling simulator, to qualify the results from the experiments to full-scale operations. The ES algorithm is automatically making changes to the applied WOB to optimize the ROP. To ensure that the algorithm does not steer the WOB to values which will result in, e.g., the torque exceeding its maximal limit, a combination of a predictive and a reactive constraint handling technique is investigated in the lab and in simulation scenarios. The constraint handling is based on real-time measurements while drilling and is demonstrated for the case of a maximal limit imposed on the surface torque (still, the method is generic and can be applied on various drilling parameters). The proposed optimization scheme is able to handle the process and measurement noise inherent to the drilling process, which can have a strong effect on the algorithm performance. Compared to the classical filter-based ES scheme (see e.g. Aarsnes, Aamo and Krstić [16]), the proposed method is also adjusted to ensure easier tuning of the system by using a least-squares method to estimate the gradient, which reduces the number of tuning parameters in the algorithm.

The remainder of the paper is organized in the following way: In Section 2, we present the background for the challenge of drilling with the optimal WOB. Section 3 describes the Extremum Seeking algorithm and its application in drilling operations. In Section 4, we detail approaches for constraint handling and instantaneous ROP estimation. Experimental setup and results are provided in Section 5. Section 6 details simulations performed on a high-fidelity drilling simulator. A discussion of the results and conclusions are given in Sections 7 and 8, respectively.

2. BACKGROUND

Drilling is a complicated process with a multitude of factors affecting the ROP, such as personnel and rig efficiency, formation characteristics, mechanical and hydraulic factors, and drilling fluid properties [3]. These many and often interconnected effects make accurate modelling of the process in real-time a complex task, as many of the parameters needed to correctly model the situation are not measured directly and will change over time. However,

the general mechanics of the interaction between the bit and formation are well understood [19]. The instantaneous ROP can be described by

$$ROP = f(WOB, \boldsymbol{r}), \tag{1}$$

where $\boldsymbol{r}$ is a vector containing all parameters other than the WOB which affect the ROP, such as RPM, flow rate, bit condition, bottomhole pressure and formation properties. The nonlinear function f which governs the relationship between the WOB, $\boldsymbol{r}$ and the ROP is not known explicitly, but for any set of values for the parameters contained in $\boldsymbol{r}$ it is assumed that f as a function of WOB inhibits several characteristic drilling regimes. Fig. 1 shows a nominal relationship between the ROP and the applied WOB, where it is assumed that the values of the parameters in $\boldsymbol{r}$ are constant. The ROP-WOB relationship is characterized by three distinct phases: 1) Inefficient drilling caused by low WOB, where the depth of cut is inadequate, 2) efficient drilling where increased WOB is transferred to cutting action at the bit at peak efficiency in a straight-line fashion, and 3) inefficient drilling caused by foundering effects [10,19]. The locations of the different phases in the ROP-WOB relationship are subject to change as parameters in the vector $\boldsymbol{r}$ vary, but the general shape of the three regions is expected to remain. A change in formation properties or an increase in RPM could alter the WOB at which foundering occurs, but WOB at or slightly lower than the foundering value would still correspond to efficient drilling and WOB values above the founder point would constitute inefficient drilling. The shape of the third region depends on what type of inefficiency is causing it, which could be inadequate cuttings removal at the bit or excessive vibrations such as stick-slip and whirl. Drilling with these types of dysfunctions can be detrimental for the bit and downhole tools and should be avoided to extend the lifetime of the equipment. Depending on the cause of founder, its onset could be delayed by manipulation of combinations of drilling parameters or reengineering of the system [10,11], but these approaches are beyond the scope of this paper.

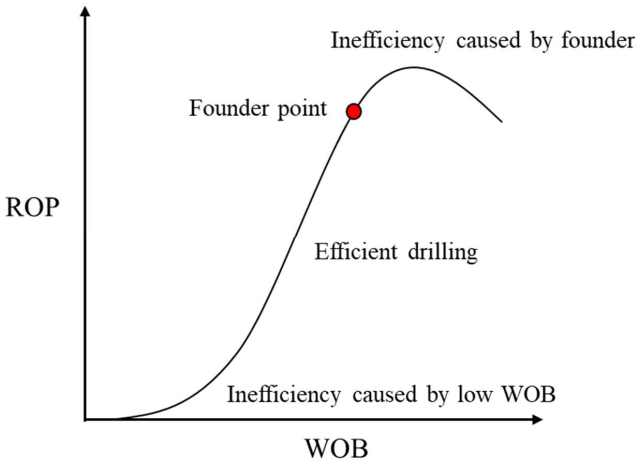

Fig. 1 Nominal relationship between the ROP and WOB, modified from Dupriest and Koederitz [10].

The transition between the last two regions in Fig. 1 is referred to as the founder point, and it is drilling at WOB which corresponds to this point or slightly below that is mainly desired. In this way, the possibly detrimental effects causing the founder as well as the bit wear resulting from a large increase in WOB for a small increase in ROP can be avoided. A convenient way of approaching this situation is to try and maximize not the ROP itself, but a performance function on the form

$$J = ROP - \mu WOB, \tag{2}$$

where μ is a tuning parameter which penalizes the use of excessive WOB [16]. As the ES optimization scheme, outlined further in Section 3, is driven by an estimated gradient of J with respect to the WOB, the algorithm seeks the optimum given by

$$\frac{\partial J}{\partial WOB} = \frac{\partial ROP}{\partial WOB} - \mu = 0. \tag{3}$$

From Eq. (3), the physical meaning of μ can be interpreted as a limiting value at which the ROP gradient is deemed too low to want to further change the WOB, even though the maximal ROP is not yet achieved. A larger value for μ will therefore correspond to a more conservative estimate of what the optimal operating point is.

In practice, the drilling process is subject to constraints which might limit how much WOB can be applied, so that drilling at the founder point may not be feasible. A multitude of constraints like this have been identified by Dupriest and Koederitz [10] and Chapman et al. [2], such as available BHA weight, solids handling capacity and top drive torque rating. A method of avoiding violation of limitations while searching for the founder point is outlined in Section 4.

3. EXTREMUM SEEKING FOR ROP OPTIMIZATION

The ES algorithm is a gradient ascent (or descent) method which requires a process with well-defined steady-state characteristics, so that for a given constant input, the system settles to a constant output within a reasonable time. It also needs the existence of a unique extremum in the output which corresponds to some value in the input variable(s) within the operational envelope. A more thorough review of these conditions and convergence criteria can be found in Tan et al. [13] or Ariur and Krstić [12]. When the system conditions are satisfied, the ES algorithm will automatically seek and maintain the value of the optimal input variable(s), without knowing the details of the relationship between the system's input and output.

The variables that the driller or an algorithm can readily control from the rig floor to affect the ROP are the WOB, the RPM and the flow rate. In this paper, we consider the case of optimizing the ROP by means of controlling the WOB in a constrained ES approach, with constant RPM and flow rate. The method is illustrated in Fig. 2, where an excitation signal is applied to the WOB to investigate the steady-state characteristics of an output performance function defined by Eq. (2). Under the assumption that the ROP-WOB relationship is subject to the different drilling regimes outlined in Section 2, the drilling process has a unique

optimal WOB at which foundering starts to occur and is well suited for optimization with ES.

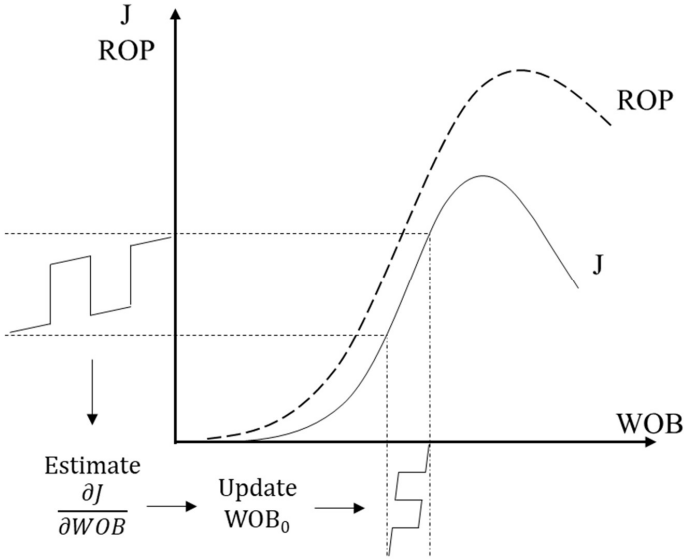

Fig. 2 Concept illustration of Extremum Seeking applied for drilling optimization.

Although drilling is a continuous process, the sampled measurements and the commands given to the control system on the rig are performed in discrete time. This motivates the notation used here: t is the current time, Δt is the time interval between both measurements of drilling parameters and updated setpoints provided to the autodriller (here assumed to be the same), so that $t + \Delta t$ signifies a value for the coming timestep.

The ES algorithm can be divided into three main components: 1) The excitation signal, which introduces a variation in the input of the system, 2) the gradient estimator, used to quantify how the system reacts to the excitation, and 3) the optimizer, which changes the input WOB based on the estimated gradient. These components are described in detail in the following.

3.1 The Excitation Signal

Some best estimate of the optimal input value, WOB_0, is initially applied to the system. This estimate could be based on a drill-off test, calculations from an available drilling model or experience from a similar offset well. While drilling ahead, the ES algorithm continuously explores the neighborhood of WOB_0 and how the system responds to small variations in the WOB by conducting a series of micro-tests. This is done by automatically varying the WOB-setpoint provided to the autodriller according to

$$WOB(t) = WOB_0(t) + d(t, A, P). \tag{4}$$

The last term in Eq. (4) is the excitation signal, which is given by

$$d(t, A, P) = A \cdot sgn\left(sin\left(\frac{2\pi t}{P}\right)\right) \tag{5}$$

In Eq. (5), *sgn* is the signum function which takes on a value of 1 when the argument is positive, a value of -1 when the argument is negative and a zero value for a zero argument. This signal is a square wave with an amplitude of A kg and a period of P seconds, which oscillates symmetrically about WOB_0. For each period, the magnitude of A approximately determines the extent of the WOB-interval which is being investigated by the algorithm. The amplitude should be small enough to not detrimentally affect the overall drilling process, but at the same time be large enough to elicit a measurable change in the ROP which can be used for gradient estimation. A square wave signal is used in this work, as this will yield the maximal output (ROP) signal power for a given amplitude [20], which will enable the ES algorithm to estimate more accurate gradients in the presence of noisy measurements. It is also expected that a square signal shape is easier to realize with a standard autodriller functionality, compared to the sinusoidal signal often used in ES algorithms.

The period of the excitation signal determines the amount of historical data used to estimate the gradient of the performance function and needs to be tuned accordingly. The

parameter P should be designed large enough to generate a dataset that contains enough information so that it can be used for gradient estimation when the data is noisy. At the same time, it must be considered that a very large value for P will result in a lot of previous drilling data (which might no longer be representative of the current drilling conditions) being used for gradient estimation.

3.2 Gradient Estimation

The applied WOB and the resulting values of J calculated from Eq. (2) are stored in buffers containing P seconds of history for these two parameters. At each update of measurements, the past values of J and WOB stored in the buffers are used to solve the 1st-order least-squares problem given by

$$\sum_{i=0}^{P/\Delta t-1} \left(J(t-i\Delta t) - (aWOB(t-i\Delta t)+b)\right)^2 \rightarrow \min_{a,b} \tag{6}$$

where a and b are the slope and intercept of the least-squares fit, respectively. These two parameters represent a linear approximation to how J has changed with the varying WOB for the past P seconds. The slope parameter a is used as an estimate of the gradient of the performance function at the current timestep,

$$\left.\frac{\partial J}{\partial WOB}\right|_{WOB_0(t)} \approx a(t). \tag{7}$$

In this way, a sliding window of data corresponding to one full period of the excitation signal is used to estimate the current gradient of J. On average, this estimate corresponds to the formation which was drilled $P/2$ seconds earlier, as this is the center of the sliding window. The excitation signal is symmetric about the slowly varying WOB_0, so that Eq. (7) represents a gradient evaluated approximately at WOB_0.

This way of calculating the gradient is robust with respect to noise and sensor bias, since much of the noise is filtered out over the least-squares window, and any sensor bias is captured by the *b*-parameter which is not used by the ES algorithm. Still, if the measurements are very noisy, the data should be low pass filtered before being analyzed with Eqs. (6) and (7) to get a better gradient estimate. The least-squares technique used here is also easier to apply than the classical filter-based ES method. This is because the least-squares gradient estimation does not require tuning of the filters used in the classical approach.

3.3 Optimizer

From Fig. 2 it can be seen that the performance function has a positive slope when drilling with a WOB to the left of the maximal value of *J*, and a negative slope for WOB values beyond this point. The gradient obtained from Eqs. (6) and (7) can thus be used to determine how the WOB should be altered to increase the performance function, *J*. This is done by calculating an updated WOB_0 value for the coming timestep from

$$WOB_0(t + \Delta t) = WOB_0(t) + \gamma \frac{\partial J}{\partial WOB}(t)\Delta t, \tag{8}$$

which will move the drilling system to a slightly higher value of *J* if the estimated gradient indicates that this is possible. The parameter γ is a gain which determines the *learning dynamics* of the algorithm. That is, how fast the ES scheme should vary WOB_0 as a response to the estimated gradient of *J*. The new WOB_0 value calculated from Eq. (8) is used to update the WOB which will be sent to the autodriller in the next timestep, as dictated by Eq. (4) evaluated at the coming timestep, $t + \Delta t$. The algorithm will subsequently repeat the process of estimating a new gradient based on new measurements and adapting to the newest information. It is worth noting that this update takes place at each timestep, with γ tuned so that WOB_0 varies relatively slowly compared to the variations in WOB caused by the excitation signal.

A block diagram of the described optimization structure is shown in Fig. 3. Each timestep constitutes a loop through this diagram, where the algorithm will vary the WOB according to Eq. (4), record and quantify the system response with Eqs. (6) and (7) and use this information in Eq. (8) to update the WOB which should be applied to initiate a new iteration of the algorithm.

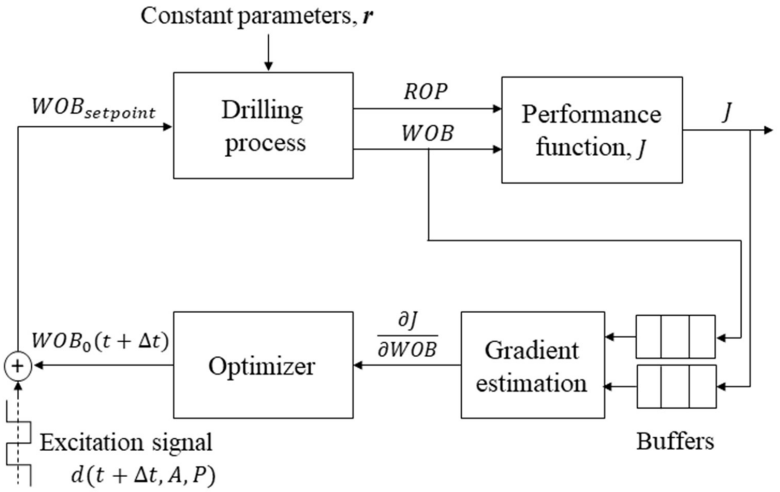

Fig. 3 ES scheme for drilling optimization.

4. CONSTRAINT HANDLING AND PRACTICAL CONSIDERATIONS

The optimization algorithm described in the previous section will be able to steer the drilling system to the optimum dictated by the performance function, given that the drilling process adheres to the general ROP-WOB relationship described in Section 2. In practice, drilling at the founder point might not be feasible. Some reasons for this could be that the required WOB might exceed the available BHA weight or allowable WOB, there could be a maximal ROP limit related to cuttings transport or handling of cuttings at the surface, or the torque generated at the bit or at the surface could exceed the allowable values. Two methods for making the ES algorithm avoid violation of this type of constraints while searching for the optimum is presented in the following. The methods are illustrated for a maximal limit

imposed on the surface torque, but the techniques are generic and could also be used on other limiting parameters. The underlying assumption for these techniques in the case of a torque constraint, is that the torque and WOB are positively correlated.

4.1 Predictive Constraint Handling

The changes in the drilling process caused by varying the WOB can be a good source of information about the current system conditions and how other drilling parameters are affected by the WOB. The same methodology as was used to extract an estimate of the gradient of J in Eqs. (6) and (7) is also able to estimate gradients of other drilling parameters and how they vary with the changing WOB. By storing measured values of the surface torque in an additional buffer containing P seconds of data, the gradient of the surface torque with respect to the WOB can be calculated from

$$\sum_{i=0}^{P/\Delta t-1} \left(T(t-i\Delta t) - (\alpha WOB(t-i\Delta t)+\beta)\right)^2 \rightarrow \min_{a,b}, \tag{9}$$

$$\left.\frac{\partial T}{\partial WOB}\right|_{WOB_0(t)} \approx \alpha(t). \tag{10}$$

The parameters α and β are the slope and intercept of the least-squares fit, respectively. The gradient estimate given by Eqs. (9) and (10) can be used to predict how the torque will react to further changes in the WOB, and how to avoid violation of constraints based on this information.

The recorded surface torque is often plagued by noise, both from inaccurate measurements and process noise in the form of drillstring vibrations. Because of this, there is some uncertainty as to what the value of the torque is. To remedy this issue, the average value that spans P seconds of data, T_{avg}, is taken as the surface torque, which approximates the torque experienced by the system when drilling with a weight on bit of WOB_0. This averaging will reduce the amount of noise in the torque value used by the algorithm, but it

will also introduce a time delay in the averaged torque value corresponding to half of the averaged period, the same delay that is inherently present in the gradient calculated in Eqs. (9) and (10). Additional measures to counteract the effects of noisy torque and WOB on the analysis is to use filtered values for these parameters in Eq. (9), as well as increasing the summation interval to analyze e.g. data from two periods of the excitation signal.

To avoid the WOB being steered to values which cause a violation of the allowable torque, T_{limit}, the gain parameter γ in Eq. (8) is calculated as

$$\gamma = \begin{cases} \gamma\,, & \left(T_{avg} + A\frac{\partial T}{\partial WOB}(t)SF\right) < T_{limit} \\ 0\,, & \left(T_{avg} + A\frac{\partial T}{\partial WOB}(t)SF\right) \geq T_{limit}\ and\ \frac{\partial J}{\partial WOB} > 0 \end{cases}, \tag{11}$$

where SF is a safety factor greater than 1. Because the algorithm varies the weight on bit about WOB_0 with a magnitude of A kg, Eq. (11) will stop the optimizer from exceeding the torque limit with a margin dictated by the SF parameter. This method also allows the excitation signal to continue the micro-testing for changes in the drilling conditions, even when the torque is close to the highest allowable value. The positive gradient condition in Eq. (11) is included to avoid a situation where the ES algorithm wants to reduce the WOB to drill more efficiently but is precluded from doing so because it is currently close to the maximal allowable torque. The value for T_{limit} used in Eq. (11) should be lower than the maximal limit the drilling system can handle, as an added safety measure.

4.2 Reactive Constraint Handling

In some instances, the predictive constraint handling detailed in Eq. (11) might not be enough to ensure that the torque stays within the allowable boundaries. This could be caused by either very noisy measurements which makes the calculated torque gradient inaccurate, or abrupt changes in drilling conditions, such as a formation change, which alters the torque in a short span of time. To ensure safe operations, a reactive constraint handling technique is implemented to reduce the WOB and consequently the torque if the limit is exceeded. This

technique uses a variable which is equal to zero if the constraint is not violated and proportional to the violation if the torque limit is surpassed,

$$e(t) = \begin{cases} 0\,, & T_{avg} < T_{limit} \\ T_{filt}(t) - T_{limit}\,, & T_{avg} \geq T_{limit} \end{cases}. \tag{12}$$

In Eq. (12), T_{filt} is a low pass filtered torque value, designed to remove most of the noise while still being representative of the current torque level. This filtered parameter is introduced so that the constraint handling routine will not react to very short-term spikes in the measured surface torque. If the variable e is larger than 0, this indicates that the constraint is violated and the adaptation gain, γ, is set to zero. The value for T_{limit} should be lower than the actual system limit, because the reactive constraint handling will only start to affect the system when T_{filt} is larger than T_{limit}. The variable e from Eq. (12) is used to calculate a penalty variable, λ, by use of a discrete Proportional-Integral (PI) controller,

$$\lambda(t) = K_P e(t) + K_I \Psi(t) \Delta t, \tag{13}$$

$$\Psi(t) = \begin{cases} 0, & T_{filt} < T_{limit} \\ \sum_{i=n}^{t} e(i), & T_{filt} \geq T_{limit} \end{cases}. \tag{14}$$

In Eq. (13), K_P and K_I are the proportional and integral gain, respectively, which are the tuning parameters that determine how aggressively the controller should penalize torque values above the limit. The parameter Ψ in Eqs. (13) and (14) is an integral term which will continue to grow as long as the torque constraint is violated and consequently make adjustments of increasing size in the WOB as a response to the limitation not being adhered to. If the torque constraint is not violated, the parameter n in Eq. (14) is set equal to the current timestep, to reset the calculated integral to a zero value. The penalty term calculated from

Eqs. (13) and (14) is used to reduce the weight on bit demanded by the ES algorithm according to

$$WOB_{0,constrained}(t + \Delta t) = WOB_0(t + \Delta t) - \lambda(t). \quad (15)$$

The parameter $WOB_{0,constrained}$ is used in Eq. (4) to calculate the constrained WOB setpoint which is sent to the autodriller. If the torque limit is exceeded, the WOB demanded by the ES algorithm will be reduced until the torque is again below its limiting value. When the constraint is not violated, λ will take on a zero value and the WOB_0 value will be determined by Eq. (8).

4.3 Practical Considerations for Field Applications

The ES algorithm relies heavily on causing a change in the ROP by varying the WOB and being able to quantify this change. The standard industry practice for estimating the instantaneous ROP is based on calculating the time derivative of the position of the travelling block [21]. This practice works well during steady state conditions when the WOB is constant, but because of drill string elasticity it can give large errors during transient periods when the WOB is non-constant. Specifically, the ROP calculated from the movement of the block alone will overestimate the ROP in transient periods where the WOB is increased and underestimate the ROP in periods when the WOB is decreased [21]. This is caused by the average tension in the drill string being reduced when more weight is supported by the bit, which results in a shortening of the drill string, and vice versa when less weight is applied at the bit. Using a purely block-based ROP estimate in the ES algorithm is therefore not desirable, as the relatively frequent adjustments in WOB can interfere with accurate ROP estimation. Because of the symmetry of the excitation signal, elasticity effects will mostly be cancelled out when estimating the gradient, but this effect should still be accounted for in the ES method to produce more accurate gradient estimates.

The relation between the bit position, h_{bit}, and block position, h_{block}, can be expressed as

$$h_{bit} = h_{block} + C_a g WOB - L, \tag{16}$$

where C_a is the axial drill string compliance, g is the gravitational acceleration and L is the length of the drill string at zero WOB and the current mud flow rate [21]. A low pass filtered WOB value should be used in Eq. (15) when the measured WOB is noisy. In general, the *L* parameter in Eq. (15) is not required to calculate the ROP since it is a constant that will be cancelled out when differentiating. To estimate the instantaneous ROP based on noisy measurements, a Kalman filter (KF) based on the following state space model is used in this work,

$$\begin{bmatrix} h_{bit} \\ ROP \end{bmatrix}(t + \Delta t) = \begin{bmatrix} 1 & -\Delta t \\ 0 & 1 \end{bmatrix} \begin{bmatrix} h_{bit} \\ ROP \end{bmatrix}(t). \tag{17}$$

Additional details on the use of the KF can be found in [22] for general position tracking and in [15] for the case of ROP estimation from noisy data.

5. EXPERIMENTS ON A DOWNSCALED DRILLING RIG

5.1 Experimental Setup

This experimental rig used in this study was built to compete in the annual Drillbotics competition [23] hosted by the Society of Petroleum Engineers (SPE), allowing students and researchers to get hands-on experience with drilling automation technologies. The miniature rig is designed to work in an analogous fashion as a full-scale drilling rig. It consists of a steel framework with integrated motors, sensors, hydraulic circulation system and other functionalities that are needed to drill through rock samples. A more detailed description than the one provided here of the miniature rig and its use for other drilling automation applications can be found in [24-26]. Fig 5 shows the experimental drilling together with a schematic that highlights key components.

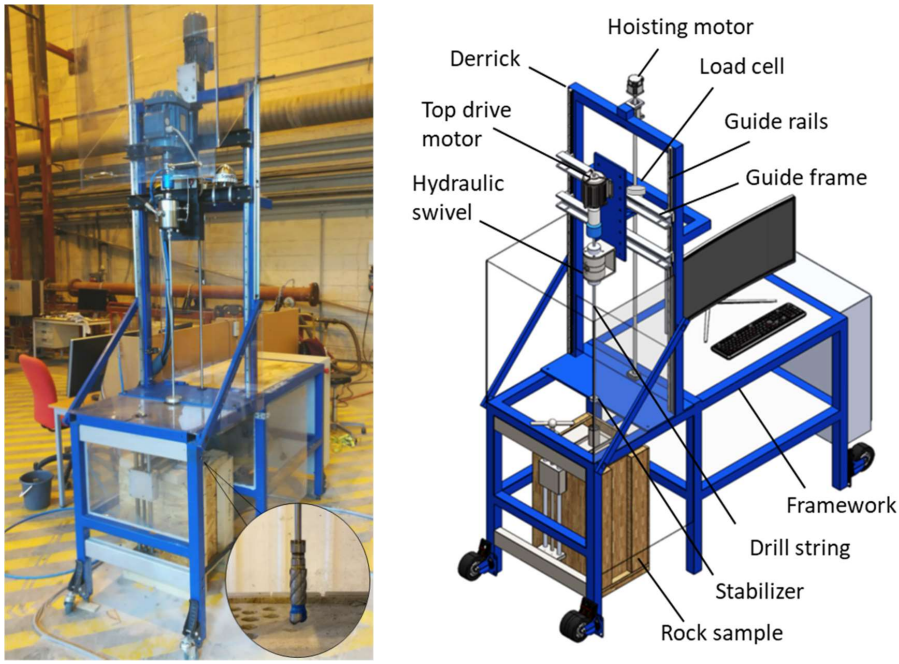

Fig. 4 The experimental rig. (**a**) Rig photo, highlighting the BHA. (**b**) Rig schematic with key components.

At the top of the derrick, approximately 2.85 m above floor level, a hoisting motor provides rotational energy which is translated to vertical movement of the top drive assembly and drill string through a ball screw system. The top drive assembly is comprised of a motor to provide drill string rotation and a hydraulic swivel to facilitate circulation of drilling fluid while rotating. These components are mounted on a frame which slides along guide rails to ensure that all movement of the top drive and drill string is vertical, similar to the functionality of a full-scale top drive system. Fresh water from a standard water outlet is circulated through the drill string to transport cuttings out of the annulus and to cool and lubricate the bit. The drill string has a length of approximately 0.9 m and is made up of a hollow steel drill pipe, connection joints, a stabilizer sub, and a generic two-wing PDC bit

with an outer diameter of 2.8 cm. Because of the reduced scale of the drilling rig, adequate WOB cannot be applied through high-weight drill string components as is done in full-scale operations. Instead, WOB is applied by the top drive assembly pushing down on the drill string, placing the entire string in compression. The drill pipe is passed through a radial ball bearing stabilizer on the "rig floor" to mitigate buckling by reducing the effective length of the string.

A load cell located by the hoisting system's nut bracket provides measurements of the total load from the bit and from the weight of the guide frame and top drive, which is converted to WOB by subtracting the weight of the mechanical components. Internal sensors in the top drive and hoisting motors supply measurements of drillstring rotational speed, (surface) torque, and the guide frame position. From the position measurement, an estimate of the ROP is calculated with a Kalman Filter by approximating the downhole ROP as the surface velocity of the travelling block (guide frame), as described in [15]. Because of the reduced scale of the system, the drill string elasticity detailed in Eq. (15) can be neglected. The rig's control system is implemented in LabVIEW, where all communication with the motors and sensors is done with a 50 Hz update frequency. The top drive and hoisting motors are controlled by supplying them with requested setpoint for RPM and hoisting velocity, respectively, which are translated to the apposite motor rotational rates by factory tuned internal Proportional-Integral-Derivative (PID) controllers. To run experiments with WOB control, a PID autodriller was implemented in LabVIEW to convert requested WOB setpoints to the appropriate velocity setpoints for the hoisting motor.

Blocks of concrete with two different material strengths were cast in 0.6 m tall wooden boxes and used as rock samples to be drilled by the experimental rig. The Concrete *A* is designed to have an Unconfined Compressive Strength (UCS) of 25 MPa, and Concrete *B* is designed to have a UCS value of 35 MPa. Fig. 5 shows the relationship between WOB and ROP in these two formations, where the data stems from active drill-off tests performed with a constant RPM value of 200 and a moving average filter is used to smooth the data.

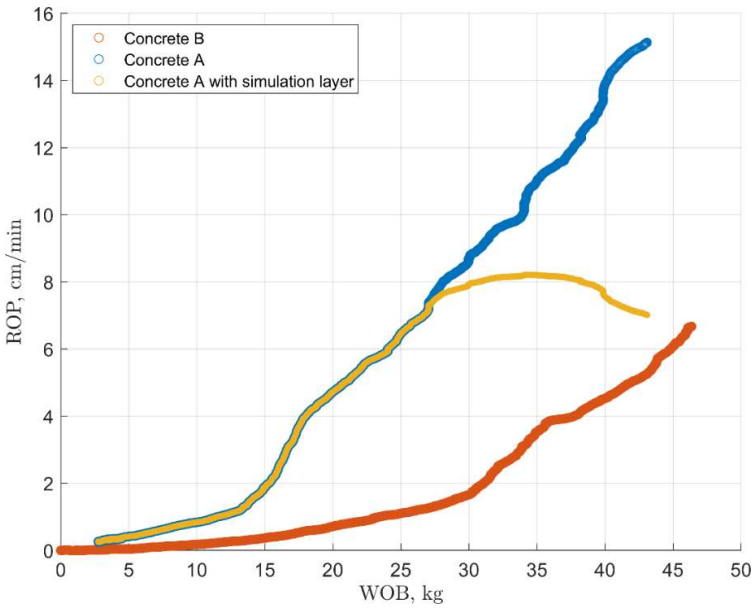

Fig. 5 Active drill-off test in concrete blocks *A* and *B* at a constant RPM of 200.

It can be observed from Fig. 5 that the blue and red datasets show drilling in phase 1 and phase 2, as described in the Background section, with a higher WOB threshold for entering phase 2 drilling in the harder formation. However, these two datasets do not show any foundering tendencies within the investigated WOB interval. The amount of WOB that can be applied is limited by the top drive motor, which stalls out at a continuous torque values above 7,2 Nm, which typically occurs at WOB values around 50 kg. This is a prime example of a factor limiting energy input, where drilling at the founder point is not feasible because of a system constraint [10]. In other words, a mechanical limit on the rig precludes drilling at higher WOB values where it is expected that the ROP at some point will deviate from the straight-line phase 2 trend [10,19].

To be able to investigate the ES algorithm's performance in drilling scenarios where the ROP-WOB relationship deviates from straight line phase 2 drilling and enters the foundering region (within the allowable WOB range of 0-50 kg), a simulation layer was added to the

experiments. The simulation layer is implemented by emulating a reduction in the recorded ROP values when they exceed a certain ROP threshold, according to

$$ROP_{sim} = \begin{cases} ROP_{mea}, & ROP_{mea} \leq ROP_{threshold} \\ ROP_{mea} - c \cdot (ROP_{mea} - ROP_{threshol}\ )^{d}, & ROP_{mea} > ROP_{threshold} \end{cases} \quad (17)$$

In Eq. (17), ROP_{sim} is the simulated ROP value, ROP_{mea} is the ROP estimated from the movement of the guide frame, $ROP_{threshold}$ is a threshold value of 7 cm/min at which the simulated foundering occurs, c and d are model parameters with values of 0.35 and 1.5, respectively, that determine how much the simulated ROP is reduced when the threshold is exceeded. The values for c and d were chosen to get a generic ROP-WOB relationship that simulates a foundering effect where the ROP response "flattens out" at higher WOB values, as could be the case for e.g. stick slip vibrations [19]. The effect of the simulation layer can be observed in the yellow dataset in Fig. (5), where it is seen that the ROP deviates from the straight-line trend when the ROP exceeds the threshold value of 7 cm/min at approximately 28 kg WOB. It is the value of ROP_{sim} that is sent to the ES algorithm for WOB optimization. If we are e.g. drilling at a WOB of 40 kg in Concrete *A*, the rig will be drilling with an ROP of about 13 cm/min, but the ES algorithm will receive a simulated ROP value of approximately 8 cm/min. Experiments in concrete *B* are not affected by the simulation layer, as the ROP values observed in this formation are in general below 7 cm/min.

5.2 Experimental Results

To investigate the proposed ES algorithm for drilling optimization, a series of experiments were performed on the miniature drilling rig described in the previous section. Before each run, a 4-5 cm pilot hole was drilled with an additional stabilizer mounted directly above the BHA. This was done to reduce the amount of whirl seen at low WOB in combination with the BHA not being in contact with borehole walls to stabilize the string. After removing the additional stabilizer and turning on the water circulation system, the experiments were performed with the rig in autonomous mode. In this mode of operation, the

rig executes a tagging sequence to place the bit in contact with the formation and ramps the RPM up to the requested value, before increasing the WOB setpoint linearly up to the initial value of WOB_0 kg. Following a few seconds of drilling with constant WOB, a single period of the excitation signal is performed without any adaptation, to get an initial estimate of how the objective function relates to the applied WOB. After the initial excitation, the WOB requested by the rig follows Eqs. (4) through (9). The experiments were carried out with the parameter values given in Table 1. The simulated ROP described in Eq. (17) was used as a substitute for the measured ROP, to emulate drilling with bit foundering when the ROP exceeds a certain threshold.

Table 1 – Parameters common for all experiments.

Parameter	*Value*	*Unit*
A	2.5	kg
P	40	s
μ	0.1	cm/min/kg
γ	0.006	kg^2/cm
Δt	0.02	s
RPM	200	rpm
Flow rate	10	lpm

The results from experiment 1 are displayed in Fig. 6, where the four tracks show time-series of the WOB, ROP, objective function and the estimated gradient, respectively.

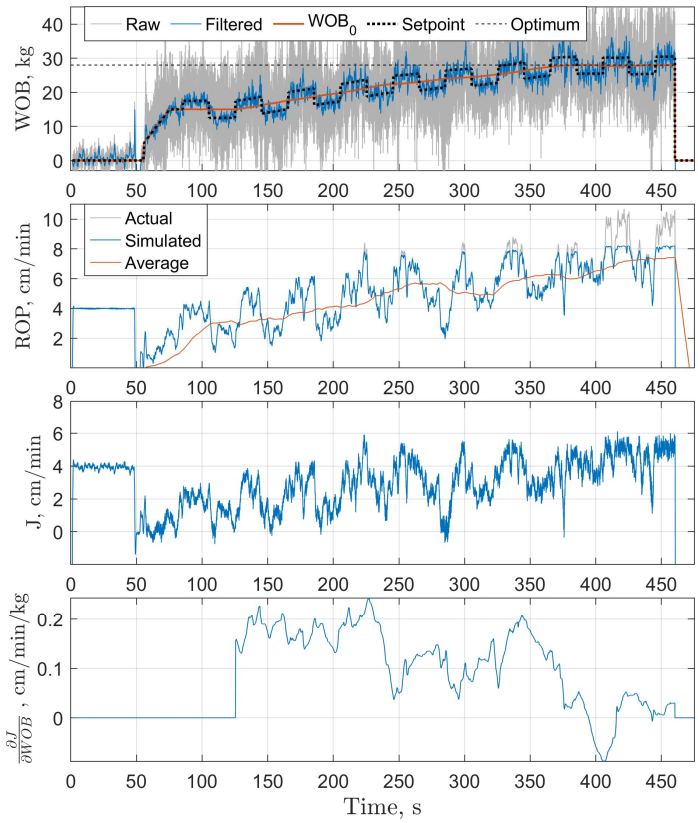

Fig. 6 Experiment 1, performed in Concrete *A* with an initial WOB of 15 kg.

This run was performed in Concrete *A* with a conservative initial guess of the optimal WOB of 15 kg. The first 125 seconds of the run show the tagging sequence, ramp-up and initial excitation of the WOB, where the average ROP at this initial WOB can be seen from the second track to be approximately 3 cm/min. At 125 seconds, the adaptation was activated, and the ES algorithm determined that the WOB should be increased to drill more efficiently (as can be seen from the positive gradient), and the following 275 seconds were spent drilling with progressively higher WOB values. About 400 seconds into the experiment, the WOB_0 value converged to an approximately constant level at 28 kg and the remainder of the run

was drilled with this value. At the end of the run, the rig was drilling with an average ROP of around 7.3 cm/min, which is an improvement of approximately 140% compared to the initial ROP. At 460 seconds, the target depth was reached, and the rig started tripping out of the drilled hole.

There are several important aspects that can be noted from Fig. 6. From the first track, it can be seen that the measured WOB is very noisy and needs to be filtered to obtain values that can be used in the ES analysis and for WOB control with the autodriller. The appropriate filtering and analysis are automatically performed by the rig's control system. The optimal WOB marked in the top track in Fig. 6 is based on the drill-on curve in Fig. 5, where the ROP deviated from straight-line behavior at a WOB of approximately 28 kg. However, the ES method had no prior knowledge of the optimal WOB value and used only information gathered from the micro-test procedure to optimize the applied WOB. In the second track, the effect of the simulation layer can be seen for ROP values higher than 7 cm/min. The gray dataset shows the actual ROP that the rig was drilling with, and the blue data denotes the simulated ROP that was used by the ES algorithm for WOB optimization. Throughout most of the run, the ROP is seen to generally increase and decrease proportionally to the variation in the WOB. After about 400 seconds, only small improvements in the (simulated) ROP are seen when the WOB is increased, which is reflected by a relatively flat response in the objective function and low gradient values. This leads the ES algorithm to reduce the rate of WOB adaptation, almost to a stop, at this point, as this tendency indicates that foundering has started to occur and the optimal WOB has been found.

Experiment 2 was designed to be identical to the first run, with the exception that in this case the constraint handling techniques described in Eqs. (9) through (14) were active with the following parameters: T_{limit} = 4.5 Nm, K_P = 0.004 kg/Nm, K_I = 0.01 kg/Nm/s and SF = 3. The results from this run are presented in Fig. 7, which shows the WOB, ROP, torque and the estimated torque gradient.

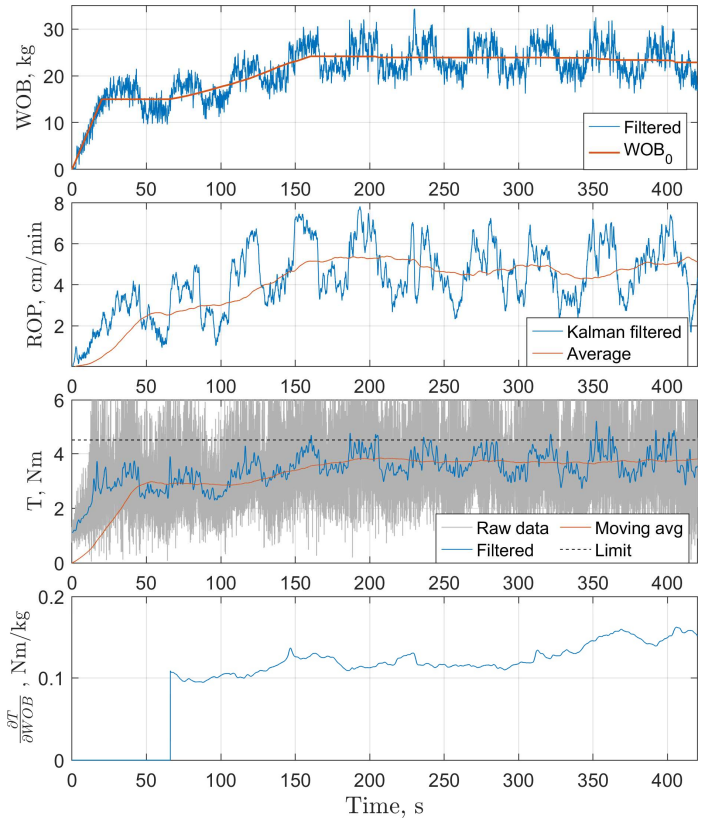

Fig. 7 Experiment 2, performed in Concrete *A* with an initial WOB of 15 kg and a maximal allowable continuous torque of 4.5 Nm.

The first 65 seconds were spent ramping up the WOB and performing the initial excitation, before the ES algorithm started increasing the WOB_0 variable towards the founder point. After 160 seconds, WOB_0 had reached a value of 24.2 kg and the constraint handler predicted that the torque would exceed the limit if WOB_0 was increased further. As a response to this, the adaptation gain, γ, was set to zero as dictated by Eq. (11). The remained of the run was drilled with almost constant WOB_0 values while the WOB was varied according to Eqs. (4) and (5). As can be seen from the third track in Fig. 7, the measured torque is very noisy, and a filtered torque value was used for the constraint handling. Several

instances of small torque-spikes exceeding the allowable limit of 4.5 Nm can be seen in this track (e.g. at around 350 and 405 seconds), which made the reactive constraint handling technique described in Eqs. (12) through (14) reduce the WOB_0 value from 24.2 to 22.9 kg. Applying the constrained ES algorithm in this case increased the ROP from 3 cm/min initially to approximately 5 cm/min, resulting in a 67 % improvement. Greater gains in ROP could have been achieved if the rig was allowed to drill with higher torque values, as was seen in Experiment 1 for a WOB_0 value of 28 kg. However, given the torque constraint, the ES algorithm sought out the WOB that resulted in maximal ROP without drilling with too high torque.

A third experiment was performed in Concrete *A,* without constraint handling and with an initial guess of the optimal WOB_0 value of 35 kg. The results from this run are depicted in Fig. 8, which shows the WOB, ROP, objective function and objective gradient. The high starting point for the WOB resulted in drilling in the founder region, as can be seen from the relatively flat (simulated) ROP response to WOB variations in the top two tracks. After having completed the initial excitation period at 75 seconds, the ES algorithm estimated a negative gradient (caused mostly by the μ parameter in Eq. (2)). The negative gradient prompted the ES algorithm to reduce the applied WOB to exit the founder region. The rest of the run was performed with WOB_0 values monotonically decreasing from 35 to 30 kg. Throughout the run, the ROP did not change much except for some transient spikes. Still, the reduction in WOB performed by the ES algorithm would be beneficial if the bit foundering was caused by e.g. vibrations, which could be detrimental for the downhole equipment to drill with.

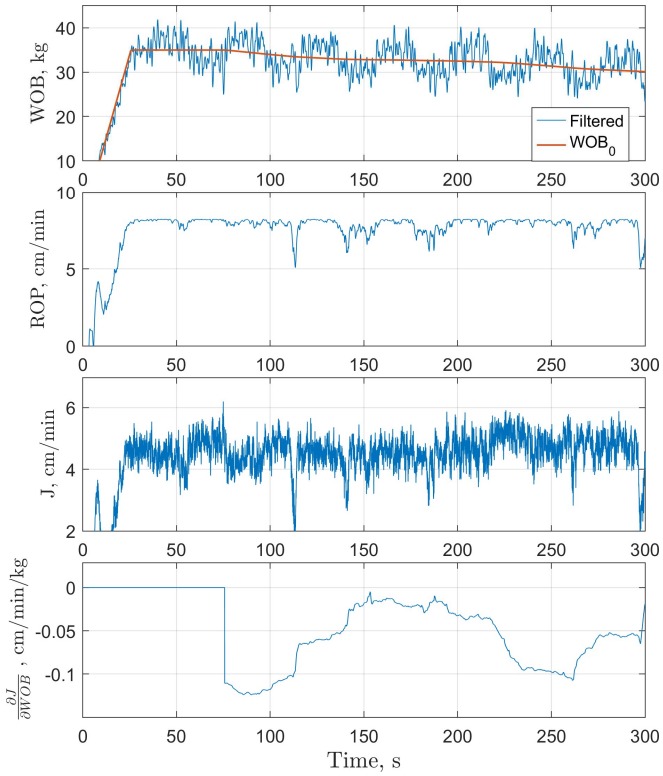

Fig. 8 Experiment 3, performed in Concrete *A* with an initial WOB of 35 kg.

The results from experiment 4 are displayed in Fig. 9. This run was performed in a concrete block consisting of 20 cm of Concrete *A* overlaying a 40 cm thick layer of the harder Concrete *B*. The initial WOB_0 value was set to 28 kg, to represent a continuation of Experiment 1 (e.g. drilling of the next stand) where this was found to be the optimal WOB value to drill with in this formation. As can be seen from Fig. 5, the harder formation *B* should be drilled with WOB that is higher than 28 kg to increase the ROP. The initial part of the run, in Concrete *A*, was spent performing the initial adaptation-free excitation and making some small reductions in the WOB_0 variable. About 110 seconds into the experiment the harder formation was encountered, which resulted in a drastic reduction in the ROP from approximately 7.5 to 2 cm/min. Drilling in Concrete B, the ES algorithm recognized that

higher WOB values would be beneficial to drill with, which resulted in the WOB_0 variable being steered to a value of approximately 42 kg at the end of the run where the average ROP was increased by about 100% to 4 cm/min.

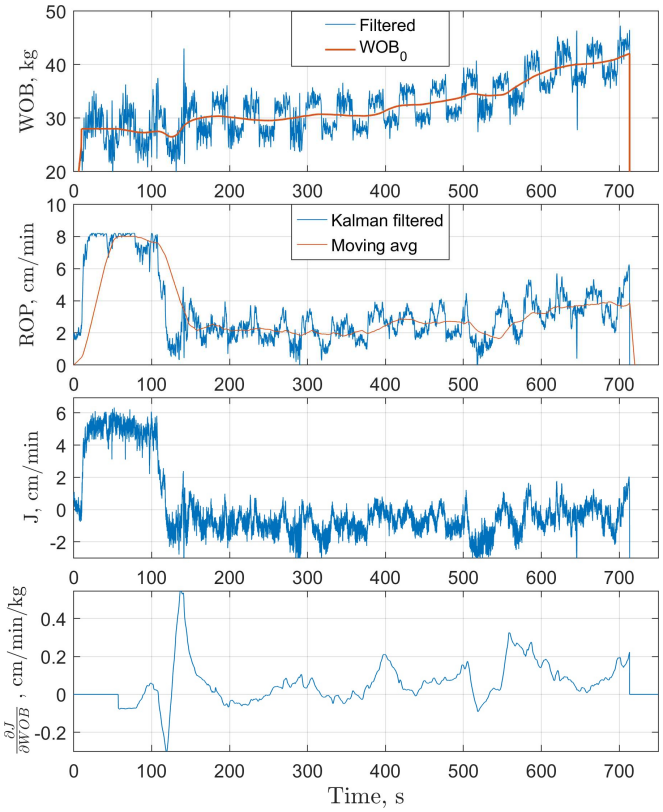

Fig. 9 Experiment 4, performed in a layered formation an initial WOB of 28 kg.

The abrupt change in drilling conditions at 110 seconds caused the estimated gradient to bounce between quite large positive and negative values for a short time interval, before more data representative of the new formation was included in the analysis and the estimated gradient again became representative of the current drilling environment. This phenomenon can be explained by the ES algorithm trying to relate any changes in ROP (which in this case

was caused by the formation shift) to the relatively small variations in the WOB. In the interval 200 – 550 seconds in Fig. 9, the WOB_0 variable can be seen to gradually increase at a quite slow pace, before it increases more rapidly from 550 – 710 seconds. As can be seen from Fig. 5, the ROP is quite unresponsive to WOB variations for phase I drilling in Concrete B. This caused the adaptation rate of the WOB_0 variable to be quite low until phase II drilling was entered and more rapid adaptation took place.

6. SIMULATIONS ON A HIGH-FIDELITY DRILLING SIMULATOR

Simulations on the high-fidelity drilling simulator OpenLab were carried out to study the performance of the ES algorithm on a full-scale rig. The simulator consists of a set of integrated numerical models covering different aspects of the drilling process, including torque and drag effects, cuttings transport, multi-phase flow and heat transfer [27]. The models on the OpenLab platform are run by supplying the simulator with setpoints for the input variables, which the simulator translates to actions on the drill-floor with built-in functions which limits the allowable rate of changes according to equipment specifications [28]. In the simulation scenarios, the ES algorithm was only allowed access to (noisy) measurements of the WOB (assumed derived from the hook load), surface torque and hook position, which would be readily available in field operations. To emulate the noisy conditions on the rig floor, a layer of white gaussian noise was added to these measurements, with the noise levels based on logged field-data. The applied WOB was controlled by a PI-autodriller which regulated the velocity of the travelling block based on the noisy WOB measurements, as would be the case in the field. The noise distribution notation for these measurement disturbances given in Table 2 can be interpreted as 99% of the measured values falling within the true value ± 3000 kg for the WOB, ± 1000 Nm for the torque and ± 0.03 m for the hook position. The ROP was calculated with the approach described in Section 4.3, with drillstring compliance included in the analysis.

The four simulation runs studied here are referred to as Sim 1, Sim 2, Sim 3 and Sim 4, and depict vertical drilling of a 12.25” section through a homogeneous formation, staring at a depth of 2500 meters. The founder point sought by the ES algorithm is found at a WOB of

12000 kg where the corresponding ROP is about 64.5 m/hr, but this information was not known by the algorithm in advance. Apart from the initial WOB_0 value in Sim 2 and Sim 4 and a maximal torque limit in Sim 3, the simulations were all performed with identical parameters, as listed in Table 2. The runs were initiated in the same fashion as in the experiments; by building up the RPM and pump flow rate to their constant values before the WOB was ramped up to the initial WOB_0. A single period of the excitation signal was performed without any adaptation to get an initial estimate of the objective function gradient, before the ES algorithm was allowed to start adjusting the WOB_0 value to increase the drilling efficiency.

Table 2 – Simulation parameters

Parameter	*Value*	*Unit*
A	500	kg
P	180	s
μ	0.0035	m/hr/kg
Δt	0.1	s
γ	1500	$kg^2hr/m/s$
RPM	100	rpm
Mud flow rate	2000	lpm
WOB_{noise}	$\sim N(0, 1000)$	kg
T_{noise}	$\sim N(0, 333)$	Nm
h_{noise}	$\sim N(0, 0.01)$	m
Initial WOB_0, Sim 1	7000	kg
Initial WOB_0, Sim 2	15000	kg
Initial WOB_0, Sim 3	7000	kg
Initial WOB_0, Sim 3	10000	kg
T_{limit}, Sim 3	6000	Nm
SF, Sim 3	3	-

The results from the four simulation runs are shown in Fig. 10. Sim 1, shown in orange, started out drilling with relatively conservative WOB_0 value of 7000 kg, resulting in an average ROP of about 30 m/hr. After performing the initial excitation, the ES algorithm started adjusting the WOB towards the optimal value, at first quite rapidly but gradually more slowly as the WOB closed in on the optimal value and the estimated gradient became smaller. At the end of the run, the average WOB and ROP were approximately 11800 kg and 64 m/hr, respectively, which is an increase of about 110 % in the ROP from the initial value.

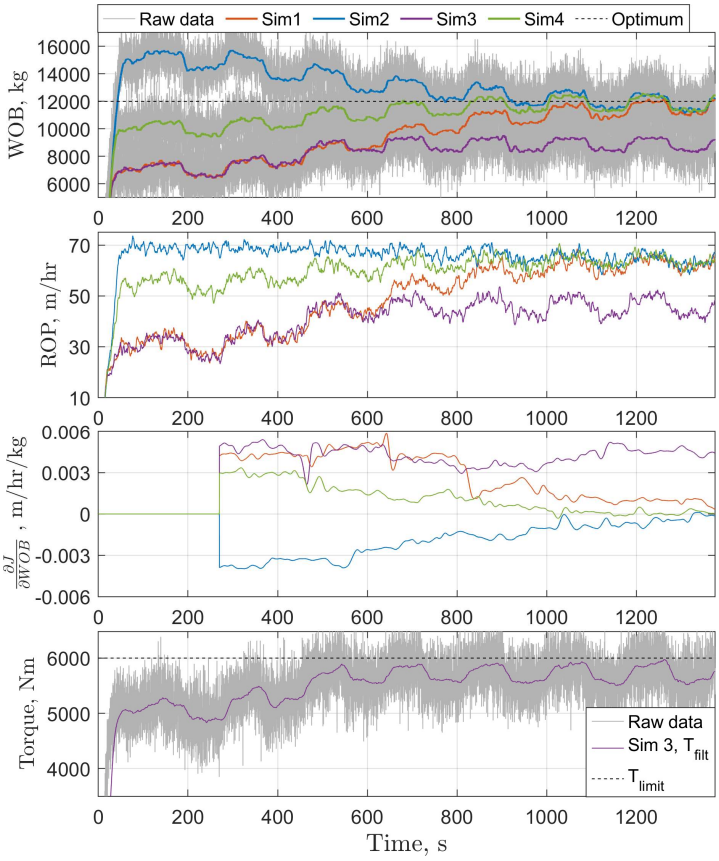

Fig. 10 Four runs with the ES algorithm performed on the high-fidelity drilling simulator OpenLab.

Simulation 2, indicated by the blue lines in Fig. 10, was initiated at a WOB_0 value of 15000 kg, where the average ROP is approximately 69 m/hr. This represents drilling in the founder region, where the ROP is slightly higher than at the founder point. Drilling in this region for prolonged periods can be damaging to the bit and downhole tools, and it should be avoided. Throughout this run, the ES algorithm is seen to reduce the WOB_0 variable towards the founder point, ending the simulation at an average WOB and ROP of 11750 kg and 64 m/hr, respectively. This is in fact a reduction in ROP of about 7% from the initial value, but drilling at this slightly reduced ROP is still the desired behavior because of the diminished potential for downhole equipment wear and tear.

The third simulation is depicted with purple lines in Fig. 10. The starting point is the same as in Sim 1, but a maximal torque limit of 6000 Nm is imposed on the system. The first 550 seconds in Sim 3 are almost identical to Sim 1. At this point, the constraint handling part of the ES algorithm predicted that further increasing the WOB_0 variable would violate the torque limitation. This behavior can be seen in the fourth track of Fig. 10, where the filtered torque remains within the acceptable bounds as the adaptation was stopped in time. From the third track in Fig. 10, the estimated gradient is seen to retain a positive value throughout the run. This indicates that the ES algorithm recognized a potential for more efficient drilling at higher WOB, which could not be realized because of the torque constraint. From 550 seconds and onwards, this run was performed with an average WOB and ROP of 8900 kg and 46 m/hr, respectively. Because the ES algorithm was not allowed to steer the WOB_0 variable to the founder point, the improvements in ROP in this run (of about 50%) are not as high as in the unconstrained Sim 1. Still, the ROP achieved from 550 seconds and onwards in this run is close to the maximal ROP that could be obtained while still adhering to the torque constraint.

A fourth simulation is detailed with green lines in Fig. 10. This run was initiated with a WOB_0 value of 10000 kg, which could represent a case where we had some prior knowledge (e.g. from drilling an offset well) of what WOB this section should be drilled with. Because the initial WOB was quite close to the optimal point, the drilling commenced at a quite high ROP of 54 m/hr. Yet, the ES algorithm recognized that higher drilling efficiency could be

achieved by increasing the WOB, resulting in the WOB_0 being steered to a value of 11900 kg where the average ROP was increased by about 19% to a value of 64.3 m/hr. The third track in Fig. 10 shows that the estimated gradient stabilized around a zero value at about 1000 seconds of simulation time, at which point the ES algorithm stopped adapting the WOB_0 variable, while still performing the WOB excitations to detect any potential changes in the drilling conditions.

It can be noted that the WOB_0 value which the ES algorithm converged to simulations 1, 2 and 4, is slightly below the pre-calculated optimum at 12000 kg. A likely explanation for this is that the ES algorithm calculates a gradient based on measurements on both sides of the WOB_0 value (at $WOB_0 \pm$ A kg), and approximates the gradient at WOB_0 through linear regression. This linearization, combined with noisy measurements and drillstring elasticity, can cause the estimated gradient to deviate slightly from the true analytical value (and show some transient spiky behavior). Still, the ES algorithm was able to navigate the WOB_0 variable sufficiently close to the founder point to achieve drilling at or close to the highest possible dysfunction-free ROP in these scenarios.

7. DISCUSSION OF RESULTS

In the experiments and simulations, the ES method was seen to autonomously perform the micro-tests and steer the WOB to achieve more efficient drilling while avoiding violation of the torque limitation in the constrained cases. How much the ES algorithm is able to increase the ROP depends on the initial WOB_0 value, which determines the potential for ROP improvements. This property is illustrated in the unconstrained simulation cases where the ROP gains were in the range -7% to 110%, dependent on the initial condition. In cases where the application of the ES algorithm resulted in reduced ROP (Simulation 3 and to a small extent Experiment 3), this was the preferred behavior as the reduction was a result of exiting the dysfunction region.

How quickly the ES algorithm is able to seek out the optimal point to drill at is dependent on the adaptation gain, γ. A large value for γ will cause rapid changes in the WOB and converge to the optimum quicker. At the same time, too aggressive tuning of γ can cause the

algorithm to make large adjustments even for small deviations in the estimated gradient caused by noise or disturbances. Thus, finding a value for γ which balances convergence rate and sensitivity to noise is an important tuning task when using the ES algorithm to optimize a noisy process such as drilling.

A related topic when considering optimization based on noisy data, is the application of appropriate filtering. The goal is to filter the data enough to extract useful information, while at the same retaining as much as possible of the underlying "true" signal. Excessively filtering the data to remove all noise will in fact eliminate most of the information which the ES method uses for gradient estimation. A balance must be struck between performing the analysis on too noisy data which can make the estimated gradient inaccurate, and overly filtering the data which eliminates most of the true signal. When considering time series analysis of filtered data, it is important that filters with the same or similar time-delays are used to be able to extract the relationships between the measured parameters.

The experiments performed on the downscaled drilling rig supports the finding that the ES algorithm can be used for optimization of full-scale operations, as the method is able to handle the vibrations and noise experienced in the lab. The experimental rig is set up to work in an analogous fashion as a full-scale drilling rig, allowing us to draw some conclusions from the experiments. Still, experiments on this small scale are not able to capture all the complex dynamics related to drill string vibrations and bit foundering seen in field operations and how the ES method would perform under these conditions. Because of the simulation layer used to emulate bit foundering, the dynamics of bit foundering and its effect on the ES algorithm's effectiveness could not be studied here. Still, the simulation layer used in the experiments is able to qualitatively mimic the foundering ROP-WOB relationship seen in field operations [10,19], which indicates that the method would be effective also in the field. Additional experimental studies on ES with a rig which can organically capture foundering effects and extending the experiments to encompass other relevant parameters for drilling optimization, such as the RPM, are promising topics for future research.

8. CONCLUSIONS

We present an optimization strategy which automatically seeks out and maintains the WOB that results in drilling at the highest possible dysfunction-free ROP. The algorithm is data-driven and does not require any model of the drilling process to be employed. The proposed method gathers information about the current drilling conditions by performing micro-tests with the applied WOB and autonomously uses the test results to perform optimization actions that increases the ROP. The micro-test procedure is run in the background while drilling ahead, with the tests performed continuously to adapt to the current drilling environment. The algorithm has been tested with experiments on a downscaled drilling rig and on a high-fidelity drilling simulator, which both capture the noisy conditions inherent to the drilling process. In both the experiments and simulations, the ES algorithm demonstrated the ability to automatically steer the WOB to the founder point without any prior knowledge of the drilling conditions. The studied cases also showed that the proposed method is able to adhere to process constraints, where the constraint handling was demonstrated with the example of a maximal limit imposed on the surface torque.

ACKNOWLEDGMENT

This research is part of BRU21 – NTNU Research and Innovation Program in Digital and Automation Solutions for the Oil and Gas Industry, www.ntnu.edu/bru21 (accessed on March 30th, 2021). The authors would also like to thank Noralf Vedvik and Steffen Wærnes Moen for their assistance with the experimental setup.

FUNDING

This research was funded by the Norwegian University of Science and Technology through the BRU21 research program.

NOMENCLATURE

Parameters

a	Least-squares slope	(m/hr/kg)
α	Least-squares slope	(Nm/kg)
A	Amplitude of excitation signal	(kg)
b	Least-squares intercept	(m/hr)
β	Least-squares intercept	(Nm)
C_a	Drill string compliance	(m/N)
d	Excitation signal	(kg)
Δt	Time increment	(s)
e	Torque limitation variable	(Nm)
g	Gravitational acceleration	(m/s^2)
γ	Adaptation gain	($kg^2 \cdot hr/m/s$)
h_{block}	Height of travelling block	(m)
h_{bit}	Bit position	(m)
J	Performance function	(m/hr)
L	Length of drill string	(m)
λ	Penalty variable	(kg)
μ	Parameter in J	(m/hr/kg)
N	Normal distribution probability density function	
P	Period of excitation signal	(s)
Ψ	Summation term	(Nm)
r	Vector of drilling parameters	
t	Time	(s)
T	Torque	(Nm)
T_{filt}	Filtered torque value	(Nm)
T_{avg}	Average torque value	(Nm)
T_{limit}	Limiting torque value	(Nm)
WOB_0	Center WOB value in d	(kg)
$WOB_{0,constrained}$	Constrained WOB_0 value	(kg)
WOB_B	Buffer with past WOB values	(kg)
y	Measurement of h_{block}	(m)

Abbreviations

ES	Extremum Seeking	
KF	Kalman Filter	
MSE	Mechanical Specific Energy	
ROP	Rate of Penetration	(m/hr)
RPM	Revolutions per Minute	(rpm)
SF	Safety Factor	
WOB	Weight on Bit	(kg)

REFERENCES

[1] Dunlop, J., Isangulov, R., Aldred, W.D., Sanchez, H.A., Flores, J.L.S., Herdoiza, J.A., Belaskie, J., and Luppens, C. "Increased Rate of Penetration Through Automation." the SPE/IADC Drilling Conference and Exhibition, Amsterdam, The Netherlands, Society of Petroleum Engineers, SPE, 1-3 March 2011 2011. doi:10.2118/139897-MS.

[2] Chapman, C.D., Sanchez, J.L., De Leon Perez, R., and Yu, H., "Automated Closed-Loop Drilling with ROP Optimization Algorithm Significantly Reduces Drilling Time and Improves Downhole Tool Reliability." Paper presented at the the IADC/SPE Drilling Conference and Exhibition, San Diego, California, USA, 6-8 March 2012. doi:10.2118/151736-MS.

[3] Sui, D., Nybø, R., and Azizi, V., "Real-time optimization of rate of penetration during drilling operation." Paper presented at the 2013 10th IEEE International Conference on Control and Automation (ICCA), 12-14 June 2013. doi:10.1109/ICCA.2013.6564893.

[4] Sui, D., and Aadnoy, B., 2016, "Rate of Penetration Optimization using Moving Horizon Estimation," *Modeling, Identification and Control: A Norwegian Research Bulletin,* 37, pp. 149-58. doi:10.4173/mic.2016.3.1.

[5] Bataee, M., Kamyab, M., and Ashena, R. "Investigation of Various ROP Models and Optimization of Drilling Parameters for PDC and Roller-cone Bits in Shadegan Oil Field." the International Oil and Gas Conference and Exhibition in China, Beijing, China, Society of Petroleum Engineers, SPE, 8-10 June 2010. doi:10.2118/130932-MS.

[6] Spencer, S.J., Mazumdar, A., Jiann-Cherng, S., Foris, A., and Buerger, S.P., "Estimation and Control for Efficient Autonomous Drilling Through Layered Materials." Paper presented at the 2017 American Control Conference (ACC), 24-26 May 2017. doi:10.23919/ACC.2017.7962950.

[7] Hegde, C., Daigle, H., Millwater, H., and Gray, K., 2017, "Analysis of Rate of Penetration (ROP) Prediction in Drilling Using Physics-Based and Data-Driven Models," *Journal of Petroleum Science and Engineering,* 159, pp. 295-306. doi:10.1016/j.petrol.2017.09.020.

[8] Hegde, C., Daigle, H., and Gray, K.E., 2018, "Performance Comparison of Algorithms for Real-Time Rate-of-Penetration Optimization in Drilling Using Data-Driven Models," *SPE Journal,* 23, no. 05, pp. 1706-22. doi:10.2118/191141-PA.

[9] Eren, T., and Ozbayoglu, M.E., "Real Time Optimization of Drilling Parameters During Drilling Operations." Paper presented at the SPE Oil and Gas India Conference and Exhibition, Mumbai, India, 20-22 January 2010. doi:10.2118/129126-MS.

[10] Dupriest, F.E., and Koederitz, W.L., "Maximizing Drill Rates with Real-Time Surveillance of Mechanical Specific Energy." Paper presented at the the SPE/IADC Drilling Conference, Amsterdam, The Netherlands, 23-25 February 2005. doi:10.2118/92194-MS.

[11] Dupriest, F.E. "Comprehensive Drill Rate Management Process To Maximize ROP." the SPE Annual Technical Conference and Exhibition, San Antonio, Texas, USA, Society of Petroleum Engineers, SPE, 24-27 September 2006 2006. doi:10.2118/102210-MS.

[12] Ariyur, K.B., and Krstić, M. *Real-Time Optimization by Extremum Seeking Control.* Wiley Online Library, 2003. doi:doi:10.1002/0471669784

[13] Tan, Y., Moase, W.H., Manzie, C., Nešić, D., and Mareels, I.M., "Extremum seeking from 1922 to 2010." Paper presented at the the 29th Chinese Control Conference, 29-31 July 2010.

[14] Banks, S., "Minimizing the Mechanical Specific Energy While Drilling Using Extremum Seeking Control." Paper presented at the the 11th International Conference on Vibration Problems, Lisbon, Portugal, 9-12 September 2013, Corpus ID: 214789826.

[15] Nystad, M., and Pavlov, A., "Micro-Testing While Drilling for Rate of Penetration Optimization." Paper presented at the the International Conference on Offshore Mechanics and Arctic Engineering, Virtual, Online, 3-7 August 2020.

[16] Aarsnes, U.J.F., Aamo, O.M., and Krstic, M., "Extremum Seeking for Real-time Optimal Drilling Control." Paper presented at the the American Control Conference (ACC), Philadelphia, PA, USA, 10-12 July 2019.

[17] Nystad, M., Aadnøy, B.S., and Pavlov, A., 2021, "Real-Time Minimization of Mechanical Specific Energy with Multivariable Extremum Seeking," *Energies,* 14, no. 5, pp. 1298.

[18] Lai, S.W., Ng, J., Eddy, A., Khromov, S., Paslawski, D., van Beurden, R., Olesen, L., Payette, G.S., and Spivey, B.J., 2020, "Large-Scale Deployment of a Closed-Loop Drilling Optimization System: Implementation and Field Results," *SPE Drilling & Completion,,* Preprint, pp. doi:10.2118/199601-PA.

[19] Dupriest, F., Hutchison, I., Oort, E.v., and Armstrong, N. *The IADC Drilling Manual - Drilling Practices.* 12th ed.: International Association of Drilling Contractors, 2014.

[20] Tan, Y., Nešić, D., and Mareels, I., 2008, "On the Choice of Dither in Extremum Seeking Systems: A Case Study," *Automatica,* 44, no. 5, pp. 1446-50. doi:10.1016/j.automatica.2007.10.016.

[21] Kyllingstad, Å., and Thoresen, K.E., "Improving Accuracy of Well Depth and ROP." Paper presented at the SPE/IADC International Drilling Conference and Exhibition, 2019. doi:10.2118/194098-ms.

[22] Saho, K., 2017, "Kalman filter for moving object tracking: Performance analysis and filter design," *Kalman Filters-Theory for Advanced Applications*, pp. 233-52. doi:10.5772/INTECHOPEN.71731.

[23] "Drillbotics Competition." 2021, https://drillbotics.com/.

[24] Arnø, M., Thuve, A., Knoop, S., Hovda, S., Pavlov, A., and Florence, F., "Design and Implementation of a Miniature Autonomous Drilling Rig for Drillbotics 2018." Paper presented at the SPE/IADC International Drilling Conference and Exhibition, 5-7 March 2019 2019. doi:10.2118/194226-MS.

[25] Egeland, R.L., Lescoeur, A., Olsen, M., Vasantharajan, M., Hovda, S., and Pavlov, A., 2018. "Miniature Robotic Drilling Rig for Research and Education in Drilling Automation." Paper presented at the IEEE Conference on Control Technology and Applications (CCTA), 21-24 August 2018. doi:10.1109/CCTA.2018.8511506.

[26] Handeland, A.S., 2018, "Design and Optimization of a Miniature Autonomous Drillig Rig - Contributions to the Drillbotics Competition 2018." MSc, Norwegian University of Science and Technology. doi:11250/2559474.

[27] Ewald, R., Gravdal, J.E., Sui, D., and Shor, R., "Web Enabled High Fidelity Drilling Computer Model with User-Friendly Interface for Education, Research and Innovation." Paper presented at the Proceedings of The 59th Conference on Simulation and Modelling (SIMS 59), 26-28 September 2018, Oslo Metropolitan University, Norway, 2018.

[28] Saadallah, N., Gravdal, J.E., Ewald, R., Moi, S., Ambrus, A., Daireaux, B., Sivertsen, S.*, et al.*, "OpenLab: Design and applications of a modern drilling digitalization infrastructure." Paper presented at the SPE Norway One Day Seminar, 2019.

Appendix C – Article 3

Real-Time Minimization of Mechanical Specific Energy with Multivariable Extremum Seeking

Magnus Nystad, Bernt Sigve Aadnøy, Alexey Pavlov

This paper was published in the journal Energies, Special issue: Drilling Technologies for the Next Generations, February 2021. doi: 10.3390/en14051298.

energies

MDPI

Article

Real-Time Minimization of Mechanical Specific Energy with Multivariable Extremum Seeking

Magnus Nystad [1,*], Bernt Sigve Aadnøy [1,2] and Alexey Pavlov [1]

[1] Department of Geoscience and Petroleum, Norwegian University of Science and Technology, 7034 Trondheim, Norway; bernt.s.aadnoy@ntnu.no or bernt.aadnoy@uis.no (B.S.A.); alexey.pavlov@ntnu.no (A.P.)
[2] Department of Energy and Petroleum Engineering, University of Stavanger, 4021 Stavanger, Norway
* Correspondence: magnus.nystad@ntnu.no

Abstract: Drilling more efficiently and with less non-productive time (NPT) is one of the key enablers to reduce field development costs. In this work, we investigate the application of a data-driven optimization method called extremum seeking (ES) to achieve more efficient and safe drilling through automatic real-time minimization of the mechanical specific energy (MSE). The ES algorithm gathers information about the current downhole conditions by performing small tests with the applied weight on bit (WOB) and drill string rotational rate (RPM) while drilling and automatically implements optimization actions based on the test results. The ES method does not require an a priori model of the drilling process and can thus be applied even in instances when sufficiently accurate drilling models are not available. The proposed algorithm can handle various drilling constraints related to drilling dysfunctions and hardware limitations. The algorithm's performance is demonstrated by simulations, where the algorithm successfully finds and maintains the optimal WOB and RPM while adhering to drilling constraints in various settings. The simulations show that the ES method is able to track changes in the optimal WOB and RPM corresponding to changes in the drilled formation. As demonstrated in the simulation scenarios, the overall improvements in rate of penetration (ROP) can be up to 20–170%, depending on the initial guess of the optimal WOB and RPM obtained from e.g., a drill-off test or a potentially inaccurate model. The presented algorithm is supplied with specific design choices and tuning considerations that facilitate its simple and efficient use in drilling applications.

Keywords: real-time drilling optimization; extremum seeking; data-driven optimization; mechanical specific energy; rate of penetration

Citation: Nystad, M.; Aadnøy, B.S.; Pavlov, A. Real-Time Minimization of Mechanical Specific Energy with Multivariable Extremum Seeking. *Energies* **2021**, *14*, 1298. https://doi.org/10.3390/en14051298

Academic Editor: Catalin Teodoriu

Received: 18 January 2021
Accepted: 22 February 2021
Published: 26 February 2021

1. Introduction

Drilling a petroleum well is a complicated process with a multitude of factors that affect the drilling efficiency. Because of the high costs associated with well construction, the industry has for more than a century sought to improve drilling performance, in particular through automation and mechanization; a process which has been traced by Eustes [1]. The current state of drilling automation mainly consists of separate functionalities that can aid the driller by performing tasks like providing envelope control [2,3], fault detection [4,5], vibration mitigation [6,7] or selection of the best suited weight on bit (WOB) and drill string rotational rate (RPM) for rate of penetration (ROP) optimization [8,9]. The focus of this study is on developing an automatic system for real-time drilling optimization that automatically seeks out and maintains the WOB and RPM resulting in optimal and safe drilling for the current downhole conditions.

To apply any automated algorithm to drill more efficiently, an objective function is needed to quantify what is meant by optimal drilling conditions. In this work, we employ the mechanical specific energy (MSE) as the objective function to be minimized. The MSE is a measure of the energy required to excavate a unit volume of rock and can

be expressed as a ratio between the rate of energy usage to the rate of penetration [10], which provides a relative measure of the drilling efficiency [11]. The MSE is strongly dependent on the relationship between the ROP and the applied WOB and RPM. It is expected that for a certain region of WOB and RPM values, the bit will drill at peak efficiency [12]. Increasing the WOB or RPM inside the efficient drilling region will result in corresponding proportional gains in the ROP, while the MSE decreases or stays constant. At some threshold value, often referred to as the *founder point*, further increases in WOB or RPM will no longer yield a proportional response in ROP. The lower than expected response in ROP is caused by a drilling dysfunction such as vibrations, bit- or bottomhole balling, which reduces the drilling efficiency and drastically increases the MSE. The founder point can therefore be identified as the combination of WOB and RPM that corresponds to the minimum MSE. If there is no specific operating point that results in minimal MSE, but rather a range of WOB and RPM values at which the MSE is minimal and nearly constant, the founder point can be identified by increasing the WOB and RPM until the MSE starts to grow [12].

It is important to note that drilling at the founder point results in high ROP and the most energy-efficient drilling, but moderately higher ROP can in most cases be obtained by increasing the WOB and/or RPM somewhat past the point of founder. Drilling with dysfunctions can however be deleterious for the bit, downhole tools and borehole quality [12,13], which can result in equipment wear and NPT by having to pull the bit prematurely [14]. The ROP that is achieved when the MSE is at its minimal value is therefore the maximal "good ROP" that can be attained without re-engineering drilling equipment or procedures [11].

In addition to drilling dysfunctions that should be avoided, there are also process constraints that the driller or an algorithm controlling the drilling must adhere to. Drilling at the founder point might not be feasible because of process constraints such as a maximal allowable ROP related to hole cleaning, an upper limit on the WOB to prevent bit damage or top-side energy constraints. In these constrained cases, the authors consider the optimal drilling conditions to be at the smallest MSE value that can be attained without violating the process constraints.

Selecting the optimal WOB and RPM is not a trivial task. Available drilling models might not be accurate enough in predicting the relationship between the ROP and related drilling parameters [15,16]. Varying downhole conditions such as changes in pore pressure or formation properties as well as degradation of the bit teeth/cutters can alter drilling efficiency so that the combination of WOB and RPM that was optimal a short time ago might no longer be the best solution. Historically, designated testing procedures like the Drill-off test [12] or five-point test [17] have been used to empirically explore how the ROP responds to various combinations of WOB and RPM. The downside of this type of "one-time testing" is that the results are only valid for the current downhole conditions, and as soon as the conditions change, the test will have to be repeated.

An alternative to optimization based on models and on "one-time testing" are approaches employing "testing on the fly". In these approaches, the relation between the WOB and/or RPM and an objective function such as the ROP or MSE is explored by performing tests while drilling ahead and selecting more optimal WOB and RPM based on the obtained information. As the downhole conditions change, the repeated tests can identify how the WOB and RPM should be adjusted to drill more efficiently, given the new circumstances. Rommetveit et al. [18] describe an approach of making changes in the WOB and RPM to gather information on how the ROP reacts to these changes. The gathered information can then be used to generate recommendations for the driller or for closed loop control by an optimization algorithm [18]. An automated golden search algorithm that varies the WOB to identify drilling with minimal MSE has been tested on a lab-scale drilling rig [19]. Field trials of advisory systems that can suggest variations in the applied WOB and RPM to search for the drilling conditions that yield the lowest MSE have been described in [20,21]. In recent years, several authors have investigated a data-driven

method called extremum seeking (ES) for drilling optimization. This method relies on continuous testing and optimization based on the test results. Banks [22] explored single variable ES to minimize the MSE with a laboratory drill rig. Aarsnes et al. [23] showed with simulations that ES can be used to seek out the optimal WOB to drill with. A method for adhering to process constraints while optimizing the applied WOB with ES has also been investigated [24]. A drilling optimization system that employs multivariable ES has been tested in the field with good results [25], although no specific details on the algorithm have been provided in that paper.

Extremum seeking is a model-free control algorithm that provides a framework for automatically conducting small tests of the current operating conditions and adapting to the results of the tests to optimize the process. ES has previously been utilized in a variety of engineering systems; an extensive list is provided by Tan et al. [26]. In the context of drilling optimization, the ES algorithm can be employed to find the combination of WOB and RPM which minimizes the MSE (or some other objective function). While drilling ahead, small periodic variations in the WOB and RPM are automatically implemented by the algorithm to test the current drilling conditions. How the MSE responds to these variations is calculated and logged from real-time measurements of the relevant drilling parameters. This generates a local linear "map" of how the MSE is related to the WOB and RPM, which is used by the ES algorithm to make small adjustments in the WOB and RPM in the direction that lowers the MSE. By iteratively performing this procedure of testing and adapting to the results, the WOB and RPM will be steered to the values which result in drilling with minimal MSE. As new tests are performed and new data is recorded, older measurements are discarded from the analysis so that the information used by the algorithm is up to date and representative of the current downhole conditions. In this way, the algorithm will be able to adapt to downhole changes like drilling into a new formation where new values of WOB and RPM might be more beneficial to drill with.

The main advantage of applying the ES method for drilling optimization is that it is model-free, and therefore requires limited a-priori knowledge about the current drilling environment to be employed. When using models to predict how to drill optimally [8,9,15,16,27], the models need to be tuned based on data that is representative of the current downhole conditions. When the conditions change, the models will no longer be valid before they are re-tuned to the new circumstances, which can limit their applicability for real-time optimization. Nevertheless, the drilling models are still a valuable tool that can be combined with data-driven approaches such as Extremum Seeking. The models can provide an initial estimate of the optimal WOB and RPM to drill with, which the ES method can use as a starting point to further improve the drilling efficiency.

In this paper, we present a multivariable ES algorithm that automatically adjusts the WOB and RPM to reach drilling with a minimal MSE value. Although an application of multivariable ES to drilling was presented in [25] with successful field trials, limited details of the algorithm were provided. The algorithm presented in our paper is given in detail with a description of specific design choices and tuning considerations that lead to its simple and efficient use for drilling applications. In addition to that, the presented algorithm can automatically handle operational constraints relevant to safe drilling. The paper details several options on how this functionality can be implemented. Finally, to test the algorithm, a new qualitative model that links the ROP, WOB, RPM and Torque as well as drilling dysfunctions is presented. Without dysfunctions, the model coincides with the drilling model developed by Detournay et al. [28]. This combined model is qualitative when it comes to modelling the dysfunction effects. Yet, it represents phenomena observed in field operations where drilling with dysfunctions result in reduced ROP and high MSE [12–14], and can be utilized for testing of ES algorithms as well as other data-driven (model-free) drilling optimization approaches.

The remainder of the paper is organized in the following way: in Section 2, we formulate the challenge of achieving safe and efficient drilling as an optimization problem and present models that qualitatively describe the relations between the drilling efficiency

in terms of MSE, drilling dysfunctions and operational constraints. These models will be used for testing the proposed algorithm in a simulation environment. In Section 3, the multivariable extremum seeking method and different techniques for constraint handling are detailed together with practical aspects on how to apply and tune the algorithm. Section 4 presents simulation results that demonstrate the performance of the proposed algorithm and highlight its properties. Section 5 contains a discussion of the results of the study, while Section 6 presents conclusions and directions for further work.

2. Safe and Efficient Drilling as an Optimization Problem

The overall goal in drilling optimization (when it comes to mechanical aspects of drilling) is to ensure *WOB* and *RPM* that result in drilling that is both safe for the on-site personnel and drilling equipment (including wear minimization) and provides high efficiency. To achieve this goal, the concept of *MSE* can be used as a performance index to identify the most efficient drilling conditions, which will generate high *ROP* without exposing the bit and downhole tools to excessive vibrations. The latter can accelerate equipment wear and reduce the *ROP*.

Although it is theoretically possible to develop accurate models describing both the rock cutting process and various dysfunctions (e.g., using bit-rock interaction models [28] and advanced proprietary drill string models [14]), such models can be of limited value for real-time drilling optimization. They require detailed knowledge of downhole conditions like mechanical rock properties, the current bit wear state and formation characteristics such as heterogeneity, anisotropy and interbedding [14,28], parameters that change over time and are hard, if possible at all, to measure while drilling. Field experience do however show that at certain combinations of *WOB* and *RPM*, downhole vibrations that can be detrimental to the *ROP* and drilling equipment do occur [9,14,29]. Situations where the drilling efficiency is hampered by vibrations should therefore be accounted for in any optimization approach that attempts to seek out the optimal *WOB* and *RPM* to drill with.

To study drilling optimization in the presence of vibrational effects, we have chosen an approach which qualitatively includes vibrational dysfunctions into a drilling model for polycrystalline diamond compact (PDC) bits [28], and refer to this combined model as the *extended model*. The extended model accounts for vibrations by reducing the *ROP* and thus the drilling efficiency when drilling with combinations of *WOB* and *RPM* that places the operation in regions with expected vibrations. The extended model is qualitative when it comes to modelling the dysfunction effects. Yet, it represents phenomena observed in field operations where drilling with dysfunctions result in reduced *ROP* and high *MSE* [12–14]. When applying static models to replicate the bit/rock interaction, as is commonly done in the literature [28,30], the model variables such as the *WOB*, *RPM* and *ROP* need to be averaged over a suitable time-window for the model to be representative [28]. The same logic is applied in the extended model; it will not capture the dynamics of the dysfunction effects, but it will on average qualitatively represent drilling responses that could be seen in field operations. Because the underlying drilling model [28] in the extended model is defined for PDC bits, we focus on vibrational dysfunction effects, which tend to dominate bit dysfunction with PDC bits [12]. Yet, the extended model could be applied to qualitatively account for other types of dysfunction such as bit- and bottomhole balling as well.

2.1. Drilling Model

The drilling model developed by Detournay et al. [28] is used in this work as a base case scenario to simulate the drilling response of a PDC bit operating under ideal conditions. What is meant here by ideal conditions is that the drilling response for a given bit and formation is fully determined by the interface laws proposed by Detournay et al. [28], which define static relationships between the *WOB*, *RPM*, *ROP* and the bit torque (T) based on bit and formation properties. Drilling dysfunctions such as vibrations are however not covered by this drilling model and will be introduced in the next section. The Detournay

model relies on the existence of three distinct drilling regimes that relate the amount of applied *WOB* and the resulting *ROP* (for a given *RPM*), separated into

- *Phase I drilling*, where the *WOB* is not adequate to force the cutters to fully engage the formation, resulting in inefficient drilling. It is postulated that this inefficiency is caused by the cutters having a blunt underside, a *wear flat*, which supports some of the WOB and is a source of friction that does not contribute to the excavation of rock. In phase I, drilling with higher *WOB* will increase the depth of cut, which translates to higher *ROP*. At the same time, the increased depth of cut will expose a larger area of the wear flats to contact with the formation, which in turn makes the wear flats carry more *WOB*. The *WOB* being translated partly to increased cutting action and partly as friction on the wear flats continues until a threshold *WOB* which marks the onset of the next drilling phase. An ideally sharp bit will in theory never drill in phase I, as it has no wear flats.
- *Phase II drilling*, which is characterized by efficient drilling with the bit acting incrementally as an ideally sharp bit. At the onset of phase II drilling the contact forces between the wear flat and the formation are fully engaged. Further increases in *WOB* value will result in the rock deforming beneath the cutters without any increase in the contact area between the wear flat and formation. An increase in *WOB* while in phase II will be transferred solely to increasing depth of cut and correspondingly increasing *ROP* at peak efficiency, up to a point where a drilling dysfunction starts diminishing the efficiency of the cutting action.
- *Phase III drilling*, where an increase in contact forces between the bit and formation results in less of the applied *WOB* being translated to cutting action, which leads to a reduction in depth of cut and less efficient drilling. The onset of phase III drilling is referred to as the founder point and is often considered the optimal conditions to drill at [12,31].

The relationship between the applied *WOB* and *RPM* and the resulting bit torque (T) and *ROP* in phase I and phase II drilling can be expressed as [28]:

$$ROP(WOB, RPM) = \begin{cases} \frac{c_1 \cdot WOB \cdot RPM}{r}, \; WOB \leq WOB_* \\ \frac{c_2 \cdot (WOB - WOB_*) \cdot RPM}{r} + ROP_*, \; WOB > WOB_* \end{cases}, \quad (1)$$

$$T(WOB) = \begin{cases} c_3 \cdot r \cdot WOB, \; WOB \leq WOB_* \\ c_4 \cdot r \cdot (WOB - WOB_*) + T_*, \; WOB > WOB_* \end{cases}, \quad (2)$$

where the asterisk subscript signifies the transition point between phase I and phase II drilling, which is determined by bit bluntness and the formation strength. The values of ROP_* and T_* correspond to the *ROP* and torque at a weight on bit of WOB_*. The parameter r is the bit radius, and c_1, c_2, c_3 and c_4 are model parameters dependent on bit and formation properties.

Equation (1) can be viewed as a calculated depth of cut per bit revolution, determined by the model parameters and the applied *WOB*, which is multiplied with the *RPM* to find the equivalent *ROP*. The torque can be observed from Equation (2) to be independent of the *RPM*, as is often assumed in drilling models [32]. The modelled drilling response from Equations (1) and (2) for a relatively sharp 12 $\frac{1}{4}$" diameter PDC bit drilling through a generic formation *A* is shown in Figure 1, where the transition between phase I and phase II drilling occurs at a *WOB* value of approximately 2700 kg. As Equations (1) and (2) do not account for phase III effects, Figure 1 shows drilling at high efficiency throughout the investigated *WOB* and *RPM* interval after the onset of phase II drilling. In real world drilling operations, the *ROP* response to increasing *WOB* and *RPM* will at some point deviate from the ideal phase II drilling, but the *ROP* response in region III is not unique and depends on the loading path [28] as well as the dysfunction which causes the foundering to occur [12,31]. Region III drilling is therefore not explicitly included in the Detournay

drilling model [28]. A qualitative way of including vibrational drilling dysfunctions in the model is proposed in the next section.

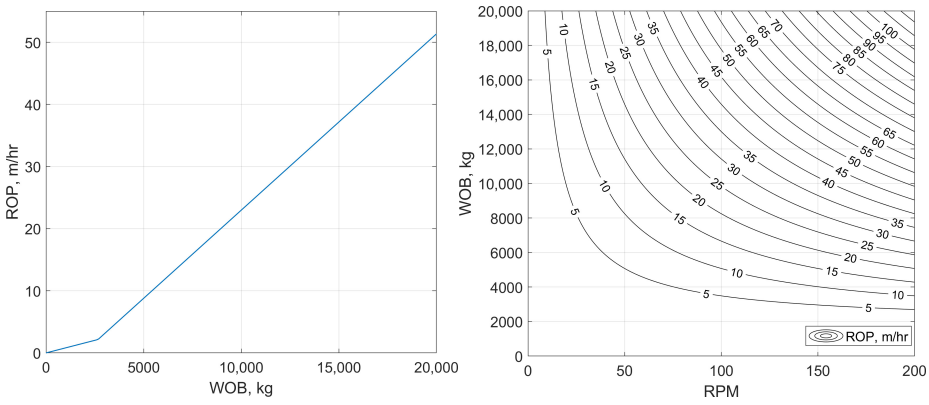

(**a**) (**b**)

Figure 1. Drilling response in phase I and phase II of the Detournay model [28] for a 12 1/4″ bit drilling in the generic formation *A*. (**a**) *ROP* as a function of *WOB* for a constant *RPM* value of 90; (**b**) Contour plot of *ROP* (m/h) as a function of applied *WOB* and *RPM*.

2.2. Drilling Dysfunctions and Constraints

There are a multitude of factors that can affect the drilling efficiency. For an efficient bit drilling with the expected depth of cut, the *ROP* will increase linearly with applied *WOB* or *RPM* as shown in Figure 1, unless a dysfunction reduces the drilling efficiency or a constraint limits the application of additional input energy [12,31]. The factors that influence the *ROP* can in general be grouped into two categories [13]

- *Foundering effects* that reduce the efficiency of energy transferal between the bit and the formation, which causes inefficient drilling. They can be caused by vibrations such as stick-slip and whirl, as well as bit or bottomhole balling. These dysfunctions will result in *ROP* values that are lower than what would be seen with an efficient bit for a given *WOB* and *RPM*.
- *Energy input limiters*, which constrain the amount of energy that can be applied through the input parameters *WOB* and *RPM* when drilling. In the case when the input energy is constrained before the onset of foundering effects, the bit would still be able to drill more efficiently at higher values of *WOB* and/or *RPM*, but because of a system constraint these parameters cannot be increased. A multitude of input energy limiters have been reported in the literature, such as a maximal *WOB* or *RPM* determined by bit or bottom hole assembly (BHA) design, a maximal *ROP* dictated by hole cleaning or solids handling capacity on the surface, a maximal top drive torque rating or top-side vibrations [8,9,13].

The onset of foundering effects and non-bit limiters can in many cases be extended to higher values of *WOB* and *RPM* through reengineering of the drilling equipment [13], but such considerations are beyond the scope of this study. Here, we rather focus on the existence of these effects and how they can be qualitatively included in a drilling model to explore the performance of a data-driven optimization technique in drilling simulation scenarios.

Critical values of *RPM* and *WOB* that trigger the onset of whirl and stick-slip vibrations are heavily affected by bit and BHA characteristics, as well as mechanical rock properties [14]. For an appropriately designed drill string, it is expected that there is a

region of *WOB* and *RPM* which is not notably affected by vibrations, while a combination of high *WOB* and low *RPM* can result in stick-slip vibrations, low *WOB* and high *RPM* can result in forward whirl, and a combination of high *WOB* and high *RPM* can induce backward whirl [9,14,29]. Figure 2 shows the concept of different regions in the *WOB-RPM* plane where the drilling process can be affected by vibrations, together with the *ROP* contours calculated from the Detournay model for formation *A*. The shaded center region in Figure 2 where one would drill with an acceptably high *ROP* while not being affected by the foundering effects was dubbed the *optimum zone* by Wu et al. [14], as it is in this region the combination(s) of *WOB* and *RPM* which results in the most efficient drilling can be found. The locations of the dysfunction regions for formation *A*, as seen in Figure 2, are generically placed in the *WOB-RPM* plane to qualitatively represent a scenario where there is an optimum zone surrounded by regions where dysfunctions will occur [14].

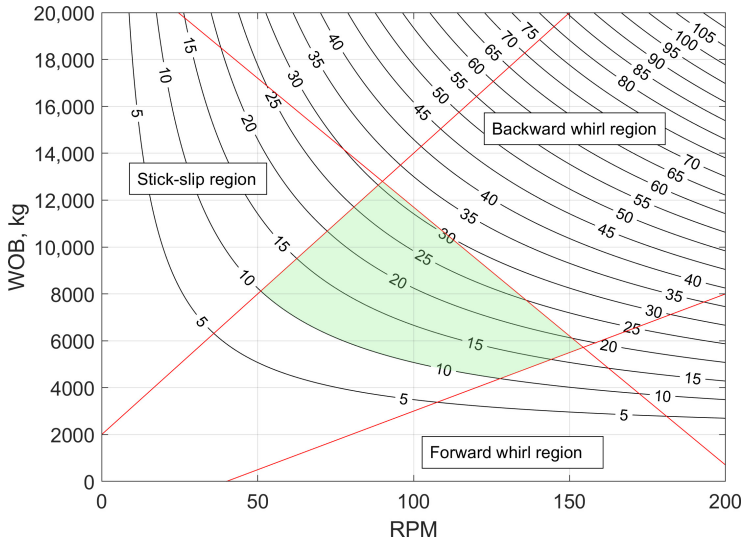

Figure 2. Contour map of dysfunction-free *ROP* (m/h) as a function of *WOB* and *RPM* in formation *A*, with generic critical values of *WOB* and *RPM* which mark the onset of vibrational foundering effects when drilling in this formation.

To incorporate vibrational foundering effects in the drilling model described by Equations (1) and (2) in a qualitative way, a penalty term proposed by the authors is included in the model. The penalty is formulated by defining limits in the *WOB-RPM* plane at which the dysfunctions start to occur, as illustrated in Figure 2. When drilling with a combination of *WOB* and *RPM* that places the operation in a region that is not affected by vibrations, the drilling response is dictated entirely by Equations (1) and (2). When drilling in the regions where vibrations are occurring, the proposed penalty term reduces the *ROP* calculated from Equation (1) by an amount that is dependent on the specific dysfunction and how far into the dysfunction region we are operating. This logic mimics the response seen in field operations for a bit drilling with a dysfunction; if we keep increasing the *WOB* and/or *RPM* further into the dysfunction regions, the experienced *ROP* will deviate further and further away from the straight-line *ROP* response that was expected if the bit was still drilling efficiently [12,13].

In this modified model, which we refer to as the extended model, the torque is not affected by the dysfunctions and is calculated from Equation (2) for all values of *WOB* and *RPM*. This property can be argued for from an *MSE* perspective. In the field, drilling with

vibrational dysfunctions can reduce the drilling efficiency to the extent that the energy consumption at the bit is more than an order of magnitude higher than what the rock strength would indicate [33]. This implies that either the torque continues to grow with the applied *WOB* also in the dysfunction region while the *ROP* is moderately reduced, or that the torque stays constant or decreases while the *ROP* is severely reduced as a response to increasing *WOB*. The former logic is applied in the extended model. Exactly how the torque and *ROP* reacts to drilling with dysfunctions cannot be captured adequately by a static model like the one we are proposing, but the model will be able to qualitatively capture the expected behavior of reduced *ROP* and increased *MSE* when drilling in the dysfunction regions.

The penalty functionality is implemented by means of straight-line functions (as shown in Figure 2) that mark the onset of drilling dysfunctions, but the method we propose is generic and could be applied to other curves as well. The method is in the following explained by an example of drilling with backward whirl, but the same logic applies to the other dysfunctions as well. If we are currently drilling ahead at an *RPM* of 150 and a *WOB* of 11,500 kg, Equation (1) predicts that the resulting *ROP* will be approximately 45 m/h in formation *A*, as can be seen from the contour lines in Figure 2. A penalty for drilling in the whirl region is calculated based on how far into the dysfunction region we are operating, which can be quantified by:

$$L = \sqrt{\left(\frac{WOB - WOB'}{WOB_{max}}\right)^2 + \left(\frac{RPM - RPM'}{RPM_{max}}\right)^2}. \quad (3)$$

In Equation (3), *WOB* and *RPM* are the current operating parameters, *WOB′* and *RPM′* signifies the point on the dysfunction curve closest to the operating parameters, and WOB_{max} and RPM_{max} are normalizing values of 20,000 kg and 200 *RPM*, respectively. The normalization is performed to assign approximately equal weight to the *WOB* and *RPM* when calculating the parameter *L*, which is a normalized measure of how far into the dysfunction region we are operating. When drilling in regions that are not affected by the dysfunctions, the parameter *L* is set equal to zero. Equation (3) is used to find the magnitude of the penalty, *R*, from:

$$R = S(mL) = \begin{cases} 3(mL)^2 - 2(mL)^3, & 0 < mL < 1 \\ 1, & mL \geq 1 \end{cases}, \quad (4)$$

where *S* is the *smoothstep function*, which is a clamping function that gives smooth s-shaped output values between 0 and 1. Using Equation (4) to calculate the penalty, the *ROP* will only be marginally reduced when drilling slightly into any of the dysfunction regions where *L* will take on small values, and more severely affected as *L* grows. The parameter *m* in Equation (4) is a model constant that can be used to customize how much the *ROP* is penalized by the different dysfunctions, so that e.g., whirl can have a stronger negative impact on the *ROP* than stick-slip [12]. In this work, the authors have used generic values of $m = 1$ to calculate the penalty in the forward and backward whirl regions, and $m = 0.5$ for the stick-slip region. When drilling at a point that simultaneously falls within two dysfunction regions, e.g., in the intersection between the stick-slip and backward whirl regions at an *RPM* value of 100 and a *WOB* value of 16,000 kg, the calculated penalty is the sum of the penalties incurred for drilling in both dysfunction regions.

The output *ROP* from the extended model is calculated from:

$$ROP = (1 - R)ROP_D, \quad (5)$$

where the parameter ROP_D signifies the *ROP* calculated from the "ideal" Detournay model in Equation (1), while *R* is calculated from Equations (3) and (4). From Equation (5), the penalized *ROP* that would be output from the model when operating at a *WOB* of 11,500 and an *RPM* of 150 is reduced from 45 to 36 m/h. Figure 3 displays how the *ROP* varies

as a function of *WOB* and *RPM* when the proposed extended model is applied to model drilling in formation *A*. Figure 3a shows a drilling curve for a constant *RPM* value of 90, where it can be observed that *WOB* values above 12,900 kg correspond to drilling with dysfunction, which reduces the *ROP* compared to the straight-line response predicted by the Detournay model. At even higher values of *WOB*, the penalty is further increased and the *ROP* starts decreasing. In Figure 3b, it can be seen from the *ROP* contours produced by the extended model that drilling in the dysfunction regions reduces the *ROP* so that the highest *ROP* that can be achieved in this formation is approximately 38 m/h, which occurs in the region around a *WOB* value of 14,000 kg and an *RPM* value of 120. This maximal *ROP* value does however correspond to drilling somewhat into the backward whirl region (as can be seen from Figure 2), and it does not necessarily represent the optimal conditions to drill at, as will be explained in the next section.

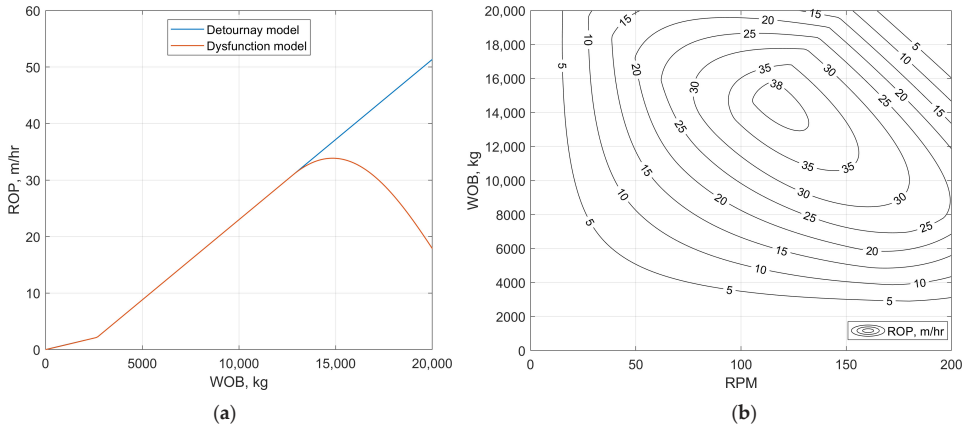

Figure 3. Drilling response with the drilling model including dysfunctions in formation *A*. (**a**) Drill-off curve for a constant *RPM* value of 90; (**b**) Contour plot of *ROP* (m/h) as a function of *WOB* and *RPM* with the extended model.

2.3. Mechanical Specific Energy

The concept of mechanical specific energy (*MSE*) was investigated by Simon [34] and Teale [10] in the sixties and has since been used for applications such as drilling optimization [11,13] and lithology identification [35]. *MSE* is defined as the energy required to excavate a unit volume of rock, and can be expressed as [10]:

$$MSE = \frac{gWOB}{\pi r^2} + \frac{120RPM \cdot \mathrm{T}}{r^2 ROP}, \quad (6)$$

where g is the gravitational acceleration constant with a value of 9.81 m/s^2. Equation (6) can be seen as the ratio between the energy input to the drilling process and the output *ROP*. This ratio will assume its minimal value when drilling at peak efficiency in the transition between phase II and phase III, with higher *MSE* values when drilling in phases I and III [13]. It can be noted that of the two right-hand terms in Equation (6), the rightmost term will normally be larger by a substantial margin and chiefly dictate the value of the calculated *MSE* [10]. To calculate an *MSE* value that reflects the actual energy expenditure at the bit, the downhole torque should be used when using Equation (6) [11,36]. This is because friction along the drill string will cause the surface torque to be higher than the torque on bit. When used as a trending tool, the *MSE* calculated from the surface torque can still be applied to identify more efficient drilling, but with the risk of possible inaccuracies in the analysis caused by fluctuations in the drill string frictional losses. The authors have

assumed in this work that we have access to the downhole torque values, which could come from either measurements from a downhole tool or be calculated from the topside torque with a torque and drag model.

Figure 4 illustrates how the *MSE* varies with *WOB* in formation *A* together with the corresponding drill-off curve. The plot is generated using the extended model detailed in Equations (1)–(5) and a constant *RPM* value of 90. From Figure 4, it can be seen that the minimum *MSE* occurs at a value of approximately 12,900 kg of *WOB*, at the founder point at which the *ROP* starts deviating from straight-line phase II drilling. Higher values of *ROP* can be achieved by increasing the *WOB* past the founder point, but this increase will come at the cost of detrimental foundering effects which can damage the downhole equipment. The minimum *MSE* will therefore correspond to the maximal "good *ROP*" that can be achieved without deleterious side-effects [11]. The shape of the *ROP*-*WOB* curve in region III will determine how rapidly the *MSE* increases when entering this region, but as long as the *ROP* deviates from the efficient phase II drilling, the *MSE* will increase at this point. This property makes the *MSE* a valuable diagnostic tool for drilling optimization; as long as the *MSE* shows an increasing trend in regions I and III (when moving "outward" from region II drilling in either direction), the most efficient drilling can be identified by seeking out the highest *WOB* that does not make the *MSE* increase.

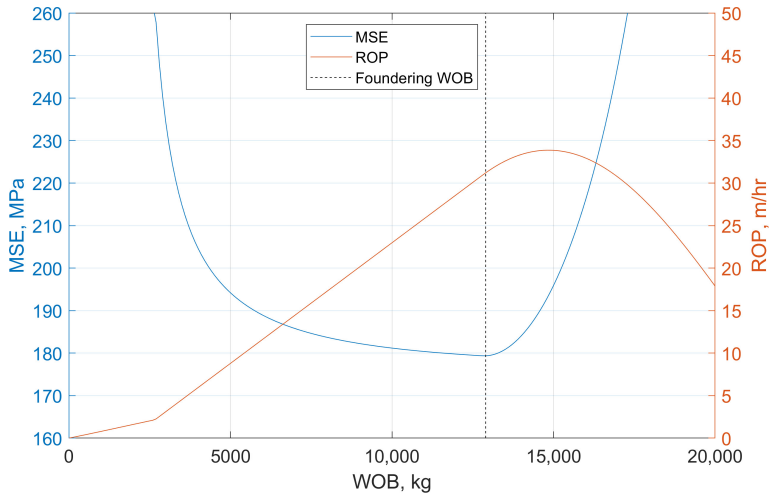

Figure 4. *MSE* and *ROP* as functions of *WOB*, illustrated for a constant *RPM* value of 90.

Figure 5 shows how the *MSE* and *ROP* varies with *RPM* for a constant *WOB* value of 10,000 kg in formation *A*. It can be observed that *RPM* values in the optimum zone, approximately 65 to 115 *RPM*, results in a flat minimum value in the *MSE*. Outside of this region, where dysfunctions affect the drilling efficiency, the *MSE* is seen to increase. This relationship can be deduced from the rightmost term in Equation (6) under the assumption that the *RPM* and torque are not coupled, as is the case with Equation (2). As long as the *ROP* scales linearly with the *RPM*, the *MSE* ratio will remain constant. In the dysfunction regions, where the gain in *ROP* is less than the expected linear relationship with the *RPM*, the numerator in Equation (6) will grow faster than the denominator. The highest *RPM* that can be applied without increasing the *MSE* above the constant minimum value in the optimum region will therefore yield the highest dysfunction-free *ROP* and the most efficient drilling.

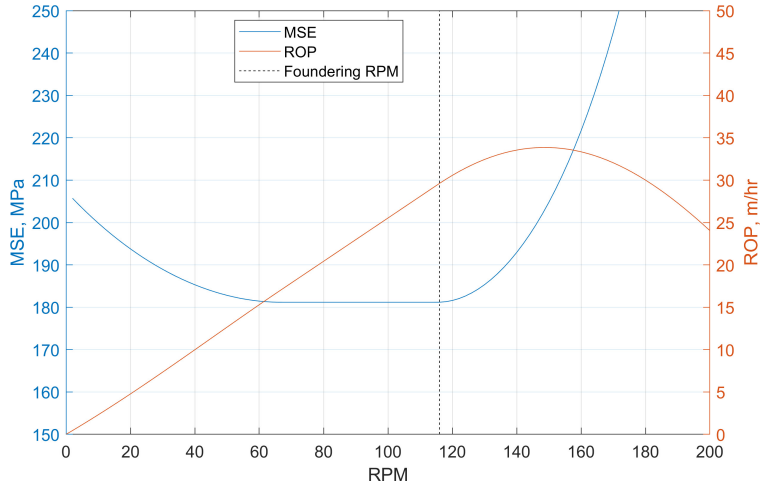

Figure 5. *MSE* and *ROP* as functions of *RPM*, illustrated for a constant *WOB* value of 10,000 kg.

A contour plot detailing how the *MSE* varies as a function of applied *WOB* and *RPM* is shown in Figure 6. This plot is generated using the proposed extended model, where the *ROP* is penalized when drilling in the three dysfunction regions (as shown in Figure 2). As can be seen in Figure 6, there is a region around the point at which the *WOB* value is approximately 12,900 kg and the *RPM* value is 90, where one would drill with the minimal *MSE* value of 180 MPa. This point corresponds to the top corner of the optimum zone depicted in Figure 2. Moving away from this low *MSE* region in any direction will increase the *MSE*; at first with small values and then progressively larger values as we move into the different dysfunction regions where drilling is less efficient. Comparing Figures 6 and 3b, it can also be observed that the highest possible *ROP* values which are found in the region around a *WOB* of 14,000 and an *RPM* of 120, correspond to drilling with a dysfunction, as is reflected by the higher *MSE* values around this point in Figure 6.

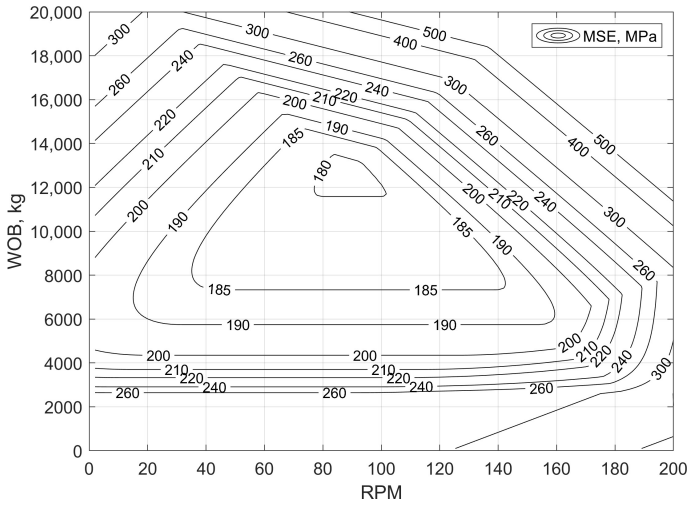

Figure 6. Contour plot of MSE as a function of WOB and RPM in formation *A*.

3. Drilling Optimization with Extremum Seeking

As detailed in Section 2, accurate modelling of the drilling process, which regions will be affected by dysfunctions and which combination(s) of *WOB* and *RPM* which will yield the most efficient drilling is a challenging task. Not knowing at which point drilling dysfunctions will be induced can cause the driller to use conservative limits imposed on the *WOB* and *RPM*, which can result in sub-optimal drilling. Accurate modeling of the drilling process will often require detailed knowledge of downhole parameters which cannot be measured directly and are therefore hard to obtain in real-time operations. The situation is further complicated by changes in downhole conditions which can cause models tuned to data from before the change to no longer be valid for the current circumstances.

Employing a data-driven optimization technique like ES can be used to solve these challenges, as the method does not rely on having detailed a priori knowledge of the downhole conditions. The ES algorithm relies instead on executing small tests while drilling ahead by varying the applied *WOB* and *RPM*. Real-time measurements of how drilling parameters such as the *ROP*, *T* and calculated *MSE* vary when the tests are performed are recorded by the algorithm. The measured response to the tests represents the most up to date knowledge on how the drilling process reacts to changes in *WOB* and *RPM* and are automatically used by the algorithm to perform optimization actions that reduce the *MSE* if possible. When a change in downhole conditions occurs, such as a formation shift, this will be reflected in the measured drilling parameters and the ES algorithm will be able to adapt to the new downhole circumstances.

Using the *MSE* as an objective function to quantify when we are drilling efficiently can be a powerful tool for drilling optimization. If the *MSE* exhibits the general shape shown in Figure 6; where drilling efficiently will result in lower *MSE* values and drilling into the dysfunction regions will make the *MSE* progressively increase, the proposed ES algorithm can be used to seek out the *WOB* and *RPM* that result in drilling with minimal *MSE*. The only a priori information that is needed is knowing the general shape of the *MSE* response to drilling efficiently and inefficiently, as well as some general drilling engineering knowledge that is needed to initiate and tune the algorithm. The ES method is an iterative algorithm, which means that it needs to be initiated when drilling at some *WOB* and *RPM* and use this as a starting point from which it can perform optimization actions. This starting point can be viewed as an "initial guess" of the optimal *WOB* and *RPM*, and can be based on the drillers experience, data from an offset well or an estimate provided by a drilling model.

3.1. The Extremum Seeking Algorithm

Extremum seeking is in essence a hill climbing optimization method that is applied to a process in real-time. ES works by systematically exciting the system to gather information about the current operating conditions by varying one or several controllable input variables. Real-time and recent measurements are used to calculate an objective function that quantifies the system's reaction to the excitations. Based on how the objective function changes with the variations in the input parameters, the ES algorithm will automatically make small changes to the input variables that steers them towards the values optimizing the objective function. This happens in an iterative fashion, where new measurements are continuously included in the analysis and old measurements are discarded. The optimization method does not require a model of the system, since all adjustments are performed based on measurements of how the process performs with different values and combinations of the input variables.

In this work, we consider a multivariable ES approach in which the controllable variables we seek to manipulate to drill more optimally are the *WOB* and *RPM*. The *MSE*, as detailed in Equation (6), is used as an objective function to quantify what combination of *WOB* and *RPM* constitutes optimal drilling. The procedure is illustrated in Figure 7, where the left-hand plot demonstrates how the ES algorithm automatically varies the *WOB* and *RPM* to investigate the drilling response in the local region marked with green shading.

The right-hand tracks show the varying input variables and the resulting *MSE* as functions of time. It can be observed from Figure 7 that, in this case, higher values of both *WOB* and *RPM* results in lower *MSE*, which would prompt the ES algorithm to slowly increase the *WOB* and *RPM*, as indicated by the dotted lines. This procedure of testing and adapting to the *MSE*-response is performed continuously and will over time drive the system to drill at the optimal conditions that minimize the *MSE*. In cases where the *MSE* does not change when the *WOB* and/or *RPM* are varied, this is interpreted by the proposed ES algorithm as a situation where it should increase the applied *WOB* and/or *RPM* further, as explained in Section 2. Several techniques for avoiding violation of drilling constraints are proposed and implemented in the following, to ensure that the ES algorithm will adhere to process limitations while seeking out the minimal *MSE*.

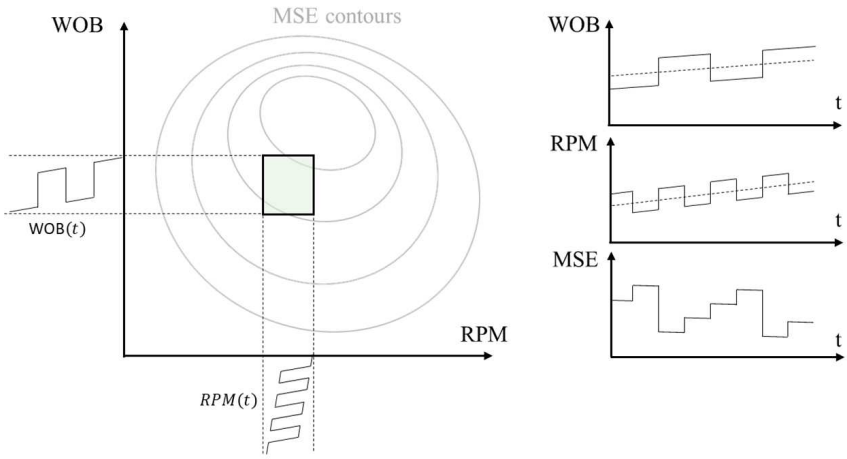

Figure 7. Concept illustration of multivariable ES applied to minimize the MSE.

The ES algorithm can be split into three main components:

- *The excitation signal*, which varies the input variables around a base value to investigate the current drilling conditions.
- *Gradient estimation*, which quantifies how the process reacts to the excitation signal by estimating partial derivatives of the objective function with respect to the input variables.
- *Adaptation*, which adjusts the base values of the input variables with a magnitude and direction determined by the estimated gradients, to seek out drilling conditions that result in lower *MSE* values.

These components are detailed in the subsequent sections. Because the measurements of drilling parameters and commands given to the control system on the rig are performed at regular intervals, discrete time notation is used. It is assumed that relevant measurements are performed at a time interval of Δt seconds, and that the top drive and autodriller can receive updated setpoints for target *RPM* and *WOB* every Δt seconds. For simplicity, Δt is set to a value of 1 s. The current timestep is denoted by t, so that a command for the coming timestep is indicated by the notation $t + \Delta t$.

3.1.1. The Excitation Signal

To probe the current drilling conditions, a periodic excitation signal is continuously applied to the input variables. Assume that we are currently drilling ahead with the base values $\overline{WOB}$ and $\overline{RPM}$ as initial guesses of the optimal input variables. These initial values could be based on e.g., data from an offset well or estimates given by a drilling model.

The ES algorithm dictates a periodic variation in the *WOB* and *RPM* about the base values according to:

$$WOB(t) = \overline{WOB}(t) + d(t, A_{wob}, P_{wob}), \tag{7a}$$

$$RPM(t) = \overline{RPM}(t) + d\left(t, A_{rpm}, P_{rpm}\right), \tag{7b}$$

where the left-hand sides signify the *WOB* and *RPM* that will be sent to the control system on the rig as setpoints. The parameters A and P are the amplitude and period of the excitation signal, d, which is given by:

$$d(t, A, P) = A \cdot \mathrm{sgn}\left(sin\left(\frac{2\pi t}{P}\right)\right). \tag{8}$$

Equation (8) describes a square wave, where *sgn* is the *signum function* which takes a value of 1 when the argument is positive, a value of 0 when the argument is zero and a value of -1 when the argument is negative. The applied *WOB* and *RPM* prescribed by Equations (7a) and (7b) will oscillate about the base values, $\overline{WOB}$ and $\overline{RPM}$, with amplitudes of $\pm\, A_{wob}$ kg and $\pm\, A_{rpm}$ rpm, respectively. Through the information gathered from the excitation signals, the ES algorithm will adjust the base values in the direction that reduces the *MSE*.

The induced variations in *RPM* and *WOB* can potentially influence the measured *MSE* to different extents and in different directions. For the ES algorithm to be able to draw conclusions as to how the two input variables individually affect the drilling efficiency, the parameters P_{wob} and P_{rpm} should be designed to minimize the coupling between the *MSE*-responses resulting from the two signals. In this work, the periods of the excitation signals are set so that $P_{wob} = 2P_{rpm}$. This tuning is illustrated in the right-hand tracks in Figure 7, where the *RPM* oscillates with twice the frequency of the *WOB*-signal. For each half-period of the *WOB* fluctuations, the *WOB* remains relatively constant while the *RPM* performs a full oscillation, from which the dependency between the *MSE* and *RPM* can be deduced by the gradient estimator. The frequency of the *RPM* signal is an even multiple of the *WOB* signal frequency, causing the average *RPM* value during each period of the *WOB* oscillation to be approximately $\overline{RPM}$. This allows for estimation of the relationship between the *MSE* and the varying *WOB* as if the *RPM* was held constant. The tuning of the excitation signals is further explored in Appendix A.

3.1.2. Gradient Estimation

To estimate a local model of the *MSE* as a function of the applied *WOB* and *RPM*, a lest-squares approach is used in this work. As we drill ahead, measurements of the *WOB*, *RPM*, T and *ROP* as well as the calculated *MSE* are stored in buffers containing a few minutes of the most recent data. These buffers contain a sliding window time series of data that represents the most up to date information that is available about the current drilling conditions. At each update of measurements, the newest measurements are included in the buffers, while the oldest are discarded. The buffers contain data from one period of the excitation signal with the longest period time, which in this case is P_{wob} seconds.

The excitation signals are designed to elicit responses in *MSE* that can be associated with each individual signal. This allows the gradient estimation to be performed by correlating the variations in measured *MSE* with the applied *WOB* and *RPM*. At each new timestep, Δt, the updated buffers are used to solve the least-squares problem:

$$\sum_{i=0}^{P_{wob}-1} \left(MSE(t - i\Delta t) - \left(a_{wob}WOB(t - i\Delta t) + a_{rpm}RPM(t - i\Delta t) + b\right)\right)^2 \rightarrow \min_{a_{wob}, a_{rpm}, b}. \tag{9}$$

In Equation (9), a_{wob}, a_{rpm} and b are the slopes and intercept, respectively, of the lest-squares fit. The parameters a and b represent a linear approximation (local model) of how

the *MSE* correlates with the input variables. The calculated slopes are used as estimates of the partial derivatives of the *MSE* with respect to *WOB* and *RPM* by setting:

$$\left.\frac{\partial MSE}{\partial WOB}\right|_{\overline{WOB}(t),\overline{RPM}(t)} \approx a_{wob}(t), \quad \left.\frac{\partial MSE}{\partial RPM}\right|_{\overline{WOB}(t),\overline{RPM}(t)} \approx a_{rpm}(t). \tag{10}$$

The gradients described by Equation (10) are based on the P_{wob} $(= 2P_{rpm})$ seconds of the most recent measurements and represent the current best estimate of how the *MSE* is related to the input variables in the local region that has been explored by the excitation signals. Because of the symmetry of the excitation signals, the average values for *WOB* and *RPM* during P_{WOB} seconds of drilling will on average be close or equal to $\overline{WOB}(t)$ and $\overline{RPM}(t)$, respectively, which is why the gradients in Equation (10) are evaluated at this point.

3.1.3. Adaptation

Assuming that there is a response in the *MSE* to the variations in the input variables, the gradients calculated from Equations (9) and (10) determine in which direction the *WOB* and *RPM* should be adjusted to reduce the *MSE*. When drilling in the optimum zone, the changes in *MSE* resulting from variations in the *WOB* and *RPM* are expected to be small. This results in zero or near zero values for the estimated gradients. When using *MSE* to increase real-time performance, a negative or zero gradient value indicates that drilling is efficient and the input *WOB* and/or *RPM* should be increased until the point of foundering [12]. To include this logic in the ES algorithm, a tuning parameter, k, is subtracted from the estimated gradients. This makes the algorithm see a zero gradient as a scenario where the corresponding input should be increased.

From the estimated gradients at the current timestep, the ES algorithm prescribes updated base values for the input variables for the coming timestep from:

$$\overline{WOB}(t+\Delta t) = \overline{WOB}(t) - \gamma_{wob}\cdot \text{sat}\left(\left.\frac{\partial MSE}{\partial WOB}\right|_{\overline{WOB}(t),\overline{RPM}(t)} - k_{wob}, \sigma_{wob}\right)\Delta t, \tag{11a}$$

$$\overline{RPM}(t+\Delta t) = \overline{RPM}(t) - \gamma_{rpm}\cdot \text{sat}\left(\left.\frac{\partial MSE}{\partial RPM}\right|_{\overline{WOB}(t),\overline{RPM}(t)} - k_{rpm}, \sigma_{rpm}\right)\Delta t. \tag{11b}$$

The left-hand sides of Equation (11) denote the new base values that will be used in Equations (7a) and (7b) in the next iteration of the algorithm. It can be observed from Equations (11a) and (11b) that for each iteration, the input base values, $\overline{WOB}$ and $\overline{RPM}$, will change incrementally from their previous values with a magnitude dictated by the rightmost terms. The magnitude of this incremental change is determined by the adaptation gain, γ, and the output of the saturation function, *sat*, which is given by:

$$sat(x,\sigma) = \begin{cases} -1, & x \leq -\sigma \\ x/\sigma, & -\sigma < x < \sigma \\ 1, & x \geq \sigma \end{cases}. \tag{12}$$

The use of Equation (12) in combination with Equation (11b) is illustrated in Figure 8. In Equation (12), σ is a tuning parameter that determines the width of the region where the saturation function shifts from negative to positive output values. The saturation function is used to limit the maximal step size that the ES algorithm is able to implement per iteration by using the principle of sliding mode extremum seeking control [37]. As the maximal output of Equation (12) is a value of ± 1, the greatest rate of change that the algorithm can demand in the input variables is given by γ. This property makes the algorithm easier to tune from a safety standpoint, as the maximal adaptation rate is explicitly stated by the parameter γ in units of kg or rpm per second.

The maximal limit on adaptation rate is useful in cases where an abrupt change in drilling conditions occurs, e.g., a formation change, as the gradients calculated by Equations (9) and (10) can be erroneous in this situation. This error would be introduced by the algorithm's assumption that any changes in the *MSE* can be attributed to the variations in the *WOB* and *RPM*. For a large change in *MSE* caused by differences in lithology, the estimated gradients could become artificially large as the algorithm relates the relatively small *WOB* and *RPM* oscillations to a large change in *MSE*. If the adaptation was directly proportional to the estimated gradients in this scenario (as is done in conventional ES algorithms, see e.g., Tan et al. [26]), it could cause the ES algorithm to demand large and rapid changes in the $\overline{WOB}$ and/or $\overline{RPM}$ that could steer the system away from the optimum and into the dysfunction regions. It should be noted that in a case like this, the estimated gradients would only be erroneous for a brief time window before the buffers would be filled with data representative of the new formation, which would produce more accurate gradient estimates. The downside of limiting the adaptation with Equation (12) is that in cases where the estimated gradients correctly indicate that large improvements in drilling efficiency could be achieved by adapting the inputs, the rate at which the inputs are adapted to more suitable values will be limited. Weighing faster adaptation versus more robust control is an algorithm design and tuning consideration, where the authors have opted to lean towards more robust control through the use of the saturation function.

The saturation function is illustrated in Figure 8, which exemplifies how this function is applied in Equation (11b) for *RPM* optimization. The example parameter values $\sigma_{rpm} = 2$, $k_{rpm} = 1$ and $\gamma_{rpm} = 1$ are used in Figure 8. It can be seen that for a gradient value of zero, the saturation function will yield an output of -0.5, which will translate to an increase of $\gamma_{rpm}/2$ in the base value $\overline{RPM}$ for the next timestep. When drilling in the optimum zone, the estimated gradient is expected to have a low or zero value, and the proposed ES algorithm relies on the parameter k_{rpm} to indicate that the *RPM* should be increased to reach the foundering point, see Section 2.3. With this configuration, the algorithm will request increasing *RPM* until the estimated gradient is equal to k_{rpm} in magnitude and the saturation function's output is zero. At some point, the ES algorithm will drive the value of $\overline{RPM}$ close to the dysfunction region. Because the *MSE* is expected to increase drastically when drilling dysfunctions occur [13], the gradients estimated past this point will take on relatively large, positive values. A suitably small value of k_{rpm} will therefore provide increasing $\overline{RPM}$ values up to the limit at which foundering starts to occur. If, for some reason, drilling outside of the optimal region occurred, the large estimated gradients would make the ES algorithm adapt at its maximal rate of γ_{rpm} rpm/s to exit the dysfunction region as quickly as possible. The same logic as described above also applies to the adaptation in *WOB* determined by Equation (11a).

A block diagram of the proposed ES algorithm is shown in Figure 9. A loop through this diagram represents an iteration of the ES algorithm, which is continuously repeated every Δt seconds. Starting from the lower left corner, the updated base values and excitation signal values are combined to produce new values for the *WOB* and *RPM*, which are fed as setpoints to the control system on the rig. The resulting *ROP*, torque, *WOB* and *RPM* values are measured and used to calculate the current *MSE* value. The new measurements are subsequently included in the buffers, while the oldest measurements are discarded. The updated buffers are used to estimate the current gradient values, which are translated to updated base values that are employed in the next iteration of the algorithm.

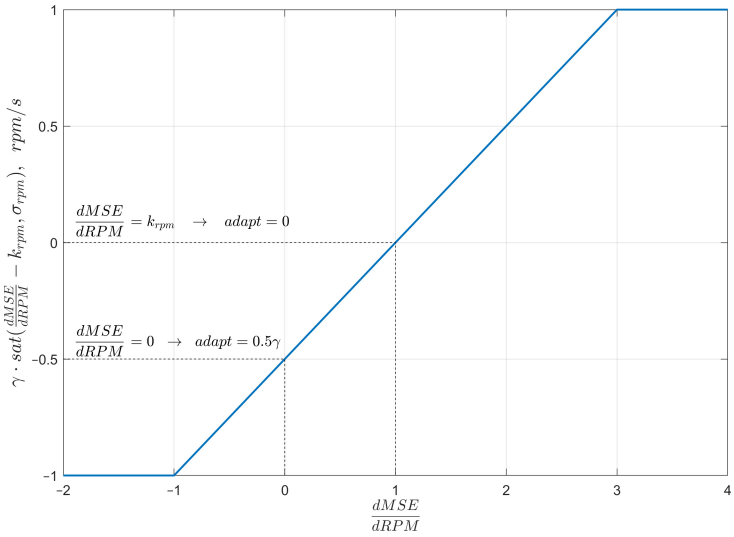

Figure 8. Illustration of the saturation function and how it is applied in Equation (11b), with the example parameter values $\sigma_{rpm} = 2$, $k_{rpm} = 1$ and $\gamma_{rpm} = 1$.

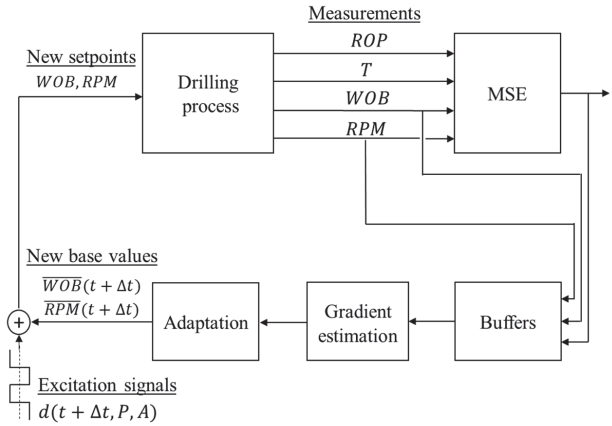

Figure 9. Block diagram of multivariable extremum seeking applied to minimize the *MSE*.

3.2. Algorithm Design Choices

The Extremum Seeking method provides a whole range of algorithms and tools suitable for various applications, starting with the fundamental ES controllers described in [26,38]. The ES algorithm presented in this paper is a result of selection various elements from this toolbox to make it robust and well suited for drilling applications.

In particular, the square wave excitation signal was chosen because this is the signal shape that, for a given amplitude, gives the maximal (output) signal power and results in faster convergence to the optimal values at least for the standard ES algorithm configurations [39]. It is also expected that square excitation waves are more suitable for realizing *WOB* variations with a standard autodriller functionality.

We can expect that due to transients and various disturbances acting on the drill string, the actual *WOB* and *RPM* realized by the autodriller and top drive may noticeably deviate from the corresponding setpoints requested by the ES algorithm. Gradient estimation by the selected least-squares method is less affected by these deviations. In addition to this, the selected gradient estimation technique accounts for changes in $\overline{WOB}$ and $\overline{RPM}$ (caused by adaptation) and will therefore calculate more accurate gradients than the standard ES method.

Finally, we have opted to use the saturation function in the adaptation block defined in Equation (11), to limit the rate of change for $\overline{WOB}$ and $\overline{RPM}$. This makes the algorithm more robust when experiencing sudden changes in downhole conditions, e.g., a formation shift.

3.3. Constraint Handling

The ES algorithm detailed in the previous section will automatically steer the *WOB* and *RPM* towards the optimal values that minimize the *MSE*. As the *MSE* will increase greatly when foundering occurs, the ES algorithm will inherently try and avoid these dysfunctions by seeking out dysfunction-free combinations of *WOB* and *RPM*. There are however many situations where drilling at the minimal *MSE* is not feasible, as the drilling process is restricted by energy input limiters, as described in Section 2.2. It is imperative that the ES algorithm does not exceed these process constraints in the search for the minimal *MSE*.

A distinction can be made between constraints that are known a priori in the *RPM*-*WOB* plane and constraints related to process output values that are not known in advance. In the former category, a maximal *WOB* associated with e.g., a buckling criterion can be implemented in the algorithm with a logic condition that would not allow for increase in the *WOB* past a certain point, even if the algorithm recognized potential for lower *MSE* at *WOB* which would exceed the buckling criterion. A similar logic condition could enforce e.g., a maximal *RPM* value related to surface vibrations. In the latter category, where e.g., a maximal *ROP* related to hole cleaning should not be exceeded, the combinations of *WOB* and *RPM* that produce too high *ROP* are not known in advance and a different approach is needed. Three techniques that can be used to ensure that the ES algorithm does not violate constraints related to process outputs while searching for the optimum drilling conditions are investigated in the following. The constraint handling techniques are generic and can be applied to different types of limitations. To demonstrate the constraint handling techniques, we apply them to maximal values imposed on the torque and the *ROP* that the ES algorithm must adhere to.

3.3.1. Modified Objective Function

A practical way of making the ES algorithm avoid e.g., *ROP* values above a given threshold, is through modification of the objective function. Instead of trying to minimize the *MSE*, an objective function on the form:

$$J = MSE \cdot \left(1 + \rho \frac{\max(0, ROP - ROP_{threshold})}{ROP_{threshold}}\right) \tag{13}$$

is used in the ES algorithm to identify the optimal combination of *WOB* and *RPM*. A function similar to Equation (13) has previously been explored to limit drilling with stick-slip [40]. In Equation (13), *max* is a function which outputs the largest of the input arguments and ρ is a tuning parameter that determines how much the objective function increases when drilling with higher than allowed *ROP*. The modified objective function, *J*, will start increasing when the threshold *ROP* is exceeded, which will make the ES algorithm avoid higher *ROP* values. Different constraining parameters can be added to Equation (13) in a similar fashion as the *ROP* term, to penalize the presence of e.g., measured vibrations or high torque, making this constraint handling technique very versatile. A downside of this approach is that if e.g., a sudden change in drilling conditions makes the *ROP* increase

by a some margin above the threshold, the time it takes for the ES algorithm to steer the *WOB* and *RPM* to better values is determined by the rather slow adaptation rate dictated by γ. A more prudent approach would then be to use a separate control loop with the ability to modify the applied *WOB* and/or *RPM* more rapidly.

3.3.2. Predictive Constraint Handling

A combination of a predictive and a reactive constraint handling technique that can be used to avoid violation of a constraint related to the torque has been tested in the case of single variable ES [24]. Here, we demonstrate that these techniques can also be applied in a multivariable ES approach. It must be noted that when using the predictive constraint handling technique, it should be combined with the reactive approach, as this ensures that the constraint handling does not make the ES algorithm "get stuck".

The predictive constraint handling method [24] relies on obtaining additional information about the downhole conditions by relating changes in measured output parameters to the known variations of the excitation signals. For this purpose, the same least-squares technique as detailed in Equation (9) can be used to estimate a gradient of how the torque relates to the *WOB*. This technique relies on the assumption that the torque is mainly a function of the *WOB*, as is commonly assumed in the literature [28,32]. Considering a sliding window time series that contains measured values of the torque and *WOB* for the past P_{wob} seconds, a gradient describing the current *T*-*WOB* relationship can be estimated from:

$$\sum_{i=0}^{P_{wob}-1} \left(T(t-i\Delta t) - (\alpha \cdot WOB(t-i\Delta t) + \beta)\right)^2 \rightarrow \min_{\alpha,\,\beta}, \tag{14}$$

$$\left.\frac{\partial T}{\partial WOB}\right|_{\overline{WOB}(t),\overline{RPM}(t)} \approx \alpha(t). \tag{15}$$

In Equations (14) and (15), α and β are the least-squares slope and intercept, respectively. As the parameter α is a linear fit to how the torque has changed recently as a function of *WOB*, α can be used to predict what the torque will be if the *WOB* is increased or lowered in the region around $\overline{WOB}$. As long as a reasonably accurate estimate of the torque gradient can be obtained, it can be used to stop the *WOB* from being steered to a region where the torque is higher than allowed, assuming that we are operating at a point where the torque constraint is currently not violated.

Let T_{avg} denote the average measured torque value for the past P_{wob} seconds. The torque constraint which we do not want to exceed is represented by T_{limit}. To avoid the *WOB* being steered to values which would cause the torque to grow past the allowable limit, the following rule is imposed on the *WOB* adaptation gain:

$$\gamma_{wob} = \begin{cases} \gamma_{wob}, & \left(T_{B,avg} + A_{wob}\alpha(t)SF\right) < T_{limit} \\ 0, & \left(T_{B,avg} + A_{wob}\alpha(t)SF\right) \geq T_{limit} \end{cases}. \tag{16}$$

The rule formulated in Equation (16) takes advantage of the fact that during one oscillation of the excitation signal, the weight on bit will take on values in the range $\overline{WOB}(t) \pm A_{wob}$. Assuming that the adaptation gain is low, the value of $\overline{WOB}$ will be nearly constant in this time interval and the average weight on bit will be approximately equal to $\overline{WOB}$. The average torque value, T_{avg}, will therefore correspond to drilling with a weight on bit of $\overline{WOB}$ kg. The product $A_{wob}\alpha(t)$ is a projection of how much the torque will grow if the *WOB* is increased by a value of A_{wob} kg. This product is multiplied by a safety factor with a value greater than 1, which determines how far away from the torque limit we wish to stop the *WOB* adaptation. Using e.g., a safety factor of 2, Equation (16) will stop the *WOB* adaptation when $\overline{WOB}$ is $2A_{wob}$ kg away from the weight on bit value which would make the torque exceed its limit. Stopping the adaptation with some margin will allow the ES algorithm to continue performing the *WOB* excitations without the torque limitation being violated.

3.3.3. Reactive Constraint Handling

There are instances where Equation (16) will not be adequate to avoid violation of the torque constraint. The torque measurements are commonly very noisy, which can cause the estimated gradient to be inaccurate. Changes in downhole conditions could affect the torque in a way that cannot be predicted by the gradient, causing the torque to exceed its maximal limit. In this case, a reactive constraint handling technique should be used in combination with the predictive method to automatically steer the *WOB* back to the safe region if the torque constraint is violated [24]. At each timestep a variable, e, is calculated that quantifies if the constraint is violated and in which case by how much:

$$e(t) = \begin{cases} 0, \ T(t) < T_{limit} \\ T(t) - T_{limit}, \ T(t) \geq T_{limit} \end{cases}. \tag{17}$$

If the variable e takes on a value larger than 0, this indicates that the constraint is violated and the adaptation gain, γ_{wob} is set to zero. In Equation (17), T is the measured torque value at the current timestep. If the torque measurements are very noisy, the torque used in Equation (17) should be filtered to avoid that the constraint handling reacts too aggressively as a response to noise [24]. The variable e from Equation (17) is used as the error term in a discrete proportional-integral (PI) controller which calculates a penalty, λ, from:

$$\lambda(t) = K_P e(t) + K_I \Psi(t) \Delta t, \tag{18}$$

$$\Psi(t) = \begin{cases} 0, \ T(t) < T_{limit} \\ \sum_{i=n}^{t} e(i), \ T(t) \geq T_{limit} \end{cases}. \tag{19}$$

In Equation (18), K_P and K_I are the proportional and integral gains, respectively. These parameters are used to tune the controller and determine how fast the *WOB* will be adjusted if the torque exceeds the imposed limit. If the torque constraint at some point in time is violated, the summation term, Ψ, will continue to grow and make the penalty term larger until the torque is adjusted down to acceptable levels. At the time when the torque is returned to a level below the limiting value, the summation term is reset by setting the parameter n equal to this time, t, essentially forgetting that the torque constraint has previously been violated and continuing optimization with the ES algorithm from this point on.

The *WOB* that is requested by the ES algorithm is adjusted based on the penalty according to:

$$\overline{WOB}_{constrained}(t + \Delta t) = \overline{WOB}(t + \Delta t) - \lambda(t). \tag{20}$$

The first term on the right-hand side of Equation (20) is the $\overline{WOB}$ value calculated from Equation (11a). The variable $\overline{WOB}_{constrained}$ is used in Equation (7a) as the base *WOB* value when the constraint handling is activated. As long as the torque limit has not been violated, λ will be equal to zero and the WOB will not be adjusted by Equations (17)–(20). The penalty term, λ, will grow if we are drilling with torque values above the allowable limit, which will cause the applied *WOB* to be reduced according to Equation (20) until the torque is within the allowable bounds and λ is reset to a zero value. Making these adjustments to the $\overline{WOB}$ with Equation (20) rather than Equation (13) allows the algorithm to reduce the applied *WOB* faster, which will cause the torque constraint to be violated for a shorter period of time. It can be noted that the reactive constraint handling method will not make any adjustments to the *WOB* until the torque limit is exceeded. For this reason, a lower value for T_{limit} than the actual system's limit should be used in Equations (17) and (19).

3.4. Practical Requirements and Algorithm Tuning

Implementation of the proposed algorithm requires the following measurements: *WOB*, *RPM*, bit torque (either calculated or measured), and calculated *ROP*. These measurements are used to calculate the *MSE* from Equation (6). In essence, the components of

the ES algorithm act like filters when calculating the gradients and performing adaptation of the *WOB* and *RPM* values. Yet, if the measurements are too noisy, appropriate filtering should be applied before using them in the algorithm.

The algorithm automatically adjusts the setpoints for the *WOB* and *RPM*, which are then used by the autodriller to control the actual *WOB* and by the top drive to control the actual *RPM*. The internal control algorithms in the autodriller and top drive must be able to realize the requested small changes in the setpoints corresponding to the excitation signals. This places a lower bound on the excitation signals' amplitudes, based on the resolution of these control systems.

There are several key parameters in the ES algorithm that need to be tuned. These parameters are the period (P) and amplitude (A) of the excitation signals (defined in Equations (7a), (7b) and (8)), as well as the adaptation rate (γ) and the tuning parameter k in Equations (11a) and (11b). These parameters should be tuned taking into account the guidelines presented in Table 1.

Table 1. Tuning considerations for key parameters in the ES algorithm.

Parameter	Tuning Considerations
Excitation amplitude, A	• Large enough to be realized by the autodriller and the top drive, as well as to cause a measurable response in the objective function through the *ROP*, *RPM*, *WOB* and torque. • Not too large, to avoid large disturbances to the overall process. • Scaled based on the planned range of *WOB* and *RPM* for the drilled section.
Excitation period, P	• Set $P_{wob} = 2P_{rpm}$ to minimize the interplay between the identified gradients with respect to *WOB* and *RPM* (see Appendix A). • Larger P_{wob} and P_{rpm} result in gradient estimates less sensitive to noise. • Trade-off between noise sensitivity and responsiveness to changes in drilling conditions
Adaptation rate, γ	• Larger γ results in faster convergence to the optimal *WOB* and *RPM* and higher responsiveness to changes in downhole drilling conditions. • Overly large γ makes the algorithm too sensitive to gradient estimation errors, e.g., when a formation shift occurs. • Trade-off between fast convergence and robustness.
k parameter	• As small as possible, yet leading to increase in *WOB* and *RPM* in the optimum zone (see Section 3.1.3)

4. Simulation Results

To simulate the dynamics of a control system on the rig that receives setpoints for *WOB* and *RPM* from the ES algorithm and steers the input variables to the requested setpoints as a function of time, the following functions were used to emulate this effect:

$$WOB(t) = WOB(t-1) + \frac{1}{\tau_{wob}}[WOB_{SP}(t-1) - WOB(t-1)], \tag{21a}$$

$$RPM(t) = RPM(t-1) + \frac{1}{\tau_{rpm}}[RPM_{SP}(t-1) - RPM(t-1)]. \tag{21b}$$

In Equations (21a) and (21b), the left-hand sides represent the current values of the *WOB* and *RPM* that are applied at the bit, while WOB_{SP} and RPM_{SP} are the corresponding setpoints. How quickly the control system is able to steer the *WOB* and *RPM* from their current values to new values dictated by the setpoints is determined by the time constants,

τ. For small values of τ, the *WOB* and *RPM* will quickly converge to their respective setpoints. For larger values of τ, convergence to the setpoints will take longer time.

The optimization algorithm and constraint handling approaches detailed in the previous sections were investigated by using the proposed extended model detailed in Equations (1)–(5) coupled with Equations (21a) and (21b) as a drilling simulator. In the simulation scenarios, the ES algorithm provides setpoints for the *WOB* and *RPM*, which are translated to applied *WOB* and *RPM* through Equations (21a) and (21b). The model simulates the *ROP* and torque response to these values of *WOB* and *RPM* that could be seen in the field for a given bit and formation. The current values for the *WOB*, *RPM*, *T* and *RPM* are "measured" from the extended model and used to calculate the *MSE* with Equation (6). These updated measurements are read by the ES algorithm and used to perform the optimization actions described in Section 3. It must be re-emphasized that the ES algorithm only uses measurements taken from the simulated drilling process to minimize the *MSE*, it has neither prior knowledge about the drilling model nor the locations of the different drilling dysfunctions.

The simulations emulate drilling in two generic formations, Formation *A* and Formation *B*. Formation *A* is described in detail in Section 2, where the optimal point to drill at in this lithology was identified to be at a *WOB* of 12,900 together with an *RPM* value of 89.5, as this combination minimizes the *MSE*. Formation *B* represents a softer formation than Formation *A*, otherwise they are identical. To emulate a preference for drilling with lower *WOB* and higher *RPM* in softer rocks, the onset of dysfunctions in Formation *B* are slightly different than in Formation *A*, placing the optimal point to drill at in Formation *B* at a *WOB* of 12,000 kg and an *RPM* value of 109. The parameters c_1, c_2, c_3 and c_4 that are used by the extended model in Equations (1) and (2) are provided in Table 2. These values are generated by picking generic values for the bit and formation parameters in the ranges suggested by Detournay et al. [28], and correspond to using units of kg for the *WOB*, rpm for the drill string rotational rate and the bit radius given in meters in Equations (1) and (2).

Table 2. Parameter values used in Equations (1) and (2).

Parameter	Fm. *A* Value	Fm. *B* Value	Units
c_1	1.4×10^{-6}	1.7×10^{-6}	$m^2/(kg{\cdot}rpm{\cdot}h)$
c_2	4.9×10^{-6}	5.9×10^{-6}	$m^2/(kg{\cdot}rpm{\cdot}h)$
c_3	3.05	3.05	m/s^2
c_4	7.01	7.01	m/s^2

All the simulation scenarios are initiated by ramping up the *WOB* and *RPM* to their starting setpoints, which is an initial guess at the optimal input values, which could e.g., be based on the driller's experience, a drill-off test, data from an offset well or estimates given by a drilling model. When the *WOB* and *RPM* have reached their initial values, the ES algorithm is activated and starts testing the drilling conditions with the excitation signals described by Equations (7a), (7b) and (8). After one full period of the *WOB* excitation signal, $P_{wob} = 120$ s, the buffers needed for the gradient estimation are filled up with the relevant measurements and the algorithm starts adapting the $\overline{WOB}$ and $\overline{RPM}$ in the direction that will reduce the *MSE*. The parameter values that are common in all the simulations are provided in Table 3.

Table 3. Parameter values that are common for all the simulations.

Parameter	Value	Units
D_{bit}	$12\frac{1}{4}$	Inches
γ_{wob}	2.5	kg/s
A_{wob}	200	kg
k_{wob}	0.001	MPa/kg
σ_{wob}	0.002	MPa/kg
P_{wob}	120	s
τ_{wob}	4	s
γ_{rpm}	0.02	rpm/s
A_{rpm}	2	rpm
k_{rpm}	0.05	MPa/rpm
σ_{rpm}	0.1	MPa/rpm
P_{rpm}	60	s
τ_{rpm}	3	s

4.1. Unconstrained Drilling Optimization

This section contains the results from two runs of simulated drilling through the homogeneous Formation *A*. The theoretical optimal point in this scenario is located approximately at a *WOB* of 12,900 kg in combination with an *RPM* value of 89.5. No constraints are considered in these two simulations, meaning that the ES algorithm is free to search for the drilling conditions that will minimize the *MSE* without any limits imposed on the torque or *ROP*.

Figure 10 shows the *WOB*, *RPM*, *MSE* and *ROP* for Simulation 1. The orange lines in the *WOB* and *RPM* tracks marks the base values, $\overline{WOB}$ and $\overline{RPM}$. This run was initiated with conservative values of 8000 kg *WOB* and 60 *RPM*, which resulted in drilling at a low *ROP* of about 11.5 m/h and a calculated *MSE* of approximately 184 MPa. After performing the initial variations in the input variables, the ES algorithm detects that increasing the *WOB* and *RPM* will result in more efficient drilling. Both the *WOB* and *RPM* are steadily increased by the algorithm until they converge to the region of the founder point after drilling for about 2700 s. The rest of the interval is drilled at peak efficiency, where the average *ROP* is 31.5 m/h, which is an increase of more than 170% from the starting point. Throughout the simulation, the *MSE* is only marginally reduced by the adaptation in the input variables. This is because the initial *WOB* and *RPM* from the start of the simulation resulted in dysfunction free phase II drilling, where the *MSE* was already close to its minimal value. The proposed ES algorithm is designed to interpret small or zero *MSE*-gradients as a situation where the corresponding input variable should be increased, which is why the $\overline{WOB}$ and $\overline{RPM}$ was adapted to the optimum in this scenario.

The values of $\overline{WOB}$ and $\overline{RPM}$ where the ES algorithm converges to in Simulation 1 are approximately 13,000 kg and 90 rpm, respectively, which are slightly higher than the pre-calculated values of 12,900 kg and 89.5 rpm. The ES algorithm's convergence to this point is caused by the *k* parameters used in Equation (11). The *k* values dictate that a (small) positive gradient must be calculated before the algorithm stops adaptation, and the point at which this occurs is slightly into the dysfunction region. This property can also be seen from Figures 4 and 5; the *MSE* does not significantly grow before the *WOB* and/or *RPM* has moved slightly into the dysfunction region, which is why the ES algorithm converges to the point seen in this simulation scenario.

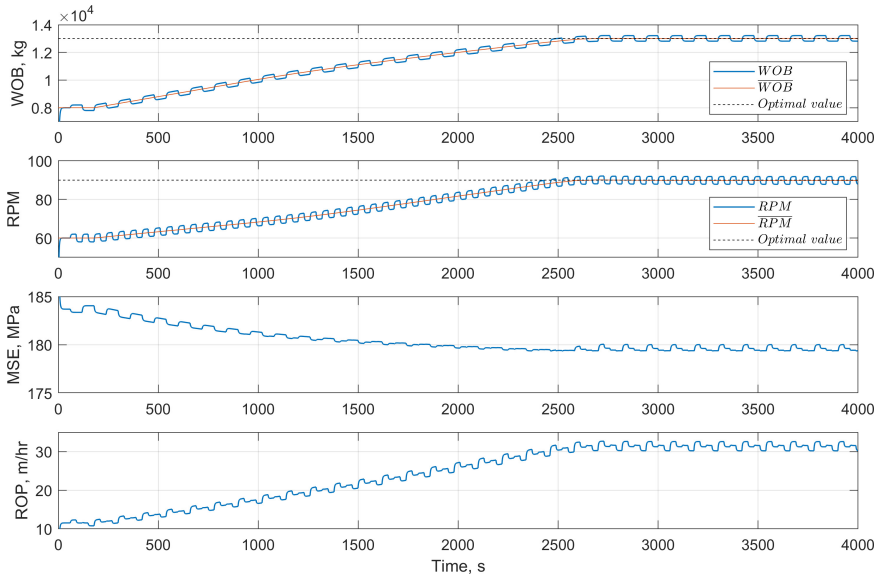

Figure 10. Simulation run 1, showing the ES algorithm converge to the optimum in the homogeneous formation *A*. The optimal *WOB* and *RPM* values indicated by the dotted lines are shown as an illustration and are not known by the ES algorithm.

Figure 11 shows the calculated gradients for Simulation 1, where it can be seen from the lower track that the estimated $\partial MSE/\partial RPM$ values show some oscillatory behavior until the *MSE* and *RPM* has converged to the optimum. This is caused by the adaptation in the *WOB* and *RPM* signals, which can sometimes interfere with accurate gradient estimation. A moving average of $\partial MSE/\partial RPM$ is plotted in the same track, which shows that the estimated gradient on average is unaffected by the oscillations. As long as the average gradients indicate which way the ES algorithm should adapt the input variables, the algorithm will be able to steer the *WOB* and *RPM* to the optimum. Figure 11 also shows the estimated gradients converging to a value equal to the k values for the respective signals, at which point the algorithm stops adjusting the $\overline{WOB}$ and $\overline{RPM}$.

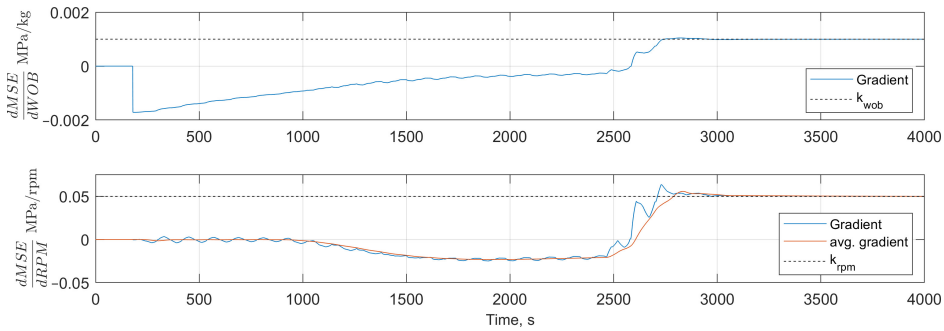

Figure 11. Estimated gradients in Simulation 1.

The results from Simulation 2 are displayed in Figure 12. This scenario is the same as Simulation 1, with the exception that the we initiate drilling at a *WOB* of 13,000 kg and with an *RPM* value of 160, which is in the dysfunction region (see Figure 2). The initial *WOB* is in fact the optimal *WOB* value, but only when combined with the appropriate *RPM*. As can be seen from Figure 12, drilling commences at a high average *MSE* value of about 300 MPa. The ES algorithm recognizes that we are drilling with a dysfunction and reduces both the *WOB* and *RPM* for the first 1800 s to exit the dysfunction region. At this point, the average *MSE* has been reduced to a value of approximately 181 MPa. As soon as the optimum zone is entered and it is safe to increase the *WOB* again, and the algorithm spends the next 3500 s converging more slowly to the optimal point. It can be noted that the adaptation in $\overline{WOB}$ and $\overline{RPM}$ that occurred during the first 1800 s happened at the algorithms maximal rate of 2.5 kg/s and 0.02 rpm/s, respectively. This is because of the large variations in *MSE* seen when drilling in the dysfunction region and the correspondingly large estimated gradients, which prompts the algorithm seek out better operating conditions as quickly as it is allowed to.

It can also be observed from Figure 12 that the adaptation that happens from 1800 s and onwards only results in small enhancements in *ROP* and *MSE*, the larger gains in drilling efficiency occurred during the early adaptation when moving out of the dysfunction region. At the start of the simulation, the *ROP* was about 33 m/h, which has been slightly reduced when compared to the *ROP* at the end of the run. The *MSE* has however been reduced substantially, which means that the drilling has become more energy efficient and possibly less detrimental for the bit and downhole tools.

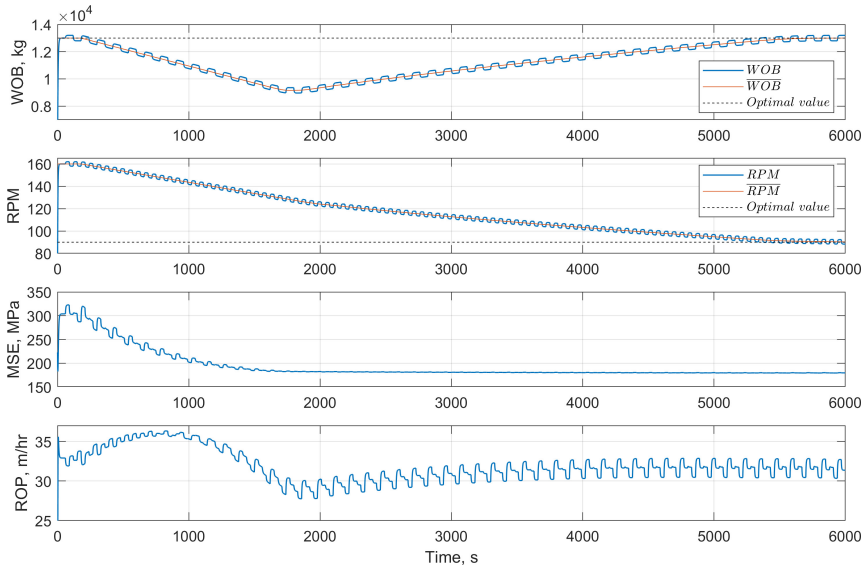

Figure 12. Simulation run 2, showing convergence for drilling initiated in the dysfunction region.

Figure 13 depicts the $\overline{WOB}$ and, $\overline{RPM}$ values from Simulations 1 and 2 in the *WOB*-*RPM* plane, together with contours which mark the *MSE* values for drilling in Formation *A*. The blue and orange datapoints can be viewed as the "path" that the ES algorithm took to converge to the founder point in these two scenarios. In the case of Simulation 2, it can be seen that the path taken by the algorithm is not the most efficient way to reach the founder point. It is however close to the most efficient path to exit the dysfunction region as quickly

as possible. Because of this "detour", more time is spent to converge to the optimum in Simulation 2, compared to Simulation 1.

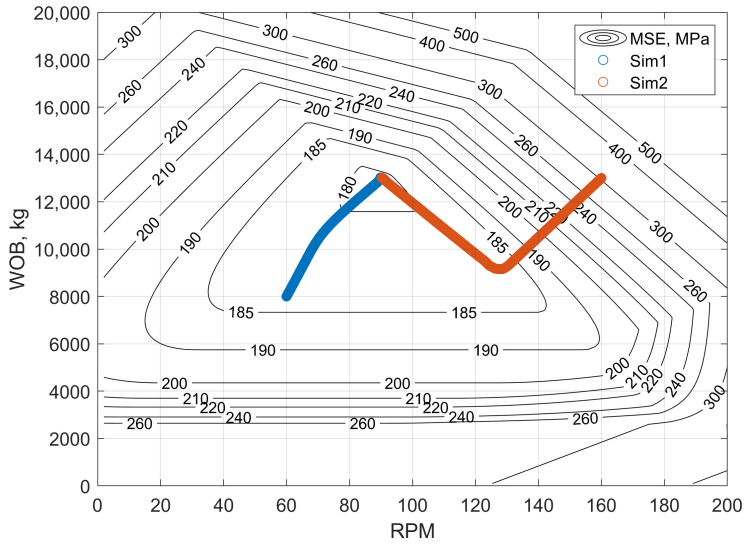

Figure 13. Contour plot of the *MSE* values for drilling in formation *A*, together with the $\overline{WOB}$ and $\overline{RPM}$ values for Simulations 1 and 2.

4.2. Constrained Drilling Optimization

In this section, the proposed constraint handling techniques are demonstrated in two simulation scenarios of drilling through the homogeneous formation *A*. In Simulation 3, we have imposed a maximal *ROP* of 20 m/h on the system through the use of Equation (13) with a ρ value of 0.1. This means that in this scenario, we seek to minimize the modified objective function given by Equation (13) and not the *MSE*. This run is initiated with the same values as in Simulation 1; a *WOB* of 8000 kg and an *RPM* value of 60. The results from Simulation 3 are shown in Figure 14, where it can be seen that the ES algorithm increases the applied *WOB* and *RPM* for the first 1300 s, before the *ROP* reaches the limiting value and the algorithm determines that any further adaptation will cause the *ROP* to exceed the allowable amount. Because of this constraint, the ES algorithm converges to the minimal *MSE* value that it can obtain while still drilling at an *ROP* at or below 20 m/h, which it finds at a *WOB* of 10,900 and an RPM of *71*. There are several operating points at which the ES algorithm could converge to in this scenario, based on the initial values for *WOB* and *RPM*. Because the MSE response in the optimal region is relatively constant, the algorithm will seek out the first combination of *WOB* and *RPM* that it can find that drills at the *ROP* limit. Any adaptation in the input variables beyond this operating point will cause the objective function to artificially grow through Equation (13), which will discourage any further changes to the *WOB* or *RPM* unless it significantly decreases the *MSE*.

In Simulation run 4, a maximal torque limit of 10,000 Nm is enforced by the predictive and reactive constraint handling approaches detailed in Equations (14) through (20). A safety factor of 2 is used in Equation (16), and the parameters K_P and K_I in Equation (18) have values of 0.05 kg/Nm and 0.001 kg/Nm·s, respectively. The initial setpoints for the *WOB* and *RPM* are 8000 kg and 100 rpm, respectively.

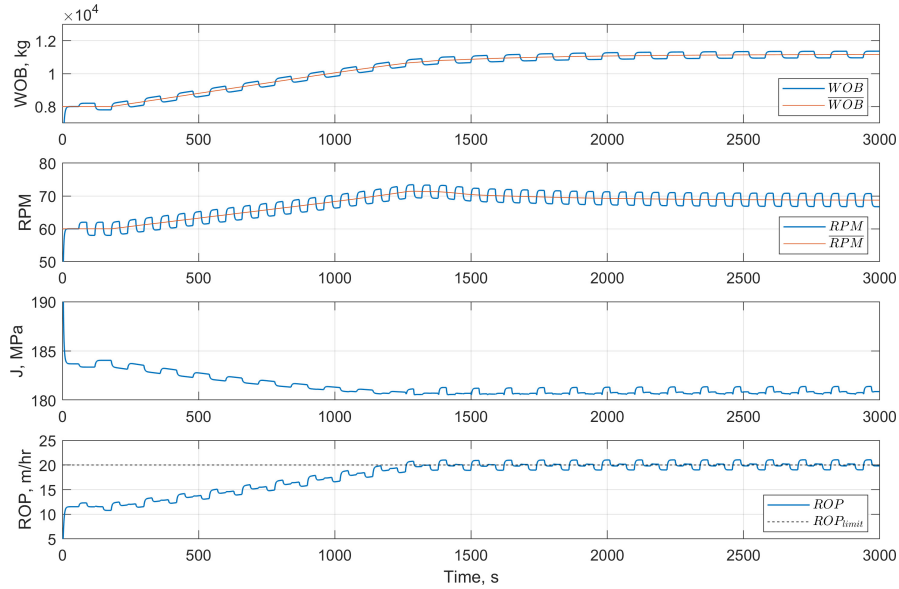

Figure 14. Simulation run 3, a scenario with a maximal limit imposed on the *ROP*.

Figure 15 displays the results from Simulation 4. In the first 1200 s, both the *WOB* and *RPM* are adapted to higher values, which results in drilling with lower *MSE* and higher *ROP*. At around 1200 s, Equation (16) predicts that the torque will surpass the allowable amount of 10,000 Nm if the *WOB* is increased any further. The adaptation in *WOB* is halted at this point and onwards, while the *RPM* continues to grow up to a value of approximately 111, where further increases in *RPM* would result in drilling in the dysfunction region. After 2000 s, an unexpected torque-increase of 1000 Nm is simulated, which makes the torque exceed its limit. This rise in torque could represent e.g., a build-up of cuttings around the BHA. As the torque is increased, the average *MSE* is elevated from about 180 to 200 MPa. The predictive constraint handler rapidly lowers the *WOB* until the torque is again within the allowable bounds, resulting in a reduction in $\overline{WOB}$ of about 900 kg. The reduction in $\overline{WOB}$ steers the drilling further away from the optimum, and the *MSE* is somewhat increased as a response. When drilling with this lower *WOB*, the ES algorithm detects that it is now safe to increase the *RPM* without encountering any dysfunctions which would increase the *MSE*. The *RPM* is seen to adapt to a value of 120, where the *ROP* is increased to approximately 29 m/h and we are drilling at the highest efficiency that can be obtained given the constraint on the torque.

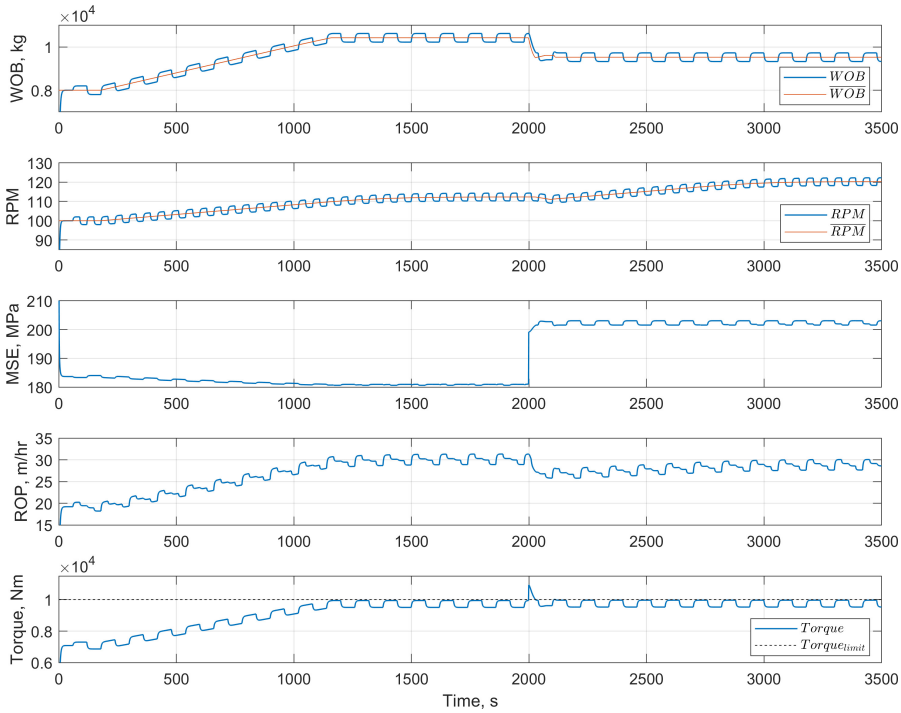

Figure 15. Simulation run 4, a scenario where the torque is not allowed to exceed 10,000 Nm.

4.3. Unconstrained Drilling with Formation Shifts

The results from Simulation 5 are shown in Figure 16, where we investigate how the proposed optimization algorithm handles abrupt formation changes. This scenario can be though as a continuation of Simulations 1 or 2, where the optimum for formation *A* was identified by the algorithm as 13,000 kg *WOB* and an *RPM* of 90. This scenario could also represent a setting where e.g., a drill-off test has been performed in formation *A*, which identified the optimal *WOB* and *RPM*. We initiate drilling with these optimal input values. After drilling 5 m in Formation *A*, we enter an 18-m-thick layer of the softer Formation *B*, at approximately 580 s. The optimal point in Formation *B* is located at a *WOB* of 12,000 kg and an *RPM* of 109, as indicated by the dotted lines in Figure 16. As we enter the softer formation, the *WOB* and *RPM* that were optimal for formation *A* are no longer the optimal input values to drill with and should be adjusted to drill more efficiently. Shortly after the formation shift occurs, the ES algorithm recognizes that the downhole conditions have changed and spends the following 1200 s converging to the optimal point in Formation *B*, where the *MSE* is minimized at an average value of 149 MPa and the average *ROP* has increased by approximately 20% from 36 to 43 m/h. At around 2200 s of simulation time, we enter Formation *A* again, and the *WOB* and *RPM* are slowly adjusted back to the optimal values that the simulation started out with. It can be seen that the "path" taken by the algorithm back to the optimum in Formation *A* consists of first reducing the $\overline{WOB}$ value before building it up to 13,000 kg, in the same manner as was done in Simulation 2 (see Figures 12 and 13) to quickly exit the dysfunction region.

Two important aspects of the proposed ES algorithm are shown in Figure 16. First, the advantage of continuously applying the excitations in *WOB* and *RPM* also even when we are operating at the current optimum, becomes apparent. When the drilled formation

suddenly changes, the information gathered by the excitation signals is used by the ES algorithm to rapidly recognize that the conditions have changed, and adjustments should be made in the applied $\overline{WOB}$ and $\overline{RPM}$ to drill more efficiently. These adjustments resulted in an increase in *ROP* of about 20%, compared to a setting where formation *B* had been drilled with constant *WOB* and *RPM* based on what was the optimal point when the simulation was initiated in formation *A*.

A second and closely related aspect is seen in the adjustments in $\overline{WOB}$,and $\overline{RPM}$ performed by the algorithm immediately after the formation change occurs at about 580 s of simulation time. In the following we consider the *WOB*, but the same analysis applies to the *RPM*. When the drilled formation becomes softer at 580 s, the calculated *MSE* is reduced. The ES algorithm relates this reduction in *MSE* to the currently applied *WOB*, which at this time was in an elevated position of $\overline{WOB} + A_{wob}$ kg. This causes the algorithm to estimate an artificially large and positive gradient for a short period of time, as higher values of *WOB* are related to a significant reduction in *MSE*. This erroneous gradient indicates that large improvements to the drilling efficiency can be made if $\overline{WOB}$ is increased. At this point, the adjustment of $\overline{WOB}$ in the wrong direction is limited by the saturation function and the adaptation gain in Equation (11), that disallows adaptation faster than 2.5 kg/s even if the estimated gradient is large. During the 50 s that the $\overline{WOB}$ is steered in the wrong direction, the $\overline{WOB}$ is only increased by about 125 kg. The requested changes in $\overline{WOB}$ would be much higher if the adaptation was directly proportional to the estimated gradient (as is usually the case in classical ES algorithms [26]). After drilling in this new formation for 50 s, the buffers used in the algorithm contain enough data sampled from the current conditions to detect that the $\overline{WOB}$ should be reduced to minimize the *MSE*, and the algorithm subsequently steers the $\overline{WOB}$ to the correct optimal value. The same effect as just described also occurs at the second formation shift at about 2200 s.

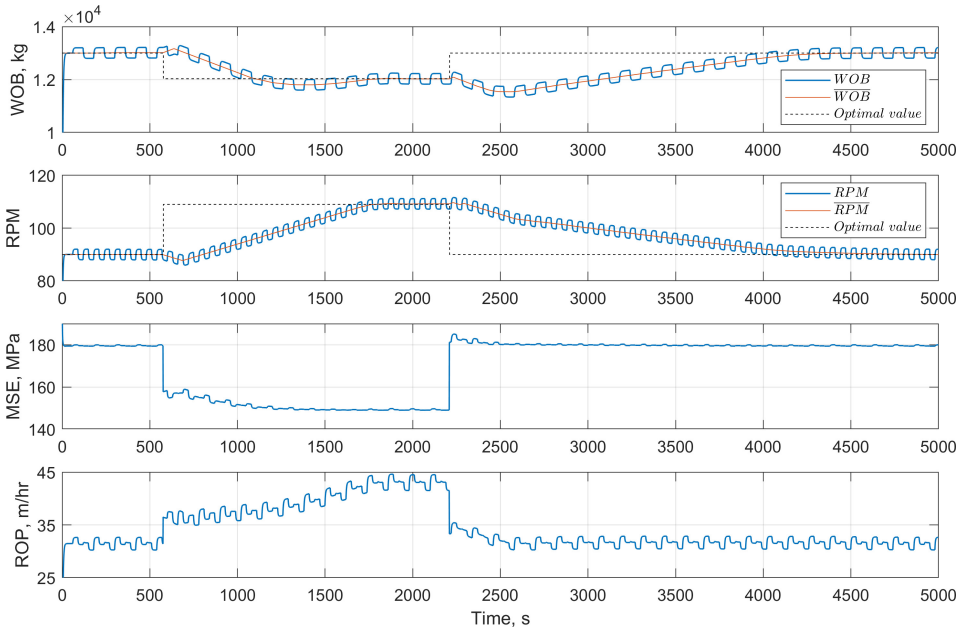

Figure 16. Simulation run 5, drilling through 5 m of formation *A*, 15 m of formation *B* and then returning to drilling in formation *A*.

5. Discussion of Results

The five simulation scenarios detailed in the previous section demonstrate how the proposed ES algorithm can be utilized to automatically steer the drilling process to the optimum conditions where the *MSE* is minimized. Since the optimization algorithm inherently requires full control of the *WOB* and *RPM* to continuously adjust these variables towards the optimal point, it is of utmost importance that the algorithm recognizes and avoids circumstances that could be damaging to the drilling equipment or could cause a contingency situation. In simulation 2 it was shown that the algorithm automatically steers away from drilling with dysfunctions, as drilling in this region resulted in high *MSE* values that could be reduced by regulating the *WOB* and *RPM*. In simulation runs 3 and 4, the possibly detrimental effects that we wish to avoid are not directly related to the *MSE*, but rather to other parameter that we wish to keep within certain limits. Simulations 3 and 4 demonstrate generic approaches to how we can avoid these types of constraints. In Simulation 4, the predictive constraint handling routine stops *WOB* adaptation before the constraint is violated. A separate control loop (the reactive constraint handling) is able to adjust the *WOB* back to the safe region when the limit is violated, much faster than if this constraint was implemented through modification of the objective function. This technique is however only applicable when the constrained output (the torque) is related to only one of the input variables, in this case the *WOB*. When several of the input variables are related to the output constraint, as is the case between the *WOB*, *RPM* and *ROP* in simulation run 3, the modified objective function described in Equation (13) is a better alternative to avoid the limit being exceeded.

The main advantage of using a data-driven algorithm like ES to optimize the drilling process is that it does not require detailed a priori knowledge of the downhole conditions or a drilling model to seek out more efficient drilling, and it can adapt to downhole changes. Both of these properties are shown in Simulation 5, where two formation shifts occurred which prompted the ES algorithm to seek out the new optimal conditions shortly after the changes happened. The ES algorithm considers a fixed window of time to perform its analysis and inherently tries to relate any change in the *MSE* to the applied excitations in *WOB* and *RPM*. If the *MSE* changes without any relation to the excitation signals, e.g., at a formation shift, the estimated gradients can become inaccurate when the data series used to estimate the gradients contain measurements from two differing downhole conditions. To avoid the algorithm having an exaggerated reaction to disturbances like this, the saturation function together with moderate values for the gain parameters, γ, is used to limit the algorithm's maximal adaptation rate regardless of the magnitude of the estimated gradients. This design encourages slow and steady adaptation towards the optimum. Faster convergence could be achieved by increasing γ, but this would also make the algorithm more susceptible to disturbances and noise.

Although the ES algorithm performs optimization actions without using a model of the system, engineering knowledge about the process is required to tune the algorithm and provide appropriate initial values for the *WOB* and *RPM*. In the simulation scenarios, the starting points were chosen to showcase different properties of the ES algorithm like constraint handling, convergence to the optimum and avoidance of drilling with dysfunctions. In simulation scenarios 1 and 5, the ES algorithm was able to increase the *ROP* by about 170% and 20%, respectively. How much the algorithm can improve the drilling efficiency (through higher *ROP* and/or lower *MSE*) is strongly related to how far away from the optimal *WOB* and *RPM* that the algorithm is initiated. In a field application, the initial *WOB* and *RPM* values should be a best guess of the optimal drilling conditions, which could be based on the driller's experience, a drill-off test, data from an offset well or estimates given by a drilling model.

There are both benefits and drawbacks to choosing *MSE* as the objective function to minimize. The *MSE* can be used to identify the founder point by seeking out the maximal *WOB* and *RPM* values that results in a decreasing or flat response in *MSE*. The expected flat region in *MSE* when operating in drilling region II can however pose some challenges

when applying the ES algorithm. When drilling in this region, the estimated gradients will have zero or near zero values and the ES algorithm depends on the parameters k_{wob} and k_{rpm} to indicate if the input variables should be increased. In field applications, the calculated *MSE* could be susceptible to noise (especially though the torque) which could make it hard to estimate zero or close to zero valued gradients. This complication could be alleviated by increasing the amplitudes and periods of the excitation signals or considering a longer sliding window time series that encompassed several oscillations of the excitation signals, which would average out disturbances. Another possible alternative could be to use a combination of *ROP* and *MSE* as the objective function, as in [25].

There are several paths for further research that could be explored. Additional studies on a more advanced drilling simulator, field trials or lab experiments are needed to investigate how dynamic effects such as vibrations affect the performance of the proposed algorithm. Tests in the field or in the lab would also provide the opportunity to compare the ES method with other optimization methods, either data-driven or model based, in a realistic setting. Testing the algorithm in e.g., a lab setting would allow us to study if the algorithm in its current form will be able to converge to the optimum if it is initiated in a region where severe vibrations occur. The extended model used to simulate drilling in this study assumes that the *MSE* will keep increasing when operating further into regions where vibrations are expected to occur (see Figures 4 and 5). If this is not the case, and the *MSE* rather reaches some plateau value that does not change as a function of *WOB* and *RPM* in these regions, the proposed ES algorithm would not be able to find the optimum if the initial point was in the *MSE* plateau region. If this is the case, a different objective function, e.g., on the form of Equation (13) could be used to remedy the issue.

A second possibility for further work relies on the ES method's inherent nature of relating measurements of drilling parameters to the known variations in *WOB* and *RPM* induced by the excitation signals. If available, additional measured and/or calculated parameters such as the magnitude of different forms of vibrations could be related to the variations in *WOB* and *RPM*. Knowing how downhole vibrations vary as a function of *WOB* and/or *RPM* could be utilized for constraint handling or be displayed as useful information for the driller.

6. Conclusions

We have presented an algorithm based on the multivariable extremum seeking method that automatically optimizes the WOB and RPM to achieve drilling with minimal MSE, while adhering to operational constraints for safe and efficient drilling. The algorithm detailed in the paper is data-driven and does not require detailed a priori knowledge or models of the drilling process. The algorithm gathers information about the current downhole conditions by continuously performing small tests with the applied WOB and RPM while drilling and automatically implements optimization actions based on the test results. To investigate the algorithm's performance in a simulation environment, a drilling model for bit-rock interaction has been extended by the authors to qualitatively account for drilling dysfunctions. The simulations demonstrate that the proposed algorithm is able to find and maintain the WOB and RPM that result in drilling with minimal MSE, while adhering to operational constraints. The constraint handling functionality has been demonstrated with limits imposed on the ROP and torque. Yet, it is generic and can be applied to other constraining factors. The simulations show that the ES method is able to track changes in the optimal WOB and RPM corresponding to changes in the drilled formation. As demonstrated in the simulation scenarios, the overall improvements in ROP can be up to 20–170%, depending on the initial guess of the optimal WOB and RPM obtained from e.g., a drill-off test or a potentially inaccurate model. Along with the algorithm's description, we provide an explanation of specific design choices and tuning guidelines that simplify the use of the algorithm in practice.

Author Contributions: Conceptualization, M.N., A.P. and B.S.A.; methodology, software, validation, formal analysis and writing—original draft preparation, M.N.; writing—review and editing M.N., A.P. and B.S.A.; visualization M.N., A.P. and B.S.A.; Supervision and project administration, A.P. and B.S.A. All authors have read and agreed to the published version of the manuscript.

Funding: This research was funded by the Norwegian University of Science and Technology through the BRU21 research program, www.ntnu.edu/bru21 (accessed on 25 February 2021).

Data Availability Statement: The simulation datasets and the Matlab code used in the model and simulations are available at: https://github.com/magnusnystad/Minimization-of-MSE-with-multivarable-ES (accessed on 25 February 2021).

Acknowledgments: This research is a part of BRU21—NTNU Research and Innovation Program on Digital and Automation Solutions for the Oil and Gas Industry, www.ntnu.edu/bru21 (accessed on 25 February 2021).

Conflicts of Interest: The authors declare no conflict of interest.

Abbreviations

BHA	Bottom Hole Assembly
ES	Extremum Seeking
MSE	Mechanical Specific Energy
NPT	Non-Productive Time
PDC	Polycrystalline Diamond Compact
PI	Proportional-Integral
RPM	Revolutions Per Minute (drill string rotational rate)
T	Torque
WOB	Weight on Bit

Appendix A. Period Selection for the Excitation Signals

The tuning of the excitation signals is an important part of the extremum seeking algorithm. To extract a gradient of how the *MSE* relates to the *WOB* and *RPM* independently, setting $P_{WOB} = 2P_{RPM}$ is suggested by the authors. Under some simplifying assumptions, it can be shown that this tuning of the excitation signal's periods allows for exact estimation of $\partial MSE/\partial WOB$ and $\partial MSE/\partial RPM$ without interference between the two excitation signals. Here, we investigate this property by considering the estimation of $\partial MSE/\partial WOB$ with a continuous-time, single-variable version of Equation (9), which is applied to a system where both the *WOB* and *RPM* is varied according to Equations (7a), (7b) and (8). A similar analysis can also be performed to show how the least-squares estimation of $\partial MSE/\partial RPM$ is not affected by the variations in the *WOB*.

Although the *MSE* is a non-linear function of both *WOB* and *RPM* when considering the entire span of *WOB* and *RPM* values (see Figures 4 and 5), the extremum seeking algorithm uses only a local region of this non-linear relationship when estimating gradients. The extent of this local region is determined by the amplitudes of the excitation signals. If suitable (not too large) amplitudes are used, it can be assumed that locally there is an approximately linear relationship between the *MSE* and the applied *WOB* and *RPM*, which is the relationship that is estimated by the least-squares gradient calculation in Equation (9). Using compact notation, let the *WOB* be denoted by $x = \overline{x} + d_x$ and the *RPM* be represented by $y = \overline{y} + d_y$, as detailed in Equations (7a) and (7b). In the neighborhood of the point $(\overline{x}, \overline{y})$, the non-linear relation between the *MSE*, *WOB* and *RPM* can be approximately described by:

$$z = \beta + \alpha xy, \tag{A1}$$

where z represents the MSE and the parameters α and β take on constant values in this local region. We further assume that the adaptation in *WOB* and *RPM* is small so that $\overline{x}$ and $\overline{y}$ are approximately constant throughout the investigated time interval of P_x seconds, as is common practice for average analysis of extremum seeking algorithms [26].

We consider a scenario where we are drilling ahead through a homogeneous formation and have varied the *WOB* (x) and *RPM* (y) according to Equation (8) while recording the *MSE* (z) for the past P_x seconds. The measured drilling data is used to solve for the least-squares slope and intercept parameters, a and b, using a continuous-time, single-variable version of Equation (9):

$$\int_{t-P_x}^{t} [z(\tau) - ax(\tau) - b]^2 d\tau \rightarrow \min_{a,b}, \tag{A2}$$

where a represents the gradient-estimate, $\partial MSE/\partial WOB$. Substituting in the previously defined relationships for x and y and approximating the response of the drilling system with Equation (A1) yields:

$$\int_{t-P_x}^{t} \left[\beta + \alpha\left(\overline{x}_y + d_x(\tau)\right)\left(\overline{y} + d_y(\tau)\right) - \alpha\left(\overline{x}_y + d_x(\tau)\right) - b\right]^2 d\tau \rightarrow \min_{a,b}. \tag{A3}$$

Further, using Equation (8) to describe the excitation signals, d_x and d_y, gives:

$$\int_{t-P_x}^{t} \left[\alpha + \beta\left(\overline{x} + A_x sgn\left(sin\left(\frac{2\pi\tau}{P_{xy}}\right)\right)\right)\left(\overline{y} + A_y sgn\left(sin\left(\frac{2\pi\tau}{P_y}\right)\right)\right) - a\left(\overline{x} + A_x sgn\left(sin\left(\frac{2\pi\tau}{P_{xy}}\right)\right)\right) - b\right]^2 d\tau \rightarrow \min_{a,b}. \tag{A4}$$

At any point in time, t, the integral in Equation (A4) can be split into intervals in which the signum function takes on constant values of ± 1. Using the relation $P_x = 2P_y$ and the assumption that $\overline{x}$ and $\overline{y}$ are constant values, Equation (A4) can be expressed as:

$$\min_{a,b}\left[P_x\left(\overline{x}_y^2 + A_x^2\right)\left(\alpha^2\overline{y}^2 + \alpha^2 A_y^2 - 2\alpha a\overline{y} + a^2\right) + 2P_x\overline{x}(\beta - b)(a - \alpha\overline{y}) + P_x(b - \beta)^2\right]. \tag{A5}$$

Taking the partial derivatives of Equation (A5) with respect to a and b and equating them to zero results in the set of equations:

$$\begin{gathered}(b - \beta) + \overline{x}(a - \alpha\overline{y}) = 0, \\ \left(x^2 + A_x^2\right)(a - \alpha\overline{y}) + 2\overline{x}(b - \beta) = 0,\end{gathered} \tag{A6}$$

which has the solution $a = \alpha\overline{y}$ and $b = \beta$. The estimated gradient, $\alpha\overline{y}$, corresponds to the slope of $\partial MSE/\partial WOB$ described by Equation (A1) evaluated at the average *RPM* value, $\overline{y}$. This shows that in an ideal scenario where the simplifying assumptions are met, the tuning $P_x = 2P_y$ allows for accurate estimation of $\partial MSE/\partial WOB$ without interference from the variations in *RPM*. The same analysis can be repeated for estimation of $\partial MSE/\partial RPM$ to find the expected gradient, $\alpha\overline{x}$, for this case. Other combinations of periods for the excitation signals can also be employed based on similar analysis, as long as one of the periods is an even multiple of the other, $P_{wob} = nP_{rpm}$ or $P_{rpm} = nP_{wob}$ where n is an even number larger than zero.

In reality, the applied *WOB* and *RPM* will exhibit dynamics and cannot be expected to perfectly follow the square wave setpoints requested by the extremum seeking algorithm. Any deviations from the setpoints will however be dealt with by the least-squares approach to gradient estimation, which will incorporate these transient periods into the analysis. Furthermore, if the system is not currently at the optimal point, there will be adaptation in both *WOB* and *RPM* which will make the base values, $\overline{x}$ and $\overline{y}$, change throughout the investigated time interval. The adaptation can cause some inaccuracies in the estimated gradients, but this effect can be kept to a minimum by choosing conservative values for the adaptation gains as well as through appropriate filtering of the data.

References

1. Eustes, A.W. The Evolution of Automation in Drilling. In Proceedings of the SPE Annual Technical Conference and Exhibition, Anaheim, CA, USA, 11–14 November 2007.
2. Chmela, B.; Gibson, N.; Abrahamsen, E.; Bergerud, R. Safer Tripping Through Drilling Automation. In Proceedings of the IADC/SPE Drilling Conference and Exhibition, Fort Worth, TX, USA, 4–6 March 2014.
3. Iversen, F.P.; Cayeux, E.; Dvergsnes, E.W.; Ervik, R.; Welmer, M.; Balov, M.K. Offshore Field Test of a New System for Model Integrated Closed-Loop Drilling Control. *SPE Drill. Completion* **2009**, *24*, 518–530. [CrossRef]
4. Gulsrud, T.O.; Nybø, R.; Bjørkevoll, K.S. Statistical Method for Detection of Poor Hole Cleaning and Stuck Pipe. In Proceedings of the SPE Offshore Europe Oil and Gas Conference and Exhibition, Aberdeen, UK, 8–11 September 2009.
5. Tarr, B.A.; Ladendorf, D.W.; Sanchez, D.; Milner, G.M. Next-Generation Kick Detection During Connections: Influx Detection at Pumps Stop (IDAPS) Software. *SPE Drill. Completion* **2016**, *31*, 250–260. [CrossRef]
6. Kyllingstad, A.; Nessjøen, P.J. A New Stick-Slip Prevention System. In Proceedings of the SPE/IADC Drilling Conference and Exhibition, Amsterdam, The Netherlands, 17–19 March 2009.
7. Runia, D.J.; Dwars, S.; Stulemeijer, I.P. A Brief History of the Shell "Soft Torque Rotary System" and Some Recent Case Studies. In Proceedings of the SPE/IADC Drilling Conference, Amsterdam, The Netherlands, 5–7 March 2013.
8. Chapman, C.D.; Sanchez, J.L.; De Leon Perez, R.; Yu, H. Automated Closed-Loop Drilling with ROP Optimization Algorithm Significantly Reduces Drilling Time and Improves Downhole Tool Reliability. In Proceedings of the IADC/SPE Drilling Conference and Exhibition, San Diego, CA, USA, 6–8 March 2012.
9. Dunlop, J.; Isangulov, R.; Aldred, W.D.; Sanchez, H.A.; Flores, J.L.S.; Herdoiza, J.A.; Belaskie, J.; Luppens, C. Increased Rate of Penetration Through Automation. In Proceedings of the SPE/IADC Drilling Conference and Exhibition, Amsterdam, The Netherlands, 1–3 March 2011.
10. Teale, R. The Concept of Specific Energy in Rock Drilling. *Int. J. Rock Mech. Min. Sci. Geomech. Abstr.* **1965**, *2*, 57–73. [CrossRef]
11. Koederitz, W.L.; Weis, J. A Real-Time Implementation of MSE. In Proceedings of the AADE National Technical Conference and Exhibition, Houston, TX, USA, 5–7 April 2005.
12. Dupriest, F.; Hutchison, I.; Oort, E.v.; Armstrong, N. *The IADC Drilling Manual—Drilling Practices*, 12th ed.; International Association of Drilling Contractors: Houston, TX, USA, 2014.
13. Dupriest, F.E.; Koederitz, W.L. Maximizing Drill Rates with Real-Time Surveillance of Mechanical Specific Energy. In Proceedings of the SPE/IADC Drilling Conference, Amsterdam, The Netherlands, 23–25 February 2005.
14. Wu, S.X.; Paez, L.; Partin, U.; Agnihotri, M. Decoupling Stick-Slip and Whirl to Achieve Breakthrough in Drilling Performance. In Proceedings of the IADC/SPE Drilling Conference and Exhibition, New Orleans, LA, USA, 2–4 February 2010.
15. Bataee, M.; Kamyab, M.; Ashena, R. Investigation of Various ROP Models and Optimization of Drilling Parameters for PDC and Roller-cone Bits in Shadegan Oil Field. In Proceedings of the International Oil and Gas Conference and Exhibition in China, Beijing, China, 8–10 June 2010.
16. Sui, D.; Aadnoy, B. Rate of Penetration Optimization using Moving Horizon Estimation. *Modeling Identif. Control A Nor. Res. Bull.* **2016**, *37*, 149–158. [CrossRef]
17. Young, F.S., Jr. Computerized Drilling Control. *J. Pet. Technol.* **1969**, *21*, 483–496. [CrossRef]
18. Rommetveit, R.; Bjørkevoll, K.S.; Halsey, G.W.; Larsen, H.F.; Merlo, A.; Nossaman, L.N.; Sweep, M.N.; Silseth, K.M.; Ødegaard, S.I. Drilltronics: An Integrated System for Real-Time Optimization of the Drilling Process. In Proceedings of the IADC/SPE Drilling Conference, Dallas, TX, USA, 2–4 March 2004.
19. Spencer, S.J.; Mazumdar, A.; Jiann-Cherng, S.; Foris, A.; Buerger, S.P. Estimation and Control for Efficient Autonomous Drilling Through Layered Materials. In Proceedings of the 2017 American Control Conference (ACC), Seattle, WA, USA, 24–26 May 2017; pp. 176–182.
20. Chang, D.-L.; Payette, G.S.; Pais, D.; Wang, L.; Bailey, J.R.; Mitchell, N.D. Field Trial Results of a Drilling Advisory System. In Proceedings of the International Petroleum Technology Conference, IPTC, Doha, Qatar, 19–22 January 2014.
21. Koederitz, W.L.; Johnson, W.E. Real-Time Optimization of Drilling Parameters by Autonomous Empirical Methods. In Proceedings of the SPE/IADC Drilling Conference and Exhibition, Amsterdam, The Netherlands, 1–3 March 2009.
22. Banks, S. Minimizing the Mechanical Specific Energy While Drilling Using Extremum Seeking Control. In Proceedings of the 11th International Conference on Vibration Problems, Lisbon, Portugal, 9–12 September 2013.
23. Aarsnes, U.J.F.; Aamo, O.M.; Krstic, M. Extremum Seeking for Real-time Optimal Drilling Control. In Proceedings of the American Control Conference (ACC), Philadelphia, PA, USA, 10–12 July 2019.
24. Nystad, M.; Pavlov, A. Micro-Testing While Drilling for Rate of Penetration Optimization. In Proceedings of the International Conference on Offshore Mechanics and Arctic Engineering, Virtual, Online, 3–7 August 2020.
25. Lai, S.W.; Ng, J.; Eddy, A.; Khromov, S.; Paslawski, D.; van Beurden, R.; Olesen, L.; Payette, G.S.; Spivey, B.J. Large-Scale Deployment of a Closed-Loop Drilling Optimization System: Implementation and Field Results. *SPE Drill. Completion* **2020**. [CrossRef]
26. Tan, Y.; Moase, W.H.; Manzie, C.; Nešić, D.; Mareels, I.M. Extremum seeking from 1922 to 2010. In Proceedings of the 29th Chinese Control Conference, Beijing, China, 29–31 July 2010.
27. Sui, D.; Nybø, R.; Azizi, V. Real-time optimization of rate of penetration during drilling operation. In Proceedings of the 2013 10th IEEE International Conference on Control and Automation (ICCA), Hangzhou, China, 12–14 June 2013; pp. 357–362.

28. Detournay, E.; Richard, T.; Shepherd, M. Drilling response of drag bits: Theory and experiment. *Int. J. Rock Mech. Min. Sci.* **2008**, *45*, 1347–1360. [CrossRef]
29. Vogel, S.K.; Creegan, A.P. Case Study for Real Time Stick/Slip Mitigation to Improve Drilling Performance. In Proceedings of the SPE/IADC Middle East Drilling Technology Conference and Exhibition, Abu Dhabi, United Arab Emirates, 26–28 January 2016.
30. Warren, T.M. Penetration Rate Performance of Roller Cone Bits. *SPE Drill. Eng.* **1987**, *2*, 9–18. [CrossRef]
31. Dupriest, F.E. Comprehensive Drill Rate Management Process To Maximize ROP. In Proceedings of the SPE Annual Technical Conference and Exhibition, San Antonio, TX, USA, 24–27 September 2006.
32. Pessier, R.C.; Fear, M.J. Quantifying Common Drilling Problems With Mechanical Specific Energy and a Bit-Specific Coefficient of Sliding Friction. In Proceedings of the SPE Annual Technical Conference and Exhibition, Washington, DC, USA, 4–7 October 1992.
33. Dupriest, F.E.; Witt, J.W.; Remmert, S.M. Maximizing ROP With Real-Time Analysis of Digital Data and MSE. In Proceedings of the International Petroleum Technology Conference, Doha, Qatar, 21–23 November 2005.
34. Simon, R. Energy Balance in Rock Drilling. *Soc. Pet. Eng. J.* **1963**, *3*, 298–306. [CrossRef]
35. Oloruntobi, O.; Butt, S. Application of specific energy for lithology identification. *J. Pet. Sci. Eng.* **2020**, *184*. [CrossRef]
36. Menand, S.; Mills, K. Use of Mechanical Specific Energy Calculation in Real-Time to Better Detect Vibrations and Bit Wear While Drilling. In Proceedings of the AADE National Technical Conference and Exhibition, Houston, TX, USA, 11–12 April 2017.
37. Yau, H.-T.; Lin, C.-J.; Wu, C.-H. Sliding Mode Extremum Seeking Control Scheme Based on PSO for Maximum Power Point Tracking in Photovoltaic Systems. *Int. J. Photoenergy* **2013**, *2013*. [CrossRef]
38. Ariyur, K.B.; Krstić, M. *Real-Time Optimization by Extremum Seeking Control*; John Wiley & Sons, Inc.: Hoboken, NJ, USA, 2003. [CrossRef]
39. Tan, Y.; Nešić, D.; Mareels, I. On the Choice of Dither in Extremum Seeking Systems: A Case Study. *Automatica* **2008**, *44*, 1446–1450. [CrossRef]
40. Payette, G.S.; Spivey, B.J.; Wang, L.; Bailey, J.R.; Sanderson, D.; Kong, R.; Pawson, M.; Eddy, A. A Real-Time Well-Site Based Surveillance and Optimization Platform for Drilling: Technology, Basic Workflows and Field Results. In Proceedings of the SPE/IADC Drilling Conference and Exhibition, The Hague, The Netherlands, 14–16 March 2017.

ISBN 978-82-326-5854-1 (printed ver.)
ISBN 978-82-326-6290-6 (electronic ver.)
ISSN 1503-8181 (printed ver.)
ISSN 2703-8084 (online ver.)

NTNU

Norwegian University of
Science and Technology